

Aus der Klinik für Dermatologie
der Heinrich-Heine-Universität Düsseldorf
Direktor: Univ.-Prof. Dr. med. Bernhard Homey

**Effects of ligand-specific activation of the
Aryl Hydrocarbon Receptor towards the
expression of the Aldo-keto reductase
1C subfamily**

Dissertation

zur Erlangung des Grades eines Doktors der Medizin der Medizinischen Fakultät
der Heinrich-Heine-Universität Düsseldorf

vorgelegt von
Sophia Katharina Bissen

2024

Als Inauguraldissertation gedruckt mit Genehmigung der Medizinischen Fakultät
der Heinrich-Heine-Universität Düsseldorf:

gez.:

Dekan: Prof. Dr. med. Nikolaj Klöcker

Erstgutachter: PD Dr. med. Stephan Meller

Zweitgutachterin: Univ.-Prof. Dr. med. Ellen Fritsche

"You cannot hope to build a better world without improving the individuals. To that end, each of us must work for his own improvement and, at the same time, share a general responsibility for all humanity, our particular duty being to aid those to whom we think we can be most useful."

- Marie Curie, 1867-1934

Parts of this work were published:

Christian Vogeley, Natalie C. Sondermann, Selina Woeste, Afaque A. Momin, Viola Gilardino, Frederick Hartung, Markus Heinen, Sophia K. Maaß, Melina Mescher, Marius Pollet, Katharina M. Rolfes, Christoph F.A. Vogel, Andrea Rossi, Dieter Lang, Stefan T. Arold, Motoki Nakamura and Thomas Haarmann-Stemmann (2022), Unraveling the differential impact of PAHs and dioxin-like compounds on AKR1C3 reveals the EGFR extracellular domain as a critical determinant of the AHR response. *Environmental International*, (158) [1]

Zusammenfassung

Die Inzidenz maligner Erkrankungen wie Hautkrebs steigt seit Jahrzehnten an, wobei der wesentliche Promotor dieser Entwicklung Umweltfaktoren sind. Forschungsbedarf besteht vor allem darin, die molekularen Mechanismen zu ergründen, da Risikofaktoren zwar bekannt, aber beteiligte Signalwege noch unverstanden sind. Neben ultravioletter Strahlung (UV) konnte nachgewiesen werden, dass auch chemische Noxen wie polyzyklische Kohlenwasserstoffe (PAH) zu Hautkrebskrankungen führen können, wie zum Beispiel im Falle von Benz(a)pyren (BaP). Es ist ein bekannter Ligand des Aryl Hydrocarbon Rezeptors (AHR), ein Transkriptionsfaktor, der in allen strukturellen Zellen der Haut vorkommt und bereits mit zahlreichen dermatologischen Prozessen wie Hyperpigmentierung, Hautalterung und Hautkrebs in Verbindung gebracht werden konnte. Der molekulare Mechanismus, über den der AHR zur Entstehung von Malignomen beiträgt, ist bis heute Gegenstand der Forschung. Eine wichtige Rolle bei der Kanzerogenese spielt die unkontrollierte Aktivierung wachstumsfördernder Rezeptoren wie der Epidermal Growth Factor Receptor (EGFR). Mitglieder dieser Rezeptorenfamilie stehen ebenso im Verdacht, bei der Entwicklung kutaner Malignome beteiligt zu sein. Ihre Aktivierung geschieht durch Ligandenbindung mit anschließender Dimerisierung. Die Liganden liegen normalerweise membrangebunden vor und müssen durch Matrix-Metalloproteinasen (MMP) herausgelöst werden. Diese werden vorher durch Proteinkinasen aktiviert, die zunächst selbst durch Tyrosinkinasen wie c-src phosphoryliert werden müssen. C-src gehört zu dem Multiproteinkomplex, in dem der AHR in gebundener, inaktiver Form vorliegt. Nach Aktivierung des AHR ist es denkbar, dass die freige-wordene Tyrosinkinase c-src den zellulären Signalweg beeinflusst an dessen Ende der EGFR aktiviert wird. Ferner aktiviert BaP nicht nur den AHR, sondern führt zu einer verstärkten Transkription von Aldo-Keto-Reduktasen (AKR), die als am Prostaglandinstoffwechsel beteiligte Enzymfamilie daraufhin die spontane Bildung von 15d-Prostaglandin J₂ (15d-PGJ₂) aus Prostaglandin D₂ (PGD₂) verhindern. Ersteres dient dem Organismus normalerweise durch die Aktivierung des Peroxisom-Proliferator-aktivierten Rezeptors gamma (PPAR γ) als pro-apoptotischer Signalwegvermittler. Wird also weniger 15d-Prostaglandin J₂ gebildet, kommt es zu einer anti-apoptotischen Stoffwechsellaage in Zellen, in der maligne Zellen potentiell bessere Möglichkeiten haben, weiter zu mutieren und zu proliferieren. In dieser Arbeit konnte gezeigt werden, dass die AKR-Familie C unter dem Einfluss des AHR zu stehen scheint, durch Liganden des EGFR verstärkt und durch Blockierung der Protein Kinase C (PKC) vermindert transkribiert wird. Zwischen dem AHR, dem EGFR und den Enzymen der AKR1C-Familie könnte es demnach Interaktionen geben, die erklären würden, wie PAH die Kanzerogenese in Hautkrebs fördern.

Summary

The incidence of malignant diseases such as skin cancer has continuously been rising for decades, the main promotor of this development being environmental factors. Therefore, it is crucial to understand the molecular mechanisms that drive carcinogenesis. Since risk factors are well known today, the focus lies upon understanding the signaling cascades that are affected by environmental changes. Besides UV radiation, polycyclic aromatic hydrocarbons (PAH) like benzo-a-pyrene (BaP) are known pollutants that induce malignant transformation in the skin. BaP is a ligand of the aryl hydrocarbon receptor (AHR), a transcriptional factor ubiquitously present in cutaneous cells and known to be involved in hyperpigmentation, skin ageing and skin carcinogenesis. Another important driver of these processes is the epidermal growth factor receptor (EGFR). Members of this receptor family are activated through ligand binding with a following dimerization process. The ligands are normally bound to the cell membrane and require shedding by matrix-metalloproteases (MMP). Those need to be activated by protein kinases (PK) that in turn require phosphorylation to be active. This normally happens due to the activity of tyrosine kinases like c-src. This kinase, in turn, is part of the multi-protein complex that holds the AHR in its inactive state. Therefore, it is possible that, after activation by BaP, the AHR releases c-src which then activates the EGFR. Interestingly, BaP not only activates the AHR, it also leads to an enhanced transcription of aldo-keto reductases (AKR), an enzyme family involved in the metabolism of prostaglandins. They inhibit the spontaneous conversion of prostaglandin D₂ (PGD₂) to 15d-prostaglandin J₂ (15d-PGJ₂). Usually, 15d-PGJ₂ activates the peroxisome proliferator-activated receptor gamma (PPAR γ), a pro-apoptotic signaling receptor. Therefore, a low quantity of 15d-PGJ₂ leads to an anti-apoptotic metabolic state, which in turn improves the conditions for carcinogenesis. In this work, it could be shown that the AKR family C depends on AHR signaling, its transcription is enhanced when exposed to EGFR-ligands and lowered by inhibitors of the protein kinase C (PKC). Therefore, a signaling cascade between the AHR, the EGFR and the AKR1C3 family that could explain how PAH drive skin carcinogenesis seems to exist.

Abbreviations

| Abbreviation | Meaning |
|---|--|
| 5 α -DHT | 5-alpha-dihydrotestosterone |
| 9 α 11 β -PGF ₂ | 9-alpha-11-beta-prostaglandin F ₂ |
| 15d-PGJ ₂ | 15-deoxy-delta-12,14-prostaglandin J ₂ |
| A/A | antibiotics/antimycotics |
| AB | Antibody |
| AD | atopic dermatitis |
| ADAM | a disintegrin and metalloproteinase |
| ADPF | AHR degradation promoting factor |
| AEV | avian erythroblastosis virus |
| AHR | Aryl Hydrocarbon Receptor |
| AHRR | AHR repressor |
| AIP | AHR interacting protein |
| AK | Actinic keratosis |
| AKR | aldo-keto reductase |
| APS | ammonium persulfate |
| AR | androgen receptor |
| ARE | antioxidant response element |
| AREG | amphiregulin |
| ARNT | AHR nuclear translocator |
| ATP | adenosine triphosphate |
| BaP | benzo[a]pyrene |
| BCA | bicinchoninic acid |
| BCC | basal cell carcinoma |
| BDE-47 | 2,2',4,4'-Tetrabromodiphenyl ether |
| bHLH | basic helix-loop-helix |
| BSA | Bovine Serum Albumin |
| BTC | betacellulin |
| cDNA | complementary DNA |
| CNS | central nervous system |
| COX2 | cyclooxygenase 2 |
| CPD | cyclobutane pyrimidine dimers |
| CR | cysteine-rich |
| cSCC | cutaneous squamous cell carcinoma |
| dEGFR | Drosophila melanogaster epidermal growth factor receptor |
| DMEM | Dulbecco's Modified Eagle Medium |

| Abbreviation | Meaning |
|----------------------------------|---|
| DMSO | dimethyl sulfoxide |
| DNA | deoxyribonucleic acid |
| DSMZ | <i>Deutsche Sammlung von Mikroorganismen und Zellkulturen</i> |
| E. coli | Escherichia coli |
| EDTA | ethylenediaminetetraacetic acid |
| eJM | extracellular juxtamembrane |
| EGF | Epidermal Growth Factor |
| EGFR | Epidermal Growth Factor Receptor |
| EGN | epigen |
| EPR | epiregulin |
| ER | estrogen receptor |
| ErbB | erythroblastosis oncogene B |
| EREG | epiregulin |
| Erk1/2 | extracellular signal-regulated kinase 1 and 2 |
| EV | empty vector |
| FCS | fetal calf serum |
| FICZ | 6-formylindolo[3,2-b]carbazole |
| G418 | Geneticin™ |
| GM3 | monosialodihexosylganglioside |
| GPCR | G-protein coupled receptor |
| H ₂ O _{DEPC} | diethylpyrocarbonate water |
| HAH | halogenated aromatic hydrocarbon |
| HB-EGF | Heparin-binding EGF-like growth factor |
| HER | human EGF receptor |
| HIF-1 | hypoxia-inducible factor-1 |
| HNSCC | head-and-neck squamous cell carcinoma |
| HRP | horseradish peroxidase |
| HSD | hydroxysteroid dehydrogenase |
| HSP90 | heat-shock protein 90 |
| IGEPAL CA-630 | Octylphenoxypolyethoxyethanol |
| iJM | intracellular juxtamembrane |
| JM | juxtamembrane |
| JMAD | juxtamembrane activation domain |
| Keap1-Nrf2 | Kelch-like ECH-associated protein 1 and nuclear factor erythroid 2-related factor 2 |
| KGF-2 | keratinocyte growth factor 2 |
| KIN I/II | keratinocytic intraepidermal neoplasia I/II |

| Abbreviation | Meaning |
|--------------------------|--|
| KLF6 | krüppel-like factor 6 |
| LRR | leucine rich repeat |
| MAPK | mitogen-activated protein kinase |
| MMP | matrix-metalloproteinase |
| NADP ⁺ /NADPH | nicotinamide adenine dinucleotide phosphate |
| NC | non-consensus |
| NER | nucleotide excision repair |
| NES | nuclear export signal |
| NF κ B | nuclear factor kappa-light-chain-enhancer of activated B-cells |
| NFDM | nonfat dried milk |
| NLS | nuclear localization signal |
| NMSC | Non-melanoma skin cancer |
| NRG | neuregulin |
| NSAID | nonsteroidal anti-inflammatory drug |
| PAH | polycyclic aromatic hydrocarbon |
| PAS | PER-ARNT-SIM |
| PBS | phosphate buffered saline |
| PC | protein kinase |
| PCB126 | polychlorinated biphenyl |
| PER | period |
| PGD ₂ | prostaglandin D ₂ |
| PI3K | phosphatidylinositol-3-kinase |
| PIC | Protease Inhibitor Cocktail |
| PKC | protein kinase C |
| PMSF | phenylmethylsulfonyl fluoride |
| PPAR γ | peroxisome proliferator-activated receptor gamma |
| PR | progesterone receptor |
| PTB | phosphotyrosine binding domain |
| PTP | protein tyrosine phosphatases |
| PVDF | polyvinylidene fluoride |
| qRT-PCR | quantitative reverse-transcriptase polymerase chain reaction |
| RNA | ribonucleic acid |
| RNAseq | RNA sequencing |
| ROI | region of interest |
| ROS | reactive oxygen species |
| RTK | receptor tyrosine kinase |
| SDR | short-chain dehydrogenases/reductases |

| Abbreviation | Meaning |
|---------------------|---|
| SDS | Sodium dodecyl sulfate |
| SFK | Src-family tyrosine kinases |
| SH2 | src homology 2 |
| shAHR | short-hairpin RNA for the AHR vector |
| SIM | single-minded |
| siRNA | small interfering RNA |
| SNP | single point nucleotide polymorphism |
| TACE | tumor necrosis factor alpha converting enzyme |
| TAD | transactivation domain |
| TCDD | 2,3,7,8-tetrachlorodibenzo-p-dioxin |
| TEMED | Tetramethylethylenediamine |
| TGF α | transforming growth factor alpha |
| TKD | tyrosine kinase domain |
| TM | transmembrane |
| TNBC | triple-negative breast cancer |
| TNF α | tumor necrosis factor alpha |
| TRIS | tris(hydroxymethyl)aminomethane |
| TTCA | transcript time course analysis |
| UV | ultraviolet radiation |
| WT | wild type |
| XAP-2 | Hepatitis B Virus X-associated protein 2 |
| XRE | xenobiotic responsive element |

Table 1: List of abbreviations

0 Contents

| | | |
|----------|---|-----------|
| 1 | Introduction | 4 |
| 1.1 | The human skin | 5 |
| 1.1.1 | General Biology | 5 |
| 1.1.2 | Epidermal architecture | 5 |
| 1.2 | Carcinogenesis | 6 |
| 1.3 | Nonmelanoma skin cancer | 7 |
| 1.3.1 | Epidemiology | 7 |
| 1.3.2 | Etiology and risk factors | 7 |
| 1.3.3 | Carcinogenesis of cutaneous squamous-cell carcinoma | 8 |
| 1.4 | The Aryl Hydrocarbon Receptor | 8 |
| 1.4.1 | Introduction | 8 |
| 1.4.2 | Structure | 9 |
| 1.4.3 | Ligands | 10 |
| 1.4.4 | Pathway | 11 |
| 1.4.5 | Function and role in the skin | 12 |
| 1.5 | Epidermal Growth Factor Receptor | 13 |
| 1.5.1 | Introduction | 13 |
| 1.5.2 | Structure | 14 |
| 1.5.3 | Ligands | 15 |
| 1.5.4 | Pathway | 17 |
| 1.5.5 | Function and role in the skin | 18 |
| 1.6 | Aldo-keto reductase 1C subfamily | 20 |
| 1.6.1 | Introduction | 20 |
| 1.6.2 | Structure | 21 |
| 1.6.3 | Metabolism | 22 |
| 1.6.4 | Function and role in the skin | 23 |
| 1.7 | Aim of the research | 25 |
| 2 | Materials and Methods | 26 |
| 2.1 | Chemicals and Reagents | 26 |
| 2.1.1 | Chemicals | 26 |

| | | |
|----------|--|-----------|
| 2.1.2 | Stimulants | 27 |
| 2.1.3 | Kits | 28 |
| 2.1.4 | Devices | 28 |
| 2.1.5 | Software | 28 |
| 2.1.6 | Antibodies | 29 |
| 2.1.6.1 | Primary antibodies | 29 |
| 2.1.6.2 | Secondary antibodies | 29 |
| 2.2 | Cell Culture | 30 |
| 2.2.1 | Cultivation of cells | 30 |
| 2.2.2 | Counting of cells and Seeding | 31 |
| 2.2.3 | Stimulation of Cells | 31 |
| 2.3 | Protein Biochemistry | 34 |
| 2.3.1 | Cell lysate preparation | 34 |
| 2.3.2 | Protein concentration determination with BCA assay | 35 |
| 2.3.3 | Sodium-Dodecyl-Sulfate Polyacrylamide Gel-Electro- phoresis (SDS-Page) | 36 |
| 2.3.4 | Western Blot | 37 |
| 2.3.5 | Antibody treatment and detection | 38 |
| 2.3.6 | Western blot quantification | 39 |
| 2.4 | mRNA Analysis | 40 |
| 2.4.1 | RNA isolation | 40 |
| 2.4.2 | cDNA Synthesis | 40 |
| 2.4.3 | Quantitative PCR | 41 |
| 3 | Results | 44 |
| 3.1 | AKR gene transcription | 44 |
| 3.1.1 | Analysis of the AHR knockdown | 44 |
| 3.1.2 | Role of the AHR | 45 |
| 3.1.3 | Role of the EGFR | 47 |
| 3.1.4 | Ligands of the EGFR regulate the expression of AKR1C genes in a dose dependent manner | 48 |
| 3.1.5 | Influence of the inhibition of the EGFR | 49 |
| 3.1.6 | Influence of the inhibition of MMPs and tyrosine kinases | 50 |
| 3.2 | AKR1C3 protein level | 52 |
| 3.2.1 | Role of the AHR | 52 |
| 4 | Discussion | 55 |
| 4.1 | Active AHR signaling influences AKR1C subfamily gene expression | 55 |
| 4.2 | The EGFR affects the AKR1C subfamily on the RNA level | 57 |
| 4.3 | The postulated pathway could not be shown on the protein level | 59 |

| | | |
|----------|---------------------------|-----------|
| 4.4 | Conclusion | 59 |
| 5 | Bibliography | 61 |
| 6 | Appendix | 86 |
| 6.1 | List of Figures | 86 |
| 6.2 | List of Tables | 87 |
| 6.3 | Amino Acid Code | 88 |

1 Introduction

Worldwide, cancer is the leading cause of death [2]. As the world's population is increasingly ageing due to improved socioeconomic developments, the threat of cancer incidences and mortality have led to the necessity of understanding carcinogenesis fundamentally. Nonmelanoma skin cancer (NMSC) presents an entity highly dependent on age, socioeconomic behavior and exposure to environmental factors such as UV radiation and chemical pollutants [3, 4]. In cutaneous squamous cell carcinoma (cSCC), the drug pioglitazone inhibits further proliferation by agonizing the proapoptotic receptor $\text{PPAR}\gamma$ [5]. The receptor requires activation by 15d-PGJ_2 , a hormone spontaneously converted out of PGD_2 [5]. Normally, PGD_2 is metabolized by AKR1C3, a member of an enzyme family involved in the metabolism of steroid hormones [6]. The enzyme was found to be overexpressed in cSCC, leading to a decreased amount of 15d-PGJ_2 [5, 7]. In other malignancies such as triple-negative breast cancer (TNBC), the expression of AKR1C3 depends on the AHR [8]. Another receptor responsible for carcinogenesis in various tissues and overexpressed in cSCC is the EGFR [9, 10]. In 2011, Lemjabbar-Alaoui et al. discovered that the subsequent development of reactive oxygen species (ROS) in lungs exposed to tobacco smoke triggered the phosphorylation of src kinase, that in turn phosphorylated PKC, which ultimately activated tumor necrosis factor alpha converting enzyme (TACE) [11]. TACE is an important member of MMPs that enable ligand binding and therefore activation of the EGFR [12, 13], while tobacco smoke triggers the activation of the AHR and src is a member of its chaperoning protein complex [14, 15]. Summarizing, there could be possible crosstalk between the AHR, the EGFR and AKR1C3 in cSCC. Hereafter, the human skin, carcinogenesis, the AHR, the EGFR and the AKR1C subfamily will be presented to gain further understanding for the topic of research.

1.1 The human skin

1.1.1 General Biology

The skin protects underlying tissues against UV radiation, environmental pollutants, water loss and possible pathogens as well as regulating body temperature, insulation and sensation. The different requirements are fulfilled by forming a multilayered organization known as the cutis and subcutis, the former divided in epidermis and dermis, the latter functioning as the insulating adipose tissue that parts the skin from muscle fasciae. As the outermost layer, the epidermis covers the underlying mesenchymal dermis, the two being connected by an intermediate basement membrane. Among others, the main cell type of the epidermis is the keratinocyte, which is followed by melanocytes, dendritic cells and inflammatory cells. Epithelial stem cells located in the basal layer of the hair follicle bulge provide its lifelong renewal, which guarantees constant protection but also leads to the general possibility of carcinogenesis [16].

1.1.2 Epidermal architecture

As the supreme layer, the epidermis is constantly exposed to the environment and is therefore composed of a multilayered keratinized squamous epithelium that provides mechanical and antimicrobial protection. Keratinization is constantly implemented by the main cell type of the epidermis, the keratinocyte, ensuring a complete renewal every four weeks [17]. Its differentiation process can be followed within the five sublayers of the epidermis: The stratum basale, stratum spinosum, stratum granulosum, stratum lucidum and stratum corneum. They are characterized by the occurrence of different types of keratin molecules, with keratin K5 and K14 being the proliferation-associated molecules in the basal layers and keratin K1 and K10 in the upper layers [17]. The differentiation is mainly driven by the epidermal growth factor (EGF), keratinocyte growth factor (KGF) and retinoic acid and is increased during wound healing [18]. Every 10th cell in the stratum basale is a melanocyte, ensuring DNA damage protection against UV radiation by concentrating melanin around the nucleus of every keratinocyte [17]. Immunological protection of the epidermis is provided by lymphocytes and the antigen-presenting *Langerhans* cells in the Stratum spinosum [17]. The least common cell type of the epidermis are *Merkel* cells, which function as mechano- and pressure-receptors [17].

1.2 Carcinogenesis

Cancer is characterized by cells showing uncontrolled proliferation even in absence of growth factors by profiting from an unlimited amount of cell divisions. Malignant growth is invasive, without restraint and not affected by contact inhibition. During their progression, they secrete angioproliferative factors that provide nutrition via angiogenesis and de-differentiate from their cellular origin. In the end, they are immune to apoptotic signaling, break loose and form secondary tumors by migrating through blood or lymphatic vessels. This process, the conversion of a normal functioning cell into a tumor cell, is called malignant transformation and begins either with somatic mutations or the infection with a tumor-promoting virus [19]. In the skin, besides UV-radiation that causes direct DNA-damage [20], also chemicals originated from environmental pollution and the individual workplace or lifestyle of a person lead to carcinogenesis [21]. These compounds are mostly polycyclic aromatic hydrocarbons (PAH) [20]. Their carcinogenic potential is fulfilled by following three different pathways: the radical cation pathway dependent on P-450 peroxidases, the diol epoxide pathway dependent on CYP1A1 and -1B1 and the o-Quinone pathway dependent on AKRs [22]. Regarding the diol epoxide pathway, the needed presence of CYP1A1 is regulated by the activity of the AHR, a receptor present in nearly every cutaneous subpopulation [15, 23]. The CYP enzyme family is mainly responsible for phase-I biotransformation, where compounds are modified to be soluble in water [20]. When oxidized by CYP1A1, a conjugation to hydrophilic moieties can be executed by phase-II metabolizing enzymes [20]. This process is eventually exhausted when exposed to PAHs permanently [20, 24]. Then, DNA-damaging ROS develop and CYP1A1 is continuously active due to the permanently activated AHR [20, 24]. Therefore, compounds undergo phase-I biotransformation without being further metabolized, which then may lead to DNA damage [20]. Within the o-Quinone pathway, CYP1A1-built chemicals are further metabolized by the AKR enzyme family [22]. Being formal phase-I metabolic enzymes, their main function is to catalyze the reduction of carbonyl to hydroxyl groups as well as the associated reverse oxidation [22, 25]. Enhanced transcription of AKRs is caused by oxidative stress due to chemical exposure or UV radiation [26]. In order to form o-quinones, AKR family members such as AKR1A1 and AKR1C1-1C4 oxidize PAH-trans-dihydrodiols previously build by CYP1A1 or -1B1 to ketols that spontaneously form catechols [22, 27]. Being unstable, those catechols quickly autoxidize into PAH o-quinones like BaP-7,8-dione [22]. Since o-quinones are electrophilic, they especially react with endogenous nucleophiles and DNA directly to cause stable adducts [22]. Furthermore, they disturb ROS-eliminating processes by conjugating with glutathione [22]. In turn, o-quinones can be reduced back to catechols enzymatically

or non-enzymatically with NADPH, causing a redox-cycle in which more and more ROS are built [22]. Regarding those mechanisms, analysis of the AHR and AKR subfamilies in the skin may contribute to a greater understanding of the formation of cSCC.

1.3 Nonmelanoma skin cancer

1.3.1 Epidemiology

With 1,198,073 new cases diagnosed in 2020, the incidence of nonmelanoma skin cancer (NMSC) has continuously increased over the past fifty years with a growth of 3% every year [2, 28]. The incidence is highest in countries with a high exposure of UV radiation such as Australia and New Zealand, with 166.2 cases per 100,000 in males and 111.0 cases per 100,000 in females [2]. The second highest rate is seen in North America with 90.4 cases per 100,000 in males and 43.3 cases per 100,000 in females. Europe follows with 37.5 cases (Western Europe), 30.2 cases (Northern Europe) and 8.5 cases (Eastern Europe) per 100,000 in males [2]. With 23.8 cases per 100,000 in males and 10.2 cases per 100,000 in females, Southern Africa is another region with a high incidence [2]. Predilection sites are the naked skin such as face, neck, lips, forearms and lower legs. Previously damaged tissues such as scars, chronic ulcers, or skin suffering from *Lupus vulgaris*, chronic lymphedema or Lichen planus also have a higher risk of developing skin cancer [29]. Although the cases of death, 63,731 in total in 2020, present one of the lowest of all cancer entities, its rising incidence, risk of metastasizing and decrease in quality of life for patients indicate that a deeper understanding of the underlying mechanisms is needed and essential for its prevention and treatment.

1.3.2 Etiology and risk factors

NMSC are tumors of malignant degenerated keratinocyte stem cells of the epidermis [30], divided into the more frequent basal cell carcinoma (BCC) with 75% of all NMSC cases and the cSCC for the remaining cases [3]. In both, the most frequent tumor initiator is UV radiation, divided into UVA with a wavelength of 320-400 nm and UVB with a wavelength of 290-320 nm [3]. While UVA, which comprises 95% of the UV radiation that reaches the biosphere, penetrates deeper into the skin and activates protein C kinases while decreasing tumor suppressor T-cell activity, UVB, the remaining 5%, damages DNA directly causing mutations such as cyclobutane pyrimidine dimers (CPDs) especially in the cell cycle controlling tumor suppressor gene p53 [31–33]. Other risk factors are smoking, ionizing radiation, immunosup-

pression, chronic inflammation, exposure to polycyclic hydrocarbons, photosensitizing drugs such as non-selective COX inhibitors, arsenic ingestion and phototherapy with psoralens [3, 4].

1.3.3 Carcinogenesis of cutaneous squamous-cell carcinoma

Exposure to tumor initiators and presence of tumor promoters such as UV radiation or chemical carcinogens may lead to precancerous lesions as, for example, actinic keratoses (AKs), developed by malignant transformed keratinocytes [30]. On the cellular level, repeated DNA damage causes enlarged, irregular and hyperchromatic nuclei [30]. Clinically, the AK is detected as lesions of coarse, skin-colored or red-brownish cornifications [29]. An increased number of degenerated keratinocytes is used to build a three-tiered grading scale defining the stage of carcinogenesis: When the lower third of basal keratinocytes are histologically atypic, the term keratinocytic intraepidermal neoplasia I (KIN I) is used, KIN II is used when two thirds are affected and KIN III when the whole epidermis shows atypical keratinocytes, defining a *carcinoma in situ* [30]. The progress from a single AK to cSCC is between 0.0025 % to 16 % per year, adjusted to the fact that many patients show at least 6 to 8 lesions 0.15 % to 80 % per year [30]. 58 % mutations in the p53 tumor suppressor gene constitute the majority of mutations induced by UVB radiation in NMSC and seem to be the most frequent initial mutations that drive the transition from AKs to cSCC [30]. Enhanced activation of the EGFR, Src-family tyrosine kinases (SFKs), both down regulating p53, and Myc were found in both cSCC and BCC [34–36].

1.4 The Aryl Hydrocarbon Receptor

1.4.1 Introduction

One mechanism defending the organism against harmful environmental compounds is the expression of half-life decreasing enzymes. The underlying physiological process is described as biotransformation, a system in which exogenously and endogenously occurring molecules are metabolized with the objective of elimination and excretion. Furthermore, several chemicals unfold their chemical potential only when metabolized during this process. It is divided into two phases guaranteeing a sequence of primary modifications by oxidation, reduction or hydrolysis and following secondary conjugations, ultimately allowing elimination. The main drivers of phase I biotransformation are cytochrome P450-dependent monooxygenases such as CYP1A1. Its expression is mainly under the control of the transcriptional fac-

tor aryl hydrocarbon receptor [37, 38]. The AHR was first discovered as a hitherto unknown binding species that enhanced CYP1A1 expression after exposure to 2,3,7,8-tetrachlorodibenzo-p-dioxin (TCDD) [39, 40]. Although it was previously known that polycyclic hydrocarbons like B(a)P were hydroxylated enzymatically by the aryl hydroxylase, the activating mechanism of this reaction was a subject of research [41]. The newly found receptor closed the search for a link between treatment with xenobiotics, enhanced aryl hydroxylase activity and intensified transcription of CYP1A1 [39, 40, 42].

1.4.2 Structure

The 96kDa AHR protein is composed of 848 amino acids [43, 44] and expressed by a gene located on chromosome 7p21 [45]. It is a ligand-activated transcriptional factor that shares its structure with the superfamily of basic helix-loop-helix PER-ARNT-SIM proteins (bHLH-PAS) [38, 43]. The bHLH domain is found at its N-terminal region. It includes two amphipathic α -helices built by conserved amino acids and attached via an unconserved loop [46]. The domain mediates both DNA binding and protein dimerization [47]. Adjacent, there is a region of basic amino acids [46] and the nuclear localization signal (NLS) [48]. The PAS domain is located in C-terminal direction to the bHLH domain. It is a motif built by the *Drosophila melanogaster* protein period (PER), the human AHR nuclear translocator (ARNT) and the *Drosophila melanogaster* protein single-minded (SIM) [46]. Originally, these proteins were independently reported. PER is a product of the *per* gene and involved in the modulation of the circadian rhythm [49, 50]. As PER, the SIM protein derives from DNA of *Drosophila melanogaster*, but regulates midline cell lineage [51]. ARNT was first revealed as an essential dimerization partner of the AHR before the discovery that it is also part of the PAS domain [52]. Furthermore, two sequences of degenerated repeats were discovered within the PAS domain and called PAS-A- and B-subdomain [51–53]. The B-subdomain partially overlaps with the binding region that is required for building the inactive cytosolic complex of the AHR [54]. It has therefore been proposed that this unique domain is required for both homotypic interactions with other PAS proteins [46], heterotypic interactions with chaperones [46] and binding of AHR ligands [55]. Additionally, the PAS domain also includes a nuclear export signal (NES) [48]. Finally, the C-terminus of the AHR contains a transactivation domain (TAD) where co-activators bind and complete target gene activation [56].

In its inactive state, different chaperones conserve the AHR, generating both protection from degradation and uncontrolled nuclear translocation as well as keeping it in a ligand-affinely conformation [55, 57]. Initially, two heat-shock protein 90

(HSP90) proteins were revealed while investigating the AHR inactively residing in the cytosol [58]. The first masks the ligand binding site within the PAS domain [59], whereas the second rests covering both the NLS in the bHLH domain and another part of the PAS domain [60]. Directly interacting with HSP90 and the AHR is the second chaperoning member, the AHR interacting protein (AIP) [61], later identified as the Hepatitis B Virus X-associated protein 2 (XAP2) [62, 63]. It protects the AHR from uncontrolled nuclear shuttling by inhibiting importin β [64], prevents ubiquitylation and proteasomal degradation [65], and seems to work as an enhancer on AHR activation [62, 63]. Degradation of the AHR is also prevented by the third member, p23 [66]. New insight revealed that p23, in contrast to earlier studies, binds to the AHR HSP90 independently and might also protect the AHR from autophagy [67]. Additionally, the chaperoned and inactive AHR is associated with the protein kinase c-src [14]. It has been revealed that it is the activation of c-src after ligand binding to the AHR that mediates especially its non-canonical pathways such as expression of cyclooxygenase 2 (COX2) [68], phosphorylation of the EGFR [69] and activation of the extracellular signal-regulated kinase 1 and 2 (Erk1/2), suppressing the expression of PPAR γ [70].

1.4.3 Ligands

The AHR provides a binding pocket for mainly planar molecules with an approximated dimension of 14 x 12 x 5 Å [71]. With the first discovered ligands being TCDD, polycyclic aromatic hydrocarbons (PAHs) and halogenated aromatic hydrocarbons (HAHs) derived from tobacco smoke, coal tar and traffic-derived particles [15, 72], it was long thought only exogenous compounds could activate the AHR. However, endogenously occurring receptors had to be developed during evolution predominantly in order to perform normal cellular functions and had to be activated by ligands of physiological origin. [38]. The first activator ever found that was not a xenobiotic was UV radiation [73]. It was revealed that particular photoproducts of the amino acid tryptophan induced by UV radiation activate the AHR with high affinity [74]. The most potent member in this class of ligands is 6-formylindolo[3,2-b]carbazole (FICZ) [75]. Further investigation classified flavonoids like diosmetin [76], polyphenols like curcumin [77], alkaloids like rutaecarpine [55] and other indole derivatives like FICZ [75] as AHR agonists. Thus, compounds especially derived from cruciferous vegetables seem to be the main source of endogenous ligands [57, 78]. Regarding xenobiotics, other synthetic agonists than dioxins, PAHs and HAHs were identified, for example the proton pump inhibitor omeprazole [79], the nonsteroidal anti-inflammatory drug (NSAID) diclofenac [80] or chemicals like thiabendazole and carbaryl, both used in pesticides [81]. In summary, agonists of anthropogenic and

natural origin both appear to activate the AHR, their number continuously growing to date. The only AHR-specific agonists used to test the hypothesis of this work were the PAH benzo[a]pyrene (BaP) and the HAH polychlorinated biphenyl (PCB126).

1.4.4 Pathway

Generally, the term "canonical pathway" is used in reference to established signaling cascades with common features. Alternative and less known pathways are labeled non-canonical. In the case of the AHR, activation of a pathway requires the binding of an agonist. Without it, the AHR resides in the cytosol in an inactive state [55]. Its activation leads to conformational change, separation from its chaperones and uncovering of the NLS in its N-terminal domain [82]. Binding of importin- β to the NLS allows translocation into the nucleus [83]. There, the AHR dimerizes with ARNT [52] via interaction of the bHLH and the PAS domains of both proteins [84]. Their conjunction is the crucial step to accomplish the following induction of gene expression since only the heterodimer of both proteins binds to the specific DNA (short for: deoxyribonucleic acid) sequence of interest, which is labeled xenobiotic responsive element (XRE) [84], a motif of a 5'-TNGCGTG-3' core surrounded by variable nucleotides [85]. Then, several co-activators, reviewed by Hankinson et al. [86], are recruited to facilitate the launch of the transcriptional machinery by loosening the chromatin structure of the DNA and relaxing the nucleosomes [55]. Finally, the ribonucleic acid (RNA) polymerase II starts DNA transcription, with the expression of CYP1A1 being the best investigated terminus addressed in the canonic pathway of the AHR [42, 82]. Other motifs controlled by the AHR are named non-consensus (NC): The 5'-GGGA-3'-tetranucleotide motif which for example codes for plasminogen-activator-inhibitor-1 [87], estrogen responsive DNA elements [88, 89] or genes also recognized by krüppel-like factor 6 (KLF6) [90]. Furthermore, several crosstalks with other cellular components like nuclear factor kappa-light-chain-enhancer of activated B-cells (Nf κ B) [91] or hypoxia-inducible factor-1 (HIF1) [92] were identified. These non-canonical pathways possibly add tissue-, cell- and microenvironment-specific functions to the AHR metabolism [20]. Rapidly after fulfilling induction of gene transcription, the AHR is exported, ubiquitinated and degraded by the 26S proteasome [93]. This process is initiated by phosphorylation of the amino acid serine 68 in the NES of the AHR [94]. For ubiquitination, the E3 ubiquitin ligase is recruited by the AHR degradation promoting factor (ADPF) [95], the latter interacting with the AHR via its C-terminal TAD [96]. Dampening AHR function is also executed by a negative feedback mechanism since binding to XRE also leads to the expression of an AHR repressor (AHR_R),

competing with the AHR on binding to ARNT [97].

1.4.5 Function and role in the skin

The AHR is a transcriptional factor first known as regulator of the dioxin response in the organism [39]. After decades of research, its presence has been demonstrated in a large variety of organs and tissues [38, 82]. This work will focus on its role in the skin, in particular in carcinogenesis of nonmelanoma skin cancer.

Investigations revealed the existence of the AHR in nearly every cutaneous sub-population [15]. Activation in cells of the skin is executed as previously described: Binding of exogenous, topic or systemically uptaken dioxins, PAHs and HAHs [98, 99] and endogenous tryptophan metabolites [100]. The latter can be induced by exposure to UV radiation or produced by skin inhabiting bacteria [101]. In the case of *Staphylococcus epidermidis*, bacteria can also activate the AHR directly [102]. Additionally, newly found agonists originate from skin-residing yeast [103]. After activation, the AHR physiologically contributes to the transcription of genes needed for epidermal [104–106] and sebocyte differentiation [107], lipid synthesis [108], melanogenesis [109] and epidermal barrier function [20, 110, 111]. However, the AHR is involved in a large spectrum of different skin diseases. The first reported hint was given when TCDD was linked to the development of chloracne [112]. Evidence of AHR-dependency in dioxin toxicity was later proven while analyzing AHR-deficient mice [113]. It is known that the AHR affects various other skin diseases such as atopic dermatitis, psoriasis, vitiligo and some types of skin cancer [20]. Due to this observation, it was found that the receptor seems to play a janus-faced role in skin metabolism, since either activation or inhibition of the receptor was of use in prevention and treatment of several skin disorders [114]. These findings suggested that executed pathways of the AHR might vary between healthy and inflamed skin [111]. Regarding initiators of skin carcinogenesis, one of the most potent drivers is UV radiation [30]. In general, it induces the generation of DNA photoproducts in the nucleus and activation of cell surface receptors [100, 115]. As a result, it increases the expression of CYP1A1 [23]. Another enzyme family that is upregulated by exposure to UV radiation c-src-dependently are COX, COX-2 in particular [68, 69]. It is responsible for generation of pro-inflammatory and anti-apoptotic functioning metabolites of arachidonic acid that are strongly linked with tumor development [116]. Additionally, UV exposed skin shows an upregulation of MMPs, an enzyme family known to contribute to tumor development [117]. The expression of all named actors is under control of the AHR [118, 119], pointing out the strong connection between UV radiation, AHR signaling and skin carcinogenesis. Additionally, the researchers associated with Dr. Haarmann-Stemmann showed that the AHR inhibits

nucleotide excision repair (NER), a mechanism needed for the removal of UV induced cyclobutane pyrimidine dimers (CPD) [120, 121]. The results strengthen the evidence of involvement of the AHR in photocarcinogenesis since inhibition of the AHR leads to p27-mediated increased NER [121]. Furthermore, the elevated risk of developing squamous cell carcinoma in smokers [122] is linked with AHR activating PAHs found in tobacco smoke [123]. In summary, AHR signaling was revealed as significantly involved in tumor cell migration and invasion in SCC [124]. Genome wide studies also showed significance regarding genomic translation [125]. Nevertheless, designating prevention and treatment recommendations regarding UV-dependent AHR signaling requires further investigation.

1.5 Epidermal Growth Factor Receptor

1.5.1 Introduction

Regarding carcinogenesis, constitutive activation of the EGFR was identified to be crucial for the carcinogenesis in various tissues and organs such as lung, colon or breast [10]. Furthermore, over 90% of primary head-and-neck SCC (HNSCC) show an overexpression of this receptor family [9, 126]. Activation depends on ligand binding that can only happen after shedding their connection to the membrane surface through MMPs like TACE. Lemjabbar-Alaoui et al. discovered that in lungs exposed to tobacco smoke, TACE was phosphorylated by PKC, which in turn was activated by src [11]. With src being a member of the chaperoning complex that surrounds the AHR in its inactive state and involved in the phosphorylation of the EGFR [69], the receptor was added as a subject of research to this work in order to test whether the AHR and AKRs would be connected through the EGFR in keratinocytes or if it would be more likely that the AHR affects AKR activity EGFR-independently. The cellular events of differentiation, proliferation, apoptosis and survival are key points in every higher organism and strictly controlled by multiple mechanisms. One of the most important mediators of these crucial processes is the evolutionary ancient epidermal growth factor receptor (EGFR) [127]. Carpenter et al. discovered in 1978 that EGF, already known as a promoter of cell differentiation [128–130], not only leads to increased cell growth but also enhances phosphorylation of cytosolic proteins [131]. Later, it was revealed that the link between EGF binding and phosphorylation of endogenous compounds was executed by the same protein, designated EGF receptor [132]. Possession of an extracellular binding site attached to an intracellular kinase that to that date was a new class of receptors, with the EGFR as its first member [133]. Its initiation of cell signaling cascades requires two members that, after ligand binding, dimerize and transphosphorylate each other's

intracellular tyrosine residues [134, 135]. Regarding its ubiquitous appearance in higher organisms, the EGFR and its three other family members that were discovered later are referred to as HER (short for: human EGF receptor) when it is needed to emphasize facts applying exclusively to the human form. Due to the discovery that the avian erythroblastosis virus (AEV) encodes a protein that is structurally homologous to the EGFR, the avian erythroblastosis oncogene B (ErbB), the term ErbB1-4 was established as another synonym [136]. This term will mainly be used in the next sections of this work. The second member of EGFR-like receptor tyrosine kinases (RTK), ErbB2 was designated HER2/*neu*, being the human counterpart of the rodent oncogene *neu* that is responsible for the formation of neuroblastomas in rats [137, 138]. The third and fourth member complete the class of ErbB receptors [139, 140]. In humans, they are found in cells of mesodermal and ectodermal origin where they are responsible for normal cellular differentiation processes but, when dysregulated, also for carcinogenesis [127].

1.5.2 Structure

Although the EGFR family members are structurally and functionally related, the locations of their encoding genes differ. The ErbB1 gene is found on chromosome 7p12 [141], ErbB2 on chromosome 17q12 [142], ErbB3 on chromosome 12q13 and ErbB4 on chromosome 2q34 [143]. They share a common structure composed of a 620 amino-acid extracellular domain that is required for ligand binding, a 23 amino-acid transmembrane domain and a 540 amino acid intracellular domain ending in a carboxy terminal tail [127, 144].

The extracellular domain is built by four subdomains of two different types, termed I, II, III and IV or L1, CR1/S1, L2 and CR2/S2 from the most amino-terminal residue in carboxy-terminal direction [145, 146]. The first and third subdomains are two large (L) members of the leucine rich repeat (LRR) family [144]. They are composed of a six turn right handed β -helix ending in a disulfide bond and an α -helix [144, 147]. The second and fourth subdomains contain multiple cysteine-rich (CR) elements that show disulfide-bonded motifs similar to tumor necrosis factor α receptor [148, 149]. Abe et al. specified that subdomain II contains eight and subdomain IV seven of these motifs [150]. Linkage between the subdomains is established between the most amino-terminal C2 motif of the first CR element and the attached L subdomain [144]. In contrast to the structural resemblance, the subdomains II and IV differ greatly in their function. An additional loop inserted in the subdomain II acts as a "dimerization arm" [151]. In the inactive monomer, dimerization is autoinhibited by molecular interactions between the subdomains II and IV, whereas after ligand binding, a conformational change allows dimerization by interaction between

the subdomain II and its corresponding domain in another ErbB molecule [148]. The extracellular domain is followed by a single transmembrane (TM) domain that links the receptor's extra- with its intracellular region [152]. Analysis of the lipid membrane of *Escherichia coli* (*E. coli*) revealed that the TM domain associates itself with the cell membrane through at least two GxxxG motifs that also take part in the linkage between two ErbB dimerization partners [153–155].

The intracellular domain is built by a tyrosine kinase domain (TKD) and a carboxy terminal tail that contains at least five tyrosine residues that work as autophosphorylation sites [152, 156]. When phosphorylated, they provide docking sites for the adaptors that initiate the different cell signaling cascades of ErbB receptors, src homology 2 (SH2) and phosphotyrosine binding domain (PTB) [157]. Interestingly, the protein kinase c-src is able to phosphorylate the EGFR at the residue Tyr-845 even in absence of an EGFR ligand [158]. Furthermore, the tail executes a twofold regulatory function by modulating both autoinhibition and active signaling [152]. The structural properties of ErbB receptors are completed by extra- and intracellular bound juxtamembrane (JM) regions that are greatly described elsewhere [152]. The description above appears to be typical for the EGFR/ErbB1. In contrast, significant differences appear among the other members of the ErbB receptor family that are of functional importance. Although ErbB2 has a ligand binding domain, no ligand has been found to date that binds with high affinity to it [127]. A hypothesis proposed that the ErbB2 could be evolved as a shared subunit for the other members [159]. Indeed, ErbB2 is the preferred dimerization partner for every other ErbB receptor family member [160]. In contrast to ErbB2, ErbB3 is capable of ligand binding, but devoid of its kinase activity [161] due to replacement of important amino acid residues in its intracellular domain [162]. New research has revealed that ErbB3 is indeed capable of binding adenosine triphosphate (ATP) and initializing autophosphorylation [162]. However, its kinase activity is about 1000-fold weaker than in measurements analyzing the EGFR/ErbB1 [162]. Finally, ErbB4 has both a potent ligand binding domain and kinase domain like the EGFR/ErbB1, but appears in two splice variants that differ in their eJM domain. A third variant that is unable to bind phosphatidylinositol-3-kinase (PI3K) due to lack of 16 amino acids in the carboxy terminal tail was designated as ErbB4 CYT-2, the originally discovered form being ErbB4 CYT-1 [163].

1.5.3 Ligands

Signaling processes that drive growth in the organism have been investigated since the 1930's and eventually led to the identification of a nerve growth factor when nerve cells stopped their expansion after removal of the limb bud [10]. It did

not take much time to reveal other members of growth regulating factors like EGF [128]. To date, seven ligands are known to bind and activate the different ErbB receptors with high affinity: EGF, transforming growth factor alpha ($TGF\alpha$), betacellulin (BTC), heparin-binding EGF-like growth factor (HB-EGF), amphiregulin (AREG), epiregulin (EREG/EPR) and epigen (EGN) [152]. They are transmembrane polypeptides with a common structure of an EGF-like domain as the amino-terminal extension linked to a JM stalk, a TM domain and a carboxy terminal cytoplasmic tail [164]. The extension regularly includes heparin-binding sites, glycosylated linkers and immunoglobulin-like domains [127], a motif of 150 amino acids that build seven to nine antiparallel β -strands [165]. Responsible for binding with ErbB receptors, the EGF module plays a central role within the general structure [164]. It is a sequence of 40 amino acids wherein six cysteine residues build three intramolecular disulfide bonds, generating a mainly β -sheet structure with three loops [127, 164]. Only one amino acid divides the second from the third loop, a feature that is believed to provide a hinge, adding flexibility to the overall structure [164]. Although being the functional relevant motif, possession of an EGF module alone does not define a high-affinity ligand for ErbB receptors. However, an onset of three additional features does: First, presence of a splice site between the fourth and fifth cysteine residues within the EGF module coded by two exons [166], second, location of the functional EGF module responsible for ligand binding within 25 residues of the TM domain [164, 167] and third, spacing of the cysteines in the sequence $CX_7CX_{4-5}CX_{10}CX_8C$ [164, 167]. Correct trafficking after their translation and delivery to the cell membrane is provided by the cytoplasmic tail, first observed regarding $TGF\alpha$ and AREG shuttling [168, 169]. Furthermore, the cytoplasmic tail, set free after shedding, enables retrograde derepression of the genes coding for its former ligand [170]. Every further deviation from the described structure distinguishes the seven high-affinity ligands from others such as the family of neuregulins (NRG) [164]. These are encoded by four genes, *NRG1-4*, and share the typical EGF domain that allows them to bind to ErbB receptors [152]. The resulting polypeptides were not used in this research and are extensively reviewed elsewhere [171]. Each ErbB receptor ligand shows tissue specificity and binding preferences. EGF, AREG, $TGF\alpha$ and EPN primarily bind to the EGFR/ErbB1 [172, 173], BTC, HB-EGF and EREG both ErbB1 and ErbB4 [172]. NRG1 and NRG2 activate both ErbB3 and ErbB4 [174–176], whereas NRG3 and NRG4 bind only to ErbB4 [172, 177, 178]. The receptors ErbB3 and ErbB4, revealed as binding partners for both neuregulins and the primary ligands, were therefore designated as "bispecific" [179]. As mentioned before, no ligand has been found to bind to ErbB2 yet [10].

1.5.4 Pathway

In their inactive condition, ErbB receptors rest as high-affinity, tethered monomers within the cell membrane. In this form, the II/S1 subdomain, responsible for dimerization, is beyond reach and autoinhibited by interactions with the subdomain IV/S2 [144, 152, 180]. Generally, eight dimeric receptor combinations are possible since neither ErbB2 nor ErbB3 form homodimers [181, 182]. Binding preferences differ largely between the receptors, but ErbB2 is the favored dimerization partner [160]. Induction of any signaling cascade of ErbB receptors begins with dimerization occurring by ligand binding [183]. As previously mentioned, the ligands are placed within the cell membrane and require shedding by proteolysis [184]. Here, release of EGF and BTC is executed by the matrix-metalloproteinase ADAM10 (short for: a disintegrin and metalloproteinase), and shedding of AREG, HB-EGF, EREG and EGN is provided by ADAM17/TACE [12, 13]. In turn, the sheddases are activated by separation from their amino-terminal pro-domain, performed by different protein kinases (PC) including src [185, 186]. The now freed ligand binds both subdomain I/L1 and III/L2 of the extracellular ErbB receptor domain, inducing a conformational change which exposes the dimerization arm of subdomain II/S1 [147, 151]. In summary, a shed ligand like EGF binds to an ErbB receptor like EGFR and builds a stable 1:1 EGF-EGFR homodimer that changes to an asymmetrical conformation. This exposes the subdomain II dimerization arm and enables bonding with the same arm of another EGF-EGFR monomer leading to an active 2:2 EGF-EGFR complex [151, 183]. Shortly after, the intracellular kinase of one receptor starts phosphorylation of the tyrosine residues of the other [187]. Here, one receptor functions primary as the activator, whereas the other presents the receiver [188]. The purpose of the phosphorylated tyrosine residues is to serve as docking sites for the next regulatory elements in the different ErbB pathways, SH2 and PTB [148, 157]. These effector proteins are essential to start further downstream signaling pathways.

In spite of the high-affinity ligands, input for ErbB receptor activation is also provided by hormones, neurotransmitters, lymphokines and mediators of the cellular stress response [189]. Furthermore, the ErbB receptors are linked to pathways under the control of G-protein coupled receptors (GPCR), which also mediate their src-dependent phosphorylation [190]. As diverse as the possible activating mechanisms are the resulting intracellular signaling cascades, depending on tissue, dimer and bound ligand. In epithelial cells alone, there are over a 1000 genes affected by active ErbB receptor signaling [191]. One of the best investigated is the mitogen-activated protein kinase (MAPK) pathway, its downstream signaling promoting cell cycle entry and regulation of proliferation, differentiation and apoptosis [192]. Aside from

the MAPK pathway, ErbB receptor downstream signaling controls many other cascades such as the lipid and protein supplying phosphatidylinositol 3-kinase (PI3K) or the JAK/STAT pathway (short for: Janus tyrosine kinase/signal transducer and activator of transcription) [193, 194]. Other pathways and crosstalks, for example with the $\text{Nf}\kappa\text{B}$ pathway are not of interest for this work and therefore disregarded here [195].

Regarding the endpoints of ErbB signaling, it needs to be highlighted that the affected genes are categorized into four groups, according to a strict time management: immediately up- or downregulated microRNA (IU-/ID-miRs), immediate early genes (IEGs), delayed early genes (DEGs) and delayed up- and downregulated genes (DUGs/DDGs) [10]. After the IU- or ID-miRs occur, it takes about 20 minutes until the expression of IEGs reaches its peak [10]. Approximately 2 hours after ligand binding, the DEGs are activated [10], and 30 minutes later, the DUGs and DDGs [10], which reach their maximum 4-8 hours after ErbB receptor activation [196]. In contrast to the other categories in which the expression decreases after reaching a maximum, the genes of the "delayed" type persist in a steady state and maintain long-term phenotypic changes [10]. Generally, the output depends on ligand, formed dimer and tissue [127].

The termination of ErbB receptor activity is mainly provided by endocytosis [127]. Shortly after ligand binding, clathrin-coated regions in the cell membrane form vesicles that mature to endosomes capable of receptor degradation or recycling [127, 197, 198]. The outcome is determined by the composition of the dimer and continued phosphorylation of the residue Tyr-1068 in the endosome.

1.5.5 Function and role in the skin

The ErbB receptor family controls cell division, migration, adhesion, apoptosis and differentiation in multiple tissues of the organism [127]. Generally, ErbB1 primarily promotes the progress of epithelial proliferation and differentiation in the skin, lung, pancreas and the gastrointestinal tract [127]. The other members were found to especially mediate cardiac development and function [199]. Together, they are crucial for the correct development of the central nervous system (CNS), although ErbB2-4 seem to be more important in this process [200]. The search for the precise biological function of a receptor often includes the creation of knockout mice. Many experiments share that EGFR knockout leads inevitably to death of the organism, although the specific moment of death ranges from embryonic lethality to death at birth to postnatal death after a period of living [201]. Nevertheless, these results emphasize the crucial need for ErbB receptor signaling beginning at the implantation of an embryo [201].

Being capable of producing the ErbB ligands TGF α , AREG and HB-EGF, keratinocytes autonomously maintain their replication as well as inhibit their apoptosis and further differentiation, due to the ErbB network [202, 203]. Already known as the main sheddase of these ligands, ADAM17 is unsurprisingly found to be the primary expressed metalloproteinase in keratinocytes [204]. Additionally, treatment of superficial wounds with the ErbB1 ligand EGF showed faster healing due to accelerated epithelialization, highlighting the impact of ErbB signaling in the skin [18]. The receptors expression varies within the different layers of the epidermis, from the highest expression in the proliferating basal keratinocytes to low expression in keratinocytes of the upper layers [205]. Besides its proliferative activity, ErbB receptor signaling is also crucial to establishing and maintaining a functioning epidermal barrier and antimicrobial response while it also controls inflammation [205–208]. If the ligands are overexpressed, the ErbB network contributes to the development of a variety of skin disorders that include hyperkeratinization, as can be seen in psoriasis [209, 210]. Further deregulation of the ErbB network leads to defective wound healing, disrupted hair follicle development and carcinogenesis [210].

Overexpression of ErbB receptors in cancer was first indicated by the observation that HER2/neu is homologous to the rat oncogene *neu* [136]. Indeed, constitutive activation of ErbB signaling was identified to be crucial for carcinogenesis of various tissues and organs like lung, colon or breast [10]. Evidence of disrupted ErbB signaling in skin cancer has been shown in HNSCC cell lines as well as in primary and metastasized HNSCC [211, 212]. Over 90% of primary HNSCC show overexpression of ErbB receptors [9], which maintain continuous proliferation and prevent terminal differentiation [126]. Aside from analyzing its downstream signaling and promotion of carcinogenesis, there have been just as many attempts at understanding how the ErbB signaling is disrupted in the first place. Being responsible for nearly 90% of SCC, UV exposure as a known initiator and promotor of DNA damage has been the major target of interest. A first link was the observation that beside its direct impact on the DNA, UV produces ROS that were found to inactivate protein tyrosine phosphatases (PTPs), enzymes responsible for the dephosphorylation of RTKs like ErbB receptors [213]. Additionally, phosphorylation of ErbB receptors by exposure to UV was shown to be dependent on ligand binding due to increased metalloproteinase activity [213]. Not only do ROS inactivate PTBs, they also trigger the cleavage of the pro-domain of TACE [214]. Additionally, Lemjabbar-Alaoui et al. found that in lungs exposed to tobacco smoke, the development of ROS triggered the phosphorylation of src kinase, that then in turn phosphorylated PKC, which ultimately activated TACE [11]. Here, a possible crosstalk between the AHR and the EGFR becomes possible.

1.6 Aldo-keto reductase 1C subfamily

1.6.1 Introduction

The enzyme AKR1C3 describes another protein which expression is upregulated in SCC [5]. Mantel et al. discovered that it protects tumor cell lines from SCC from antiproliferative effects [5]. Being mainly involved in the metabolism of steroid hormones, AKR1C3's tumor promoting effects were mostly studied in malignancies originated from the breast or the prostate [5]. In 2019, Yamashita et al. discovered that in triple-negative breast cancer (TNBC), chemotherapy efficacy is regulated by AKR1C3 in an AHR-dependent manner [8]. Taken together, the enzyme was selected to be tested whether it would be dependent on the AHR in normal keratinocytes as well or not.

Ligand controlled receptor signaling is one of the major mechanisms with which the organism regulates physiological functions. It represents the communication system besides direct cell-cell interactions and electrochemical impulses. Messenger substances serving as such ligands are designated hormones, neurotransmitters or cytokines, depending on the system in which they are active. Hormones are secreted by endocrine glands or specific tissues. Important members of this system are steroid hormones. Locally produced, they trans-activate nuclear receptors like the androgen, estrogen, progesterone, mineralocorticoid or glucocorticoid receptor [215, 216]. Prior, they undergo prereceptor modifications by a system of enzymes which interconvert their inactive precursors to potent hormones [215, 216]. These enzymes belong to the family of hydroxysteroid dehydrogenases (HSDs), which can be divided into NADPH (short for: nicotinamide adenine dinucleotide phosphate)-dependent ketosteroid reductases and NAD^+ -dependent hydroxysteroid oxidases [216]. HSDs are members of two protein superfamilies, the short-chain dehydrogenases/reductases (SDRs) and the aldo-keto reductases (AKRs) [216]. AKRs combine NAD(P)(H)-dependent oxidoreductases that are encoded by 15 genes and divided into three families and seven subfamilies [25]. They are classified by using a nomenclature based on amino acid sequence similarities established by Jez et al. in 1997 [217]. Here, a root AKR is followed by a number that designates the family in which all enzymes have 40% sequence similarity. Next, a letter indicates the subfamily where 60% sequence similarities have been revealed. Finally, another number represents the unique protein sequence. Therefore, AKR1A1 describes the first AKR in family 1, subfamily A, and AKR1C3 the third protein in family 1, subfamily C [217]. The different members are widely expressed and metabolize a variety of substrates.

1.6.2 Structure

Most AKRs are monomeric proteins composed of approximately 320 amino acids with an average mass between 34 and 37 kDa [218, 219]. Apart from this generally found composition, members of the families six and seven build dimers, or even tetramers [220, 221]. Analysis of their crystal structure revealed a triosephosphate isomerase, more specifically an $(\alpha/\beta)_8$ motif, where eight α helices that proceed antiparallel surround eight parallel β strands that merge in the center and shape the "staves" of a barrel [218, 222]. At its back, three large loops, designated A-loop, B-loop and C-terminal loop, determine substrate specificity [218]. Two additional helices, H1 and H2, are located in the C-terminal region outside of the barrel [219]. The active site of the enzyme is located in its base and built by the positions Asp-50, Tyr-55, Lys-84 and His-117 [25, 219]. The highly conserved residues Thr-24, Asp-50, Ser-166, Asn-167, Gln-190, Tyr-216, Leu-219, Ser-221, Arg-270, Phe-271, Ser-272, Arg-276, Glu-279, and Asn-280 function as the cofactor binding site [218]. Here, both NADPH and NADH can bind, although NADPH is preferred due to the additional phosphoryl group [223]. Substrate binding happens within a pocket often built by 14 residues in five loops, predominately in the A-, B- and C-terminal loop [219].

As mentioned before, members of the same family or subfamily show high sequence similarities that explain the shared structure, resembling a barrel. Residues crucial for catalytic activity seem to be conserved, whereas the residues of the loops vary greatly between the enzymes [218]. Therefore, some AKRs can change their conformation, increasing the affinity to their cofactor, and others are devoid of this ability. A great example is AKR1B1, where the residues 210 to 212 and 213 to 216 of its β -strand 7 are involved in the formation of a clamping loop that locks NADPH into the binding cleft by building van der Waals and electrostatic linkages with the cofactor [224]. In contrast, AKR1C family members do not form this conformation [219]. Regarding the stereochemical outcomes, only one single point mutation in the active site of an enzyme can lead to a different product. AKR1C1 exhibits a 20 α -HSD activity and differs from AKR1C2 by seven residues, but exchange at the position 54 in its active site with the residue found at the same position in AKR1C2 forces AKR1C1 to execute the 3 α -HSD activity of AKR1C2 [225, 226]. AKR1C3, in turn, has other unique properties, but has Leu-54 in its active site like AKR1C1 [227]. Additionally, the outcome of the chemical reaction catalyzed by AKRs is determined by various possible steroid-binding poses [219]. This explains why the AKR1C1-4 have the ability to act as 3-, 17- or 20-ketosteroid reductases [219].

AKR genes are located on chromosome 10p15 to 10p14 [228]. As being part of the defense system against oxidative stress, their gene promoters contain antioxidant

response elements (AREs) through which they can be regulated by the Keap1-Nrf2 (short for: Kelch-like ECH-associated protein 1 and nuclear factor erythroid 2-related factor 2) system [229]. Unsurprisingly, upregulation occurs through the influence of ROS, electrophiles and Nrf2 activators [219]. According to RNA sequencing (RNAseq), additional splice variants have been identified, three for AKR1C2, and two for AKR1C3. Evidence of their transcription, translation, and catalytic activity is poor and it is believed that only one transcript per AKR gene encodes for the active protein [219]. Furthermore, there exist multiple single point nucleotide polymorphisms (SNPs) that are evolutionarily conserved and/or alter the executed chemical reactions [230].

1.6.3 Metabolism

AKR enzymes are primarily located in the cytosol where they regulate ligand occupancy for steroid receptors [219]. Exceptions have been demonstrated with AKR1C1-3 additionally secreted with surfactant by alveolar type II cells, AKR1B15 found in mitochondria and AKR1B10 present in lysosomes [231–233]. Highly differentiating, AKR6 family members are associated with membrane bound voltage channels, and AKR7A2 probably with the Golgi apparatus [25, 221]. Generally, they catalyze the reduction of carbonyl to hydroxyl groups, and the associated reverse oxidation [25]. Here, due to the excess of NADPH over NAD^+ in cells, the reaction favors reduction of molecules [25]. It follows a bi-bi kinetic mechanism, where the cofactor binds first and leaves last [25, 234, 235]. The exact kinetics were exceptionally reviewed by Penning et al. 2019 [219]. The following description of the catalyzation sequence was observed in AKR1C2 and AKR1C9, the latter being the prototype of the AKR1C family [219]. The initial event that allows further reactions is the binding of a NADP(H) to the enzyme, and performed in three steps [234–236]. It is mainly mediated by the highly conserved residues Arg-276 and -270, which allow quick formation of a loose complex by building salt bridges with the 2'-phosphate of the AMP proportion of a NADP(H) molecule [237, 238]. Shortly after, a conformational change enables strengthening linkages between loop β 1, α 1, and loop B, which lead to the formation of a tunnel that locks the cofactor in its place. Then, hydrogen bonds between its nicotinamide head group and the cofactor binding residues of the enzyme are established [219, 238]. Due to the structure of NADP(H), in which its ribose moiety is bound to the nicotinamide head group by a N-glycosidic bond, these binding processes occur in anti-conformation [219]. Furthermore, the head group of NADP(H) associates with Tyr-216 by π - π stacking, its carboxamide side chain with Ser-166, Asn-167, and Gln-190 [219]. Reaching this conformation enables the 4-pro R -hydride transfer [229]. Prior, a substrate associates with the

binding pocket of the enzyme. Within the catalytic tetrad, Tyr-55 now has a key role due to its ability to act as a diprotic general acid/base [239]. Its ionization is provided by a "push-pull" mechanism, where the adjacent residues His-117 and Lys-84 facilitate proton donation and removal, respectively [239]. Regarding the favored reduction direction, protonated TyrOH₂⁺ at a pH optimum of 6 is able to polarize the carbonyl group of an AKR substrate to facilitate hydride transfer [239]. In the following, stereospecific reaction, the hydride is removed from the C4 position of the nicotinamide ring of NADP(H) and added at the C3 position of the substrate [239]. The reverse reaction, oxidation of a substrate by hydride transfer from its alcohol group to a bound NAD(P)⁺, takes place in a pH optimum of 9 and is implemented by TyrO⁻ acting as a general base [239]. As previously described, this phenolate form of Tyr-55 exists due to Lys-84, which, in turn, is salt-linked to and deprotonated by Asp-50 [239]. After the successful hydride transfer, the product leaves the enzyme first and is followed by the utilized cofactor [219]. Now, the process can begin from the start. Here, AKR1C family members especially reduce the positions C3, C5, C17 and C20 on the targeted steroid [240].

1.6.4 Function and role in the skin

The expression of AKR enzymes has been determined to steroidogenic organs. This includes the male and female reproductive system, the testis and prostate and the breast, endometrium, uterus and ovaries, respectively [6]. Furthermore, in both sexes, the enzymes are expressed in the CNS, lung, adrenal kidney, liver and adipose tissue [6, 219]. Generally, AKRs influence the availability of a ligand for their target receptors, the androgen (AR), estrogen (ER), and progesterone receptor (PR), respectively [6]. Since they catalyze both oxidation and reduction, they transform inactive metabolites into potent, active hormones and vice versa [241]. Here, AKR1C1 and -1C2 seem to act in ligand decreasing direction by favoring inactivating reactions [241, 242]. In contrast, AKR1C3 converts the weak estrogen to the potent 17 β -estradiol in women, the essential hormone for reproduction and development of the female secondary sexual characteristics [6]. In male biology, this process is mirrored by the production of testosterone out of Δ^4 -androstene-3,17-dione [6]. Furthermore, AKR1Cs are involved in virilization and the development of the genitalia by being part of the pathway that produces 5 α -dihydrotestosterone (5 α -DHT) [243]. AKR1C4 is liver-specific and needed for the reduction of 5 α -pregnane-3,20-dione to 3 α -hydroxy-5 α -pregnan-20-one [240, 244]. Notably, the residues 117-237 of AKR1C3 were found to have the ability to directly bind the AR, enabling its recruitment to androgen responsive genes [245]. Besides the metabolism of sexual hormones, both AKR1B1 and -1C3 have a prostaglandin F synthase activity [246, 247]. AKR1C3 is

able to catalyze the reduction of PGD_2 to $9\alpha11\beta$ -prostaglandin F_2 ($9\alpha11\beta$ - PGF_2) [7]. Normally, PGD_2 would spontaneously be converted into 15d-PGJ_2 , which is an agonist of $\text{PPAR}\gamma$ [5]. Absence of this agonist due to overly active AKR1C3 is therefore proposed as a tumor promoting mechanism [5]. Higher affinity and stronger catalytic activity for PGD_2 , AKR1C3 and not -1C1 or -1C2, is mainly responsible for this process [248, 249]. This statement was strengthened by the revelation that AKR1C3 is strongly expressed in the differentiated suprabasal layers of the skin and upregulated in PGD_2 promoted atopic dermatitis (AD) [241]. Unsurprisingly, the skin as well is considered to be a steroidogenic organ [250]. Here, the highest expression of AKR1C members was measured in mid-term epidermis and in the stratum spinosum [241]. The importance of sex hormone metabolism for the skin is shown by their involvement in its lipid barrier, hydration, elasticity, firmness, and wrinkle formation [251, 252]. The accompanying expression of AKR1C1 and -1C2 has been previously described in cultured human keratinocytes, although their occurrence in human skin, exact biology, and the additional expression of AKR1C3 was first noted in 2009 by Yari E. Marín [26, 253, 254]. This group demonstrated the occurrence of AKR1C family members in keratinocytes, fibroblasts, and melanocytes. The transcription of AKR1C1-3 was increased after they exposed HaCaT cells to UV or hydrogen peroxide-derived ROS, suggesting a role in keratinocyte stress response [26]. Exposure to small-interfering RNA (siRNA) against AKR1Cs led to a decreased number of living cells after incubation for 72 hours [26]. The amount was even lower when the transfected cells were exposed to UVB as well [26]. In summary, first evidence of AKRs playing a key role as survival factor for keratinocytes was concluded [26]. Their protective behavior is supported by the observation that 17β -estradiol, known to be produced by AKR1C3, prevents H_2O_2 -induced apoptosis in human keratinocytes [255]. However, mediating a general cellular survival response despite harmful pathogens is a possible mechanism that also enables carcinogenesis. Indeed, AKR1Cs were revealed as being overexpressed in the cutaneous SCC cell line A431 [256]. Downregulation of AKR1C expression again led to increased apoptosis after UV and bleomycin exposure [26, 256]. Finally, Mantel et al. revealed the overexpression of AKR1C3 in SCC samples from tumor patients [5]. Furthermore, treatment with PGD_2 , 15d-PGJ_2 , and with the $\text{PPAR}\gamma$ agonist pioglitazone inhibited further SCC proliferation [5].

1.7 Aim of the research

Understanding the mechanisms of early carcinogenesis is the key to determine preventive measures. In cSCC, AKR1C3 and the EGFR are over-expressed and for TNBC, the expression of AKR1C3 depends on the AHR. This leads to the hypothesis that the expression of AKR1C3 depends on the AHR in healthy skin as well. Additionally, it might be possible that the EGFR is a link in the signaling cascade between the AHR and AKR1C3. We suggest a possible, hitherto unknown pathway between those receptors and the enzyme. The aim of this work is to test how AKR1C3's gene transcription and protein translation depends on the activity of the AHR or the EGFR and whether the suggested pathway between the AHR, the EGFR and AKR1C3 exists. The data was collected exposing HaCaT-keratinocytes to agonists of the AHR or the EGFR and different inhibitors. Gene transcription was measured using qRT-PCR, protein expression by using Western Blot.

2 Materials and Methods

2.1 Chemicals and Reagents

2.1.1 Chemicals

| Agent | Reference |
|---|--|
| 2-mercaptoethanol | Sigma Aldrich, St. Louis, MO, USA |
| 2-propanol | Carl Roth GmbH & Co KG, Karlsruhe |
| Ammonium persulfate (APS) | Sigma Aldrich, St. Louis, MO, USA |
| Bromophenol blue | SERVA Electrophoresis GmbH, Heidelberg |
| Bovine Serum Albumin (BSA) | Carl Roth GmbH & Co KG, Karlsruhe |
| Color Protein Standard | New England Biolabs, Ipswich, MA, USA |
| Dimethyl sulfoxide (DMSO) | Carl Roth GmbH & Co KG, Karlsruhe |
| Dulbecco's Modified Eagle Medium (DMEM) | PAN-Biotech GmbH, Aidenbach |
| dNTP-Mix | Jena Bioscience GmbH, Jena |
| Ethylenediaminetetraacetic acid (EDTA) | Sigma Aldrich, St. Louis, MO, USA |
| Ethanol, denatured | Roth, Karlsruhe |
| Geneticin™ Selective Antibiotic (G418) | Biochrom GmbH, Berlin |
| Glycine | NeoFROXX GmbH, Einhausen |
| Hydrochloric Acid | Carl Roth GmbH & Co KG, Karlsruhe |
| Methanol | Carl Roth GmbH & Co KG, Karlsruhe |
| Non-fat dried milk powder | AppliChem GmbH, Darmstadt |
| Octylphenoxypolyethoxyethanol (IGEPAL CA-630) | ICN Biomedicals Inc., Irvine, CA, USA |
| Oligo (dT) ₁₅ Primer | Jena Bioscience GmbH, Jena |
| Phenylmethylsulfonyl fluoride (PMSF) | Sigma Aldrich, St. Louis, MO, USA |
| Phosphate buffered saline (PBS) | PAN-Biotech GmbH, Aidenbach |

| Agent | Reference |
|--|---|
| Polyvinylidene fluoride (PVDF) membrane | GE Healthcare, Chicago, IL, USA |
| Protease Inhibitor Cocktail (PIC) | Merck Millipore, Burlington, MA, USA |
| Restore™ WB Stripping buffer | Thermo Fisher Scientific, Waltham, MA USA |
| Reverse Transcriptase | Promega, Madison, WI, USA |
| Roctiphorese® Gel 40 (29:1) Acrylamide/Bisacrylamid solution | Carl Roth GmbH & Co KG, Karlsruhe |
| Sodium azide | Sigma Aldrich, St. Louis, MO, USA |
| Sodium chloride | Carl Roth GmbH & Co KG, Karlsruhe |
| Sodium deoxycholate | Sigma Aldrich, St. Louis, MO, USA |
| Sodium dodecyl sulfate (SDS) | Carl Roth GmbH & Co KG, Karlsruhe |
| Sodium fluoride | Sigma Aldrich, St. Louis, MO, USA |
| Sodium orthovanadate | Sigma Aldrich, St. Louis, MO, USA |
| Sucrose | Carl Roth GmbH & Co KG, Karlsruhe |
| Tetramethylethylenediamine (TEMED) | Sigma Aldrich, St. Louis, MO, USA |
| Tris ultrapure | AppliChem GmbH, Darmstadt |
| Tween® 20 | Sigma Aldrich, St. Louis, MO, USA |
| WesternBright™ ECL | Advansta, Menlo Park, CA, USA |

Table 2.1: List of chemicals

2.1.2 Stimulants

| Agent | Reference | Target structure |
|-----------------------------------|---------------------------|----------------------------------|
| Amphiregulin (AREG) | PeproTech | Epidermal Growth Factor Receptor |
| Benzo[a]pyrene (BaP) | Sigma Aldrich | Aryl Hydrocarbon Receptor |
| Bosutinib | Carl Roth | Tyrosine kinases |
| Epidermal growth factor (EGF) | Sigma Aldrich | Epidermal Growth Factor Receptor |
| Epiregulin (EREG) | PeproTech | Epidermal Growth Factor Receptor |
| Marimastat | Santa Cruz Bio-technology | Matrix metalloproteinase |
| Polychlorinated biphenyl (PCB126) | LGC Standards | Aryl Hydrocarbon Receptor |
| Transforming growth | PeproTech | Epidermal Growth Factor Receptor |

| Agent | Reference | Target structure |
|---|------------------|------------------------------------|
| factor alpha (TGF α) | | Receptor |
| Tumor necrosis factor alpha (TNF α) | R & D Systems | Tumor necrosis factor receptor 1/2 |

Table 2.2: List of stimulants

2.1.3 Kits

| Designation | Reference |
|------------------------------|---|
| peqGOLD Total RNA-Kit | VWR International, Langenfeld, NRW, Germany |
| Pierce BCA protein assay kit | Thermo Fisher Scientific, Waltham, MA, USA |

Table 2.3: List of Kits

2.1.4 Devices

| Device | Reference |
|--|--|
| Leitz Labovert inverse phase-contrast microscope | LEITZ ACCO Brands GmbH & Co KG, Stuttgart |
| HERAcell [®] 150 CO ₂ cell incubator | Heraeus Holding GmbH, Hanau |
| Hettich Mikro 22R | Andreas Hettich GmbH & Co.KG, Tuttlingen |
| OPTIMAX | PROTEC GmbH & Co. KG, Oberstenfeld |
| Rotor-Gene Q | QIAGEN N.V., Venlo, NLD |
| Tecan Infinite [®] M200 PRO | Tecan Trading AG Switzerland, Männedorf, CHE |

Table 2.4: List of Devices

2.1.5 Software

| Software | Reference |
|-----------------|---|
| Excel 365 | Microsoft |
| GraphPad Prism | GraphPad Software, Inc. |
| Tecan Software | Tecan Trading AG Switzerland |
| TexMaker | Freeware, Copyright (c) 2003-2017, Pascal Brachet |

Table 2.5: Software

2.1.6 Antibodies

2.1.6.1 Primary antibodies

| Antigene | Source | Dilution | Catalog# | Company |
|---------------------|--------|----------|------------|----------------|
| Anti-EGFR | mouse | / | #05-104 | Upstate |
| AKR1C3 | mouse | 1:1000 | #MAB7678 | R & D Systems |
| AKR1C3 | rabbit | 1:1000 | #ab209899 | Abcam |
| Akt | rabbit | 1:1000 | #9297 | Cell Signaling |
| β -Actin | mouse | 1:10000 | #3700 | Cell Signaling |
| β -Tubulin | mouse | 1:20000 | #T-7816 | Sigma Aldrich |
| EGFR | rabbit | 1:500 | #2232 | Cell Signaling |
| p44/42 MAPK | rabbit | 1:1000 | #9102 | Cell Signaling |
| phospho-p44/42 MAPK | rabbit | 1:1000 | #9101 | Cell Signaling |
| phospho-Akt | rabbit | 1:1000 | #4060 | Cell Signaling |
| phospho-EGFR | rabbit | 1:1000 | #3777 | Cell Signaling |
| phospho-Src | rabbit | 1:1000 | #6943 | Cell Signaling |
| phospho-TACE | rabbit | 1:1000 | #12033 | SAB |
| Src | mouse | 1:1000 | #05-184 | Upstate |
| TACE | mouse | 1:1000 | #sc-390859 | Santa Cruz |

Table 2.6: List of primary antibodies

2.1.6.2 Secondary antibodies

| Antigene | Source | Dilution | Catalog# | Company |
|---------------------|--------|----------|----------|----------------|
| IgG-HRP Anti-mouse | horse | 1:2000 | #7076 | Cell Signaling |
| IgG-HRP Anti-rabbit | goat | 1:2500 | #7074 | Cell Signaling |

Table 2.7: List of secondary antibodies

2.2 Cell Culture

2.2.1 Cultivation of cells

For this work, the adherent growing aneuploidy immortal keratinocyte cell line HaCaT, purchased from the *Deutsche Sammlung von Mikroorganismen und Zellkulturen* (DSMZ), and two variants previously established by the lab of Dr. Haarmann-Stemmann were used, as can be seen below (Table 3.8).

| Name | Description | Medium composition |
|-------------|---|--|
| HaCaT | aneuploidy immortalized human keratinocytes | DMEM, 10% FCS, 10 μ g/ml A/A |
| HaCaT-EV | HaCaT cells stably transfected with pCL1P.THPC (empty vector) | DMEM, 10% FCS, 10 μ g/ml A/A, 6,8 ml (0,54 mg/ml) G418 |
| HaCaT-shAHR | HaCaT cells, stably transfected with pCL1P.THPC (sh RNA for AhR vector) | DMEM, 10% FCS, 10 μ g/ml A/A, 6,8 ml (0,54 mg/ml) G418 |

Table 2.8: Human Cell Lines

The cells were constantly stored under standard conditions at 37°C and at 5% CO₂ in 175 cm² cell culture flasks. They were cultured in a solution of Dulbecco's modified eagle medium (DMEM), antibiotics/antimycotics (A/A 10,000 μ g/ml) and fetal calf serum (FCS). Geneticin™ Selective Antibiotic (G418) was added to the two variants to prevent a mix of wild type and modified cell lines. Their medium was changed every 5th day. When a confluence of 90% was reached, the cell cultures were split in a ratio of 1:60. The growth medium was removed and the cells were washed in 10 ml of phosphate-buffered saline (PBS). After the PBS had been aspirated, the cells were incubated with 2 ml of Trypsin/EDTA at 37°C for 15 minutes. When detached, 8 ml of medium were added in order to wash the cells and stop trypsinization. 600 μ l of the resulting suspension were then added to new culture flasks previously prepared with 20 ml of DMEM and directly stored under standard conditions. The remaining cells were counted, diluted again, and seeded.

2.2.2 Counting of cells and Seeding

In order to gain the fixed confluence that is needed in an experiment, the cells were counted before the seeding using the *Neubauer Zählkammer*. The average number of cells per square was used to calculate the cell concentration of the suspension using the following formula:

$$\text{Total cells/ml} = \text{Average cell count} * 10.000 \text{ cells/ml} \quad (1)$$

The seeding was done afterwards, using a solution prepared according to the following formulas:

$$\text{Cell suspension needed in ml} = (\text{cells per well} * \text{wells} + 1 \text{ well}) / \text{total cells/ml} \quad (2)$$

$$\text{Mastermix needed in ml} = 2 \text{ ml/well} * \text{wells} + 2 \text{ ml} \quad (3)$$

$$\text{Medium needed in ml} = \text{Mastermix in ml} - \text{cell suspension in ml} \quad (4)$$

After 2ml had been added to each well, they were inspected under the microscope to check if the needed confluence was reached. The dishes were finally stored under standard conditions overnight, allowing the adherent growing cells to attach and replicate.

2.2.3 Stimulation of Cells

After the cells had been incubated overnight, the medium was removed and the cells were washed twice with 2 ml of PSB, in order to remove all remaining FCS. As a promoting growth factor, it would otherwise potentially interfere with the reagents used further on and alter the result of the experiments. Therefore, after the PBS had been aspirated, 2 ml of medium without FCS were added to each well and they were again stored under standard conditions overnight. That way, the cells were synchronized within the cell cycle and the induction of receptors, enzymes and their pathways could be related exactly to both the time point when the reagents were added and their concentrations used. In all further experiments, DMSO was used as the negative and B(a)P as the positive control.

The first experiment was designed in order to test the influence of the AHR towards the expression of different AKR family members. Therefore, B(a)P and PCB126, both ligands of the AHR, were diluted in FCS-free medium to a concentration of 1,5 μM for PCB126 and 2,5 μM for B(a)P. Induction of the AKR's gene expression was analyzed via PCR afterwards by comparing the amount of transcribed AKR1C-DNA in EV- and shAhR cell lines. Therefore, the reagents were added to wells either containing starved EV- or starved shAhR-HaCaT cells in the concentrations given below.

| AHR ligands | Concentration |
|--------------------|----------------------|
| DMSO | 0.20 % |
| B(a)P | 2.5 μ M |
| PCB126 | 1.5 μ M |

Table 2.9: AHR ligands

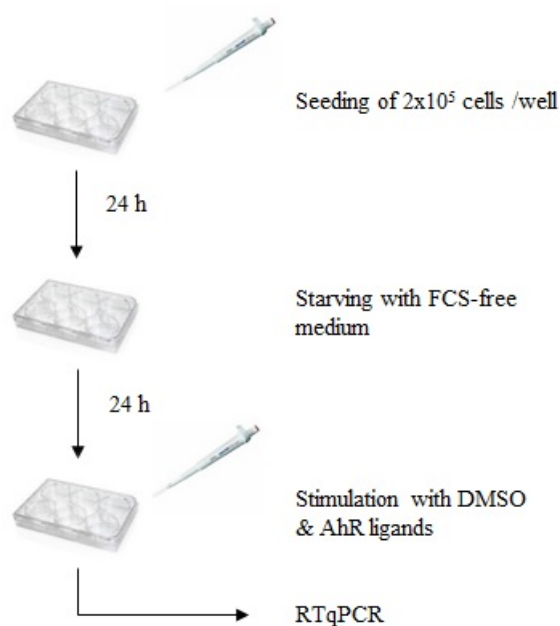


Figure 2.1: Stimulation of cells with AHR ligands

In the second experiment, WT-HaCaT keratinocytes were exposed to the EGFR-ligands EGF, TGF α , AREG and EREG to test whether the EGFR plays a role in the transcription of AKR1C DNA.

| EGFR ligands | Concentration |
|---------------------|----------------------|
| DMSO | 0.20 % |
| B(a)P | 2.5 μ M |
| PCB126 | 1.5 μ M |
| EGF | 1 μ g/ml |
| TNF α | 1 μ g/ml |
| TGF α | 1 ng/ml |
| AREG | 1 ng/ml |
| EREG | 1 ng/ml |

Table 2.10: EGFR ligands

How EGFR ligands affected the transcription of AKR1C subfamily members was tested afterwards by exposing EV- and shAHR-HaCaT cells to different concentrations of EGF or AREG, respectively.

| EGFR ligands | Concentration |
|---------------------|----------------------|
| DMSO | 0.20 % |
| B(a)P | 2.5 μ M |
| EGF | 1 μ M |
| | 10 μ M |
| | 20 μ M |
| AREG | 1 μ M |
| | 10 μ M |
| | 20 μ M |

Table 2.11: Concentration series of EGF and AREG

In order to clarify the influence of the EGFR, the amount of transcribed AKR1C DNA was measured after WT-HaCaT were exposed to an anti-EGFR antibody (AB).

| Anti-EGFR Antibody | Concentration |
|---------------------------|--------------------------|
| DMSO | 0.20% |
| B(a)P | 2.5 μ M |
| B(a)P + anti-EGFR-AB | 2.5 μ M/4 μ g/ml |

Table 2.12: Anti-EGFR antibody

The keratinocytes were also simultaneously exposed to B(a)P and Marimastat, an inhibitor of MMPs, or Bosutinib, an inhibitor of tyrosine kinases, to test the amount of AKR1C subfamily gene transcription after cell signaling that would normally activate the EGFR had been inhibited.

| Reagents | Concentration |
|--------------------|-------------------------|
| DMSO | 0.20 % |
| B(a)P | 2.5 μ M |
| PCB126 | 1.5 μ M |
| B(a)P + PCB126 | 2.5 μ M/1.5 μ M |
| B(a)P + Marimastat | 2.5 μ M/1 μ M |
| B(a)P + Bosutinib | 2.5 μ M/1 μ M |

Table 2.13: Pathway promoters and inhibitors

Whether a transcriptional factor like the AHR has an influence towards the gene expression of another receptor or a certain enzyme needs to be tested by measuring the amount of the translated, mature protein of interest as well. Here, western blot (WB) was used, testing if the mRNA translation of AKR1C family members is influenced by the AHR. Therefore, again EV- and shAHR-HaCaT cells were, after starvation, treated with either B(a)P or PCB126 for 24 hours.

| Reagents | Concentration |
|-----------------|----------------------|
| DMSO | 0.20 % |
| B(a)P | 2.5 μ M |
| PCB126 | 1.5 μ M |

Table 2.14: AHR ligands for WB

2.3 Protein Biochemistry

2.3.1 Cell lysate preparation

In order to analyze the expression levels of the proteins in question via SDS-PAGE and WB, a lysate of each sample was prepared. Therefore, the cells were washed two times with 2 ml of PSB, and re-suspended in 200 μ l of lysis buffer after the processes of starvation and incubation were finished.

| Reagent | Volume |
|---|---------------|
| Tris-HCl, pH 7,4 from a stock solution of 1 M in Aq. dest | 10 ml |
| NaCl from a stock solution of 2 M in Aq. dest | 15 ml |
| EDTA, pH 8.0 from a stock solution of 1 mM in Aq. dest | 20 ml |
| Deoxycholate from a stock of 10 % in Aq. dest | 20 ml |
| SDS from a stock of 10 % in Aq. dest | 2 ml |
| NaN ₃ from a stock of 10 % in Aq. dest | 500 μ l |
| IGEPAL CA-630 | 2 ml |
| H ₂ O | add to 100 ml |

Table 2.15: 2x RIPA buffer

The cells were scraped from the surface of the well using a cell scraper and transferred into a chilled Eppendorf[®] Tube. The tubes were incubated for 30 minutes at 4°C on the rotation wheel and then centrifuged for 15 minutes at 14.000 g at 4°C. The supernatant was transferred into a new chilled Eppendorf[®] Tube. Afterwards, the protein concentration was determined, using the bicinchoninic acid (BCA) assay.

| Reagent | Volume |
|-----------------------------------|---------------|
| 2 x RIPA buffer | 500 μ l |
| PMSF | 10 μ l |
| Protease Inhibitor Cocktail (PIC) | 4 μ l |
| NaF | 20 μ l |
| Na ₃ VO ₄ | 20 μ l |
| H ₂ O | 446 ml |

Table 2.16: 1 ml completed lysis buffer

2.3.2 Protein concentration determination with BCA assay

Analyzing the expression of a certain protein in different samples requires that the same amount of protein lysate is loaded into each well of the SDS-PAGE. The standardization procedure used in this work is the bicinchoninic acid (BCA) assay that measures the quantity of total protein in a lysate using the principle of colorimetric detection. In an alkaline medium, proteins reduce Cu²⁺ to Cu¹⁺, which forms a chelate with two molecules of BCA. This reaction product causes a strong absorbance at 562 nm that is almost linear between 20-2000 μ g/ml. The absorbance of each sample and therefore its amount of protein can then be detected with a spectrophotometer [257].

The BCA working reagent was freshly prepared by adding 50 parts of reagent A to 1 part of reagent B. In a 96-well plate, 25 μ l of previously produced BSA-standard solutions were added in triplets and 25 μ l of each protein lysate were added in doubles. To start the reaction, 200 μ l of the working reagent were mixed with the samples and incubated at 37°C for 30 minutes. Afterwards, the absorbance was measured with the Tecan Infinite[®] 200M PRO spectrophotometer and used to determine the protein concentration of each lysate. Standardization was achieved by diluting the lysates with (H₂O_{DEPC}) and 4x Laemmli buffer to a concentration of 10 μ g protein per 20 μ l.

| Reagent | Volume/Weight |
|--|----------------------|
| Sucrose | 20 g |
| Tris-HCl pH 6.8 from a stock solution of 1 M | 20 ml |
| SDS | 2 g |
| Bromophenol blue | 0.1 g |
| 2-mercaptoethanol | 1 ml |

Table 2.17: 4x Laemmli sample buffer

The finished sample solutions were then boiled at 95 °C for 10 minutes in order to unfold the proteins by breaking the secondary and tertiary structure. Disulfide bridges were cut with 2-mercaptoethanol that was added to the Laemmli buffer. This way, long, rod-like conformations were created that could easily be separated by their size. The samples were either directly used or stored at -20 °C overnight.

2.3.3 Sodium-Dodecyl-Sulfate Polyacrylamide Gel-Electrophoresis (SDS-Page)

The most common method to analyze and compare proteins in different samples is the Sodium-Dodecyl-Sulfate Polyacrylamide Gel-Electrophoresis (SDS-Page). Invented by U.K. Laemmli in 1970 [258], the method takes advantage of the fact that negatively charged proteins can be sized by their molecular weight while travelling through a sieve-like matrix in an electric field. The matrix is usually formed by a gel of polyacrylamide, its percentage determining its viscosity and therefore how fast the proteins can migrate. It is chosen in advance to gain a good separation in the region of interest. With protein sizes ranging from 42 kDa to 175 kDa, a 10 % gel was used for this work.

| Reagent | Volume running gel for 15 ml | Volume stacking gel for 6 ml |
|------------------|---|---|
| H ₂ O | 7.1 ml | 4.3 ml |
| Acrylamide | 3.8 ml | 0.8 ml |
| 1,5 μM TRIS | 3.9 ml (pH 8.8) | 0.8 ml (pH 6.8) |
| 10 % SDS | 0.075 ml | 0.03 ml |
| 10 % APS | 0.075 ml | 0.03 ml |
| TEMED | 0.006 ml | 0.006 ml |

Table 2.18: SDS-polyacrylamide gel 10 %

The added anionic surfactant sodium-dodecyl-sulfate (SDS) forms a non-covalently bound complex with the proteins, masking their intrinsic charge and leading to the required charge that needs to be negative. With 1,4 g SDS binding 1 g protein, a similar charge-to-mass ratio for all proteins in a sample is reached. Thereby, the separation of the proteins is independent from charges and results solely because of the different molecular weights.

A successful way to improve the results of the Western blot is by using a discontinuous SDS-Page system. It consists of a large pore stacking gel on top of a small pore resolving gel. With an electric field applied and running buffer added, the introduced proteins migrate fast through the upper gel while being sandwiched in a voltage gradient made up of a leading border of Cl⁻ ions in front and a trailing

border of glycinate ions behind. While the Cl^- ions are already present within the gel, the glycinate ions are added with the running buffer. Change in pore size and pH in the migration zone between both gels allows the glycinate ions to overtake the protein-SDS complexes which highly increases the protein concentration in a small zone. This allows the formation of clear and tight bands improving the overall resolution of the method. In order to measure the height and therefore the molecular weight of the different proteins, a color protein standard was added to the first and the last well of the stacking gel. For the first hour, the system was run with a current of 90 V. It was stopped when the dye front reached the migration zone and adjusted to 120 V for two hours.

| Reagent | Quantity |
|------------------|-------------------|
| Glycine | 144.1 g (0.384 M) |
| TRIS | 30.3 g (0.05 M) |
| SDS | 5.0 g (0.1 %) |
| H ₂ O | add to 1000 ml |

Table 2.19: SDS-Page, 5x Running buffer

2.3.4 Western Blot

Detection and quantification of proteins requires that they reside on a solid membrane that immobilizes them, increasing their durability and allowing specific probing with antibodies [259]. The transferring process was first described in 1979 [260, 261] and has constantly been improved since then. In this work, polyvinylidene fluoride membranes (PVDF) that bind proteins through hydrophobic interactions were used. The membrane needed to be soaked in methanol to decrease its hydrophobicity and to ease the infiltration of the transfer buffer (Table 3.18) together with the proteins. It was directly placed upon the finished polyacrylamide gel and sandwiched between two Whatmann-papers. A falcon tube was carefully rolled over the system to remove trapped air bubbles, which would have inhibited the transfer. The system was afterwards coated with two sponges and placed inside the blot carrier, which was added to the blot tank. The tank was filled with cold transfer buffer and placed in an ice bath to keep the temperature low. Migration of the proteins was achieved by running the system with a current of 100 V for 1,5 h.

| Reagent | Quantity |
|------------------|-------------------|
| Glycine | 144.1 g (0.384 M) |
| TRIS | 30.3 g (0.05 M) |
| H ₂ O | add to 1000 ml |

| Reagent | Quantity |
|---------|----------|
|---------|----------|

Table 2.20: Western blot, 5 x transfer buffer

| Reagent | Quantity |
|------------------|----------|
| Transfer buffer | 400 ml |
| Methanol | 400 ml |
| H ₂ O | 1200 ml |

Table 2.21: Western blot, 2l finished transfer buffer

2.3.5 Antibody treatment and detection

The finished PVDF membrane was cut to separate the proteins of interest and incubated in washing buffer (Table 3.19) containing either 5 % bovine serum albumin (BSA) or 5 % nonfat dried milk (NFDM) for one hour in order to block the areas that do not contain any proteins. This prevents non-specific binding of the antibodies. Depending on the blocking solution, the primary antibodies were also diluted in either 5 % BSA or NFDM following the manufacturer's instructions. After blocking, the membrane pieces were incubated with the primary antibodies at 4 C° overnight. The next morning, the membranes were washed three times with washing buffer for 10 minutes each. Depending on the source of the primary antibody, the secondary antibodies, conjugated to the enzyme horseradish peroxidase (HRP), were prepared again in 5 % BSA or NFDM, following the manufacturer's instructions, added to the blot and incubated at room temperature for 1 hour. The washing step was repeated and a 1:1 solution of WesternBright™ ECL Luminol/enhancer solution and Peroxide Chemiluminescent Detection Reagent were prepared. As a substrate of HRP, had already been added with the secondary antibody, the luminol emits light when reduced by the peroxidase in the presence of H₂O₂ [262]. Enhancement of the signal is provided by the enhancer solution containing phenol derivates [263]. The protein of interest is therefore detected by binding of the primary, protein specific antibody, binding of a matching, HRP conjugated secondary antibody and adding of a light emitting HRP substrate. Finally, the emitted light is detected by using a X-ray film in a dark room and developing the film with a X-ray developer. During this research, the PROTEC OPTIMAX was used.

| Reagent | Quantity |
|-----------|-----------------|
| TRIS | 24.2 g (20 mM) |
| NaCl | 80.0 g (137 mM) |
| Tween® 20 | 10 ml (0.1 %) |

| Reagent | Quantity |
|------------------|-----------------|
| HCl | add to pH = 7.6 |
| H ₂ O | add to 1000 ml |

Table 2.22: Western blot, 10 x washing buffer

2.3.6 Western blot quantification

The detected protein bands were analyzed using the software ImageJ, a freeware created by Wayne Rasband from the National Institute of Health (USA). After the scanning process, ImageJ was executed. The options "Mean Gray Value" and "Display label" were chosen within the "Set Measurements" option of the "Analyze" menu. Then, the image of the scanned WB was opened and set to 32bit to set the picture mode to grayscale. Within the first band of the first row, the region of interest (ROI) was defined, by selecting the "Rectangle" tool of the program and drawing the frame around the band. The ROI was saved as "Selection" so that the same rectangle would be retrievable again if the size was mistakenly changed. By pressing "*Strg + M*" on the keyboard while the frame was adjusted on the band, the mean gray value was detected. This step was repeated with every band of the row that needed to be analyzed. The resulting data was transferred to a separate spreadsheet (Microsoft Excel). Then, by placing the frame above or below the measured band, the background was measured as well and added to the spreadsheet. Calculation included the following steps:

$$\text{inverted protein } x = 255 - \text{protein } x \quad (1)$$

$$\text{inverted background } x = 255 - \text{background } x \quad (2)$$

$$\text{net protein} = \text{inverted protein } x - \text{inverted background } x \quad (3)$$

The same calculations were done with the loading control. In this work, both β -actin and β -tubulin were used.

$$\text{inverted loading control } x = 255 - \text{loading control } x \quad (4)$$

$$\text{inverted background } x = 255 - \text{background } x \quad (5)$$

$$\text{net loading control} = \text{inverted loading control } x - \text{inverted background } x \quad (6)$$

The resulted measurements first needed to be deducted from 255 as this number represents the mean gray scale of the detected image. After the calculations above were finished, the ratio between the detected protein of interest and its loading control was calculated, preventing false results due to different sample sizes. These calculated results were set in ratio with the amount of detected protein in the negative control.

$$\text{ratio protein x} = \text{net protein x} / \text{net loading control x} \quad (7)$$

$$\text{ratio negative control} = \text{ratio protein x} / \text{ratio negative control} \quad (8)$$

These steps were executed according to the protocol of Hossein Davarinejad, provided by York University. It can be found by following www.yorku.ca > yisheng > Internal > Protocols > ImageJ.

2.4 mRNA Analysis

2.4.1 RNA isolation

The question if a certain receptor or agent has an influence on any other can also be answered by analyzing the amount of expressed mRNA encoding for the protein of interest with the quantitative reverse transcription polymerase chain reaction (qRT-PCR). In this two-step procedure, purified RNA is transcribed into its complementary DNA strand (cDNA) and multiplied by thermostable DNA polymerases in a thermocycler afterwards. Purification of the RNA of each sample was conducted using the peqGOLD Total RNA-Kit by VWR International.

The previously starved and stimulated cells were washed with 3 ml of PBS after the medium had been removed. 400 μl of RNA lysis buffer T were added to each well, the cells were removed from the surface using a cell scraper, and transferred to a DNA removing column. They were spun down at 12.000 g for 1 minute and the flow-through was carefully mixed with 350 μl of 70 % ethanol to enhance the solubility of the RNA. The mixtures were added to Perfect-Bind RNA columns and again spun down at 10.000 g for 1 minute. The columns were washed afterwards with 500 μl of RNA wash buffer I, spun down at 10.000 g for 15 seconds, again washed with 600 μl of RNA washing buffer II and again spun down at 10.000 g for 15 seconds. The flow-through was discarded in every step. Before the purified RNA could be removed from the binding columns, it needed to be dried by centrifugation at 10.000 g for 2 minutes to enhance its concentration and remove any remaining buffers. Finally, 50 μl of diethylpyrocarbonate water ($\text{H}_2\text{O}_{DEPC}$), used because DEPC eliminates possibly existing RNase [264], were added to each column. They were incubated at room temperature for 3 minutes and spun down directly into fresh Eppendorf tubes at 5.000 g for 1 minute. The amount of isolated RNA was analyzed via TECAN.

2.4.2 cDNA Synthesis

After purification, each sample was diluted to a concentration of 500 ng RNA per 7.5 μl $\text{H}_2\text{O}_{DEPC}$, according to the results of the TECAN analysis. The reagents used for primer annealing (Table 3.20) were added to each sample and incubated at 60 C°

for 5 minutes. Afterwards, the reagents including reverse transcriptase (Table 3.21) were added and the probes were incubated at 37 C° for 60 minutes. The synthesis was finished at 70 C° for 10 minutes. The finished cDNA was diluted in a 1:3 ratio with H₂O_{DEPC} and could have been frozen at -20 C° at this point or directly used in the PCR.

| Reagent | Quantity |
|--|-----------------|
| Oligo (dT)15 Primer | 1.25 μ l |
| dNTP | 1.00 μ l |
| 500 ng RNA in H ₂ O _{DEPC} | 7.5 μ l |

Table 2.23: Synthesis Step 1: Primer annealing

| Reagent | Quantity |
|----------------------------------|-----------------|
| Reverse Transcriptase | 1,00 μ l |
| 5 x RT-buffer | 4.00 μ l |
| H ₂ O _{DEPC} | 5.00 μ l |

Table 2.24: Synthesis Step 2: cDNA-Synthesis

2.4.3 Quantitative PCR

Gene specific primers enclosing the DNA section that encodes for the protein of interest were prepared together with the QIAGEN SYBR Green FAST standard reagent (Table 3.22). Hereby, every sample of cDNA needed to be combined once with every primer mix to test a possible affection. A reference gene known not to be affected by the further experiments and nearly equally expressed in every sample is needed as an internal reaction control. In this research, this was fulfilled by either β -actin or β -tubulin.

| Reagent | Quantity |
|-------------------------|-----------------|
| SYBR Green FAST reagent | 7.5 μ l |
| <i>forward</i> primer | 2.5 μ l |
| <i>reverse</i> primer | 2.5 μ l |
| cDNA | 3.0 μ l |

Table 2.25: PCR reaction mixture

The finished PCR reaction mixtures were transferred to the Rotor Gene[®] Q of the company QUIAGEN. The qRT-PCR was executed cycling 40 times through the following phases:

| Phase | Time in seconds | Temperature in °C |
|--------------|------------------------|--------------------------|
| Denaturation | 15 | 94 |
| Annealing | 30 | 56 |
| Elongation | 30 | 72 |

Table 2.26: qRT-PCR Sequences

First, the double-stranded DNA was denatured at 94°C for 15 seconds. Afterwards, the added primer hybridized with the complementary single-stranded DNA at 56°C for 30 seconds (annealing). Beginning at the 3'OH-end of the primer, a DNA polymerase replicated the DNA strand at 72°C for 30 seconds (elongation). Then, the next cycle started over with the denaturation of the newly created DNA double-strands.

Quantification happens by measuring the fluorescence signal that occurs due to the reaction between the cDNA and the added DNA-binding fluorescent dye SYBR Green [265]. Here, the fluorescence signal increases linearly with the increase in DNA after each cycle. Therefore, the signal can be used to measure the amount of cDNA present in a sample.

Finally, the gene expression was calculated using the $\Delta \Delta$ Ct-method established by Livak & Schmittgen in 2001 [266]. The cycle threshold (Ct) of each RNA of interest was read out using the Rotor-Gene Q Series 2.0.2 program provided by the company QUIAGEN. The results were transferred into a Microsoft Excel[®] spreadsheet. After obtaining a sufficient amount of repeats of the same experiment, the mean Ct-value of the gene expression in cells only treated with DMSO, the negative control, was calculated. Before, the Ct-value of the control, a housekeeping gene whose expression is known not to be affected by the experimental setup, was subtracted from the Ct-value of the negative control.

$$\Delta \text{ Ct (DMSO)} = \text{Ct (DMSO)} - \text{Ct (control gene)} \quad (1)$$

$$\text{mean Ct (DMSO)} = \Delta \text{ (DMSO)} (n_1 + n_2 + \dots + n_x) / \text{number of repeats} \quad (2)$$

Then, the Ct-value of the control gene was subtracted from every other gene analyzed in the experiment as well. From this result, the mean Ct-value of DMSO was subtracted.

$$\Delta Ct (\text{target gene}) = Ct (\text{target gene}) - Ct (\text{control gene}) \quad (3)$$

$$\Delta \Delta Ct (\text{target gene}) = \Delta Ct (\text{target gene}) - \text{mean Ct (DMSO)} \quad (4)$$

Afterwards, the difference between the expression of the target gene in cells treated with the substrate was set in relation to the expression of the target gene in cells treated with the negative control.

$$\text{ratio (target gene)} = 2^{-\Delta \Delta Ct (\text{target gene})} \quad (5)$$

$$\text{fold of DMSO} = \text{ratio (target gene)} / \text{ratio (DMSO)} \quad (6)$$

Finally, the fold of DMSO was used to plot a chart that shows the difference between the expression of the target gene in WT-, EV- or shAHR-HaCaT-keratinocytes that had been treated with different stimulants.

3 Results

3.1 AKR gene transcription

The first question that needed to be investigated was whether the transcription of AKR subfamily genes is affected by the AHR at all and to what extent. Analysis answering this task was executed by culturing EV and shAHR HaCaT keratinocytes, previously established by the research group of Dr. Thomas Haarmann-Stemmann, followed by exposure to different AHR or EGFR ligands and inhibitors. Afterwards, the amount of translated DNA was measured using qRT-PCR. The tested AKR genes were selected regarding whether they contain AREs and therefore implicate involvement in the antioxidant stress response [267] or XREs, suggesting a regulation by the AHR [268]. The former are included in the genes encoding for the enzymes AKR1C family members 1-4 and AKR1B10, the latter in AKR1A1, -1B1, -7A1 and -2 [267, 268].

3.1.1 Analysis of the AHR knockdown

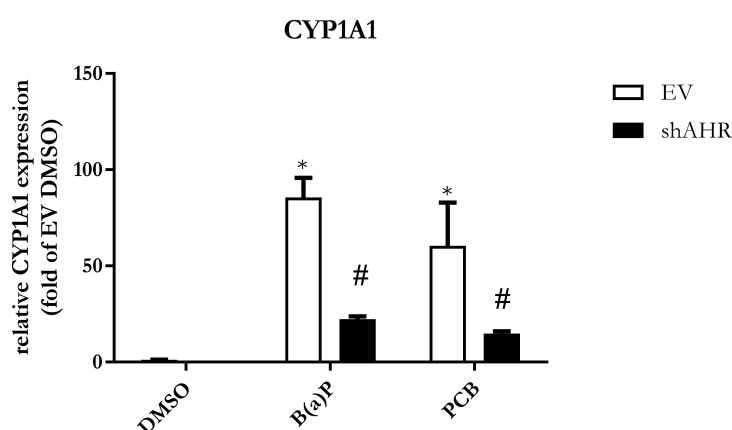


Figure 3.1: Stable knockdown of the AHR in shAHR HaCaT keratinocytes shown after exposure to the ligands B(a)P and PCB126. Two-way ANOVA, $n = 5$, $p \geq 0.05$, Tukey's multiple comparisons test, error bar = SD

As being an established outcome of the AHR's transcriptional activity, the stability of the knockdown in shAHR HaCaT keratinocytes was tested measuring the expression of CYP1A1. The transcription was significantly decreased in shAHR HaCaT cells exposed to B(a)P in comparison to HaCaT cells transfected with an empty vector. The same observation was obtained regarding exposure to the AHR-agonist PCB126.

3.1.2 Role of the AHR

The first experiment focused on the question whether the AHR has an influence on the expression of AKRs in general. After exposure to the agonists B(a)P and PCB126, the transcribed DNA was measured via qRT-PCR.

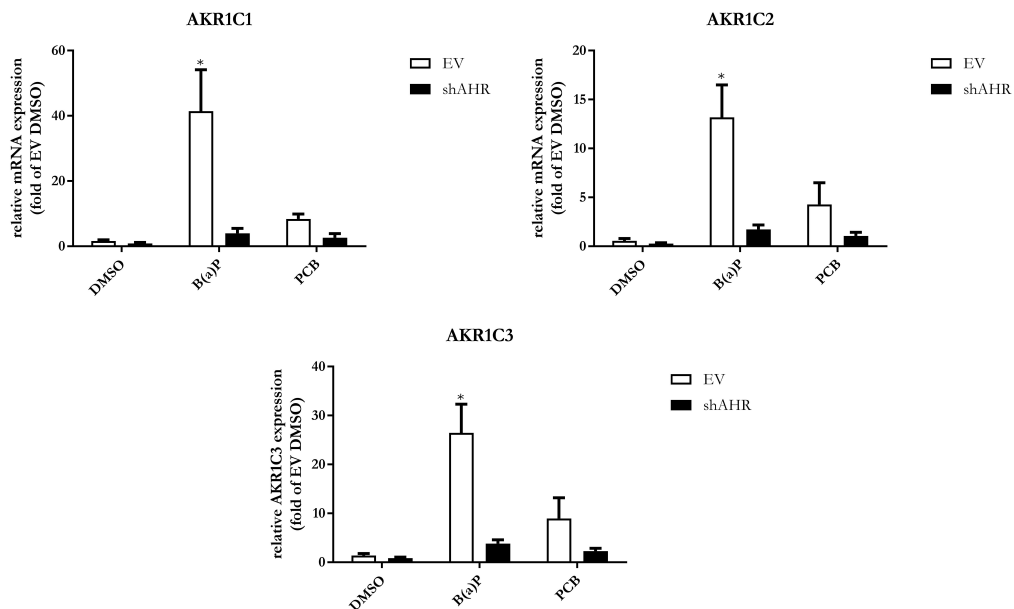


Figure 3.2: AKR1C1, -C2 and C3 transcription in EV and shAHR HaCaT after treatment with DMSO, B(a)P and PCB126. n = 6, Two-way ANOVA-test, $p \geq 0.05$, Tukey's multiple comparisons test, error bar = SD

The results of the qRT-PCR for AKR1C1, -C2 and -C3 can be seen in 3.2. Generally, the amount of transcribed AKR genes in HaCaT keratinocytes transfected with an EV is significantly higher than that measured in shAHR HaCaT cells. AKR1C1 transcription is increased up to 41.42-fold of EV DMSO, AKR1C2 13.18-fold and AKR1C3 26.46-fold in EV-HaCaT cells exposed to B(a)P. Interestingly, the transcription was not equally increased by both AHR ligands. In fact, B(a)P showed a significantly higher transcription rate of AKR genes than PCB126 did.

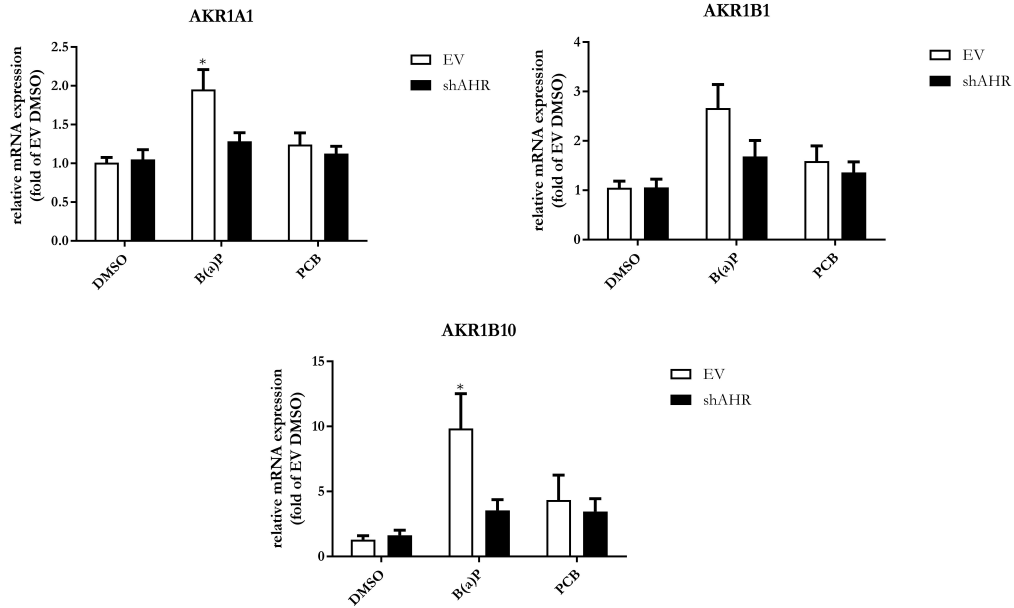


Figure 3.3: AKR1A1, -B1 and -B10 transcription in EV and shAHR HaCaT after treatment with DMSO, B(a)P and PCB126. n = 6, Two-way ANOVA-test, $p \geq 0.05$, Tukey's multiple comparisons test, error bar = SD

The increase of the expression of AKR1A1 was significant, although the amount of transcribed DNA was 1.95-fold of DMSO, which is much less compared to AKR1C subfamily's expression. Furthermore, EV- and shAHR HaCaT cells did not show a difference in AKR1A1 expression after exposure to PCB126. Although the transcription of AKR1B1 showed an increase after treatment with either B(a)P or PCB126, the result was not statistically significant. Again, a difference between EV- and shAHR HaCaT cells could not be detected, especially regarding the exposure to PCB126. The transcription of AKR1B10 showed a similar pattern compared to the AKR1C subfamily members. In EV-HaCaT cells, its expression increased significantly to a 9.84-fold of DMSO after treatment with B(a)P. Again, a significant increase was not detected in shAHR cells.

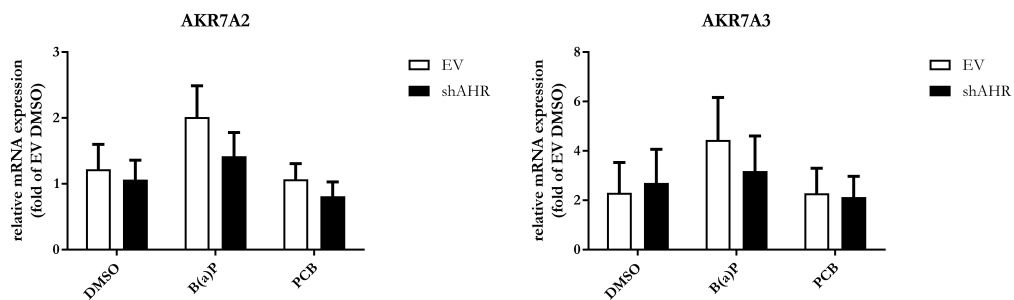


Figure 3.4: AKR7A2 & -3 transcription in EV and shAHR HaCaT after treatment with DMSO, B(a)P and PCB126. n = 6, Two-way ANOVA-test, $p \geq 0.05$, Tukey's multiple comparisons test, error bar = SD

The transcription of both AKR7A2 and -3 showed little difference between EV- and shAHR HaCaT cells. Although the transcription increased after treatment with the agonists, the result was not statistically significant.

3.1.3 Role of the EGFR

Analyses of an influence of the EGFR receptors towards the expression of AKR's were performed using the receptor's ligands EGF, TGF α , AREG and EREG. Being an activator of the MAPK pathway, TNF α was added in the experiments as well [269]. It was implemented in WT or EV-HaCaT keratinocytes to analyze if there would be any connection between EGFR signaling and AKR gene transcription.

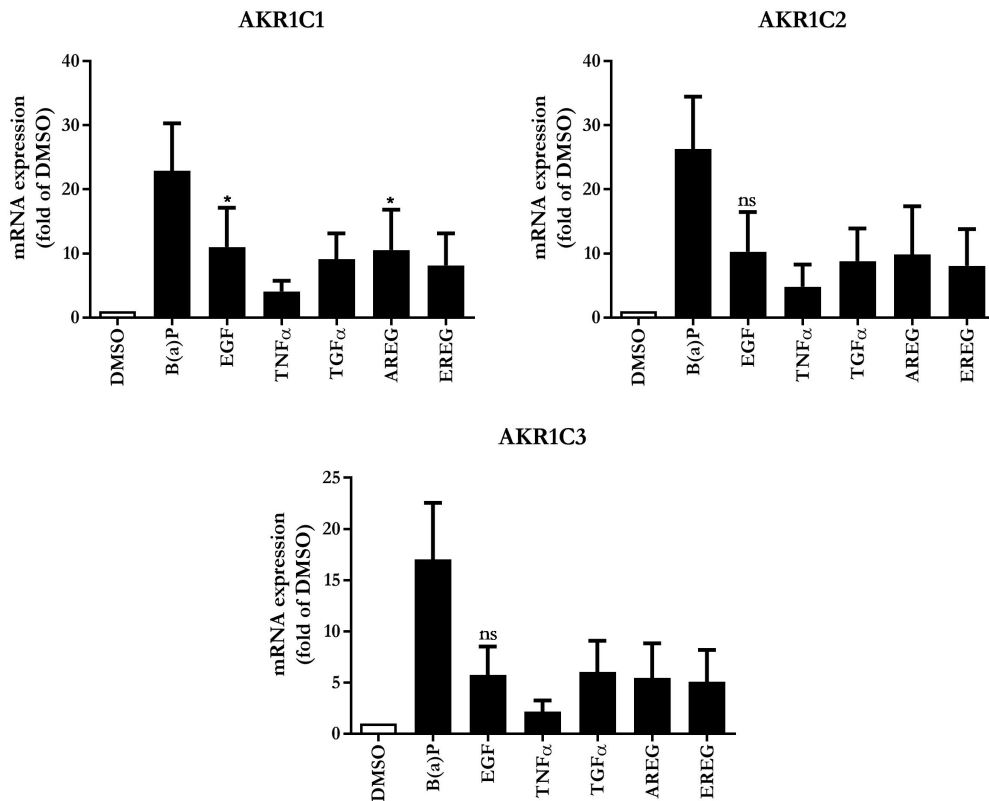


Figure 3.5: AKR1C1, -C2 and -C3 transcription in WT HaCaT after treatment with DMSO, B(a)P, EGF, TGF α , TNF α , AREG and EREG. n = 6, Kruskal-Wallis-test, p \geq 0.05, Dunn's multiple comparisons test, error bar = SD

The transcription of AKR1C subfamily genes increased in cells exposed to the AHR ligand B(a)P as expected, regarding the previous experiment. With 11-fold of DMSO, EGF enhanced the transcription of AKR1A1 significantly. The same could be seen after exposure to AREG, which increased the transcription of AKR1A1 10.52-fold of DMSO. Although the other ligands showed similar patterns, measurements were not statistically significant in every other 1C subfamily member.

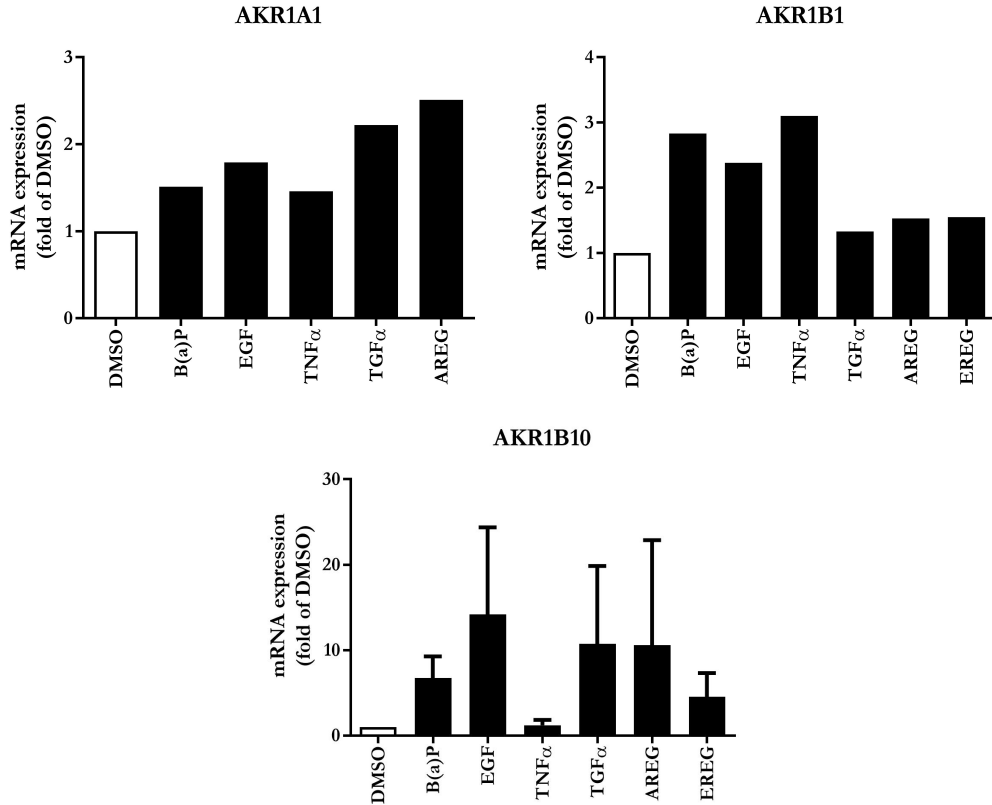


Figure 3.6: AKR1A1, -1B1 and -1B10 transcription in WT HaCaT after treatment with DMSO, B(a)P, EGF, TGF α , TNF α , AREG and EREG. $n = 1$ for AKR1A1 and -1B1, $n = 6$ for AKR1B10, Kruskal-Wallis-test, $p \geq 0.05$, Dunn's multiple comparisons test, error bar = SD

Both AKR1A1 and AKR1B1 genes did not show any enhanced transcription after exposure to ligands of the EGFR. Due to the fact that their gene transcription was not increased significantly by exposure to agonists of either the AHR or the EGFR, further experiments were performed without testing them. Additionally, AKR1B10 was disregarded in further experiments as well. Although its transcription was significantly increased after exposure to B(a)P, no statistically significant outcome resulted after the exposure to ligands of the EGFR.

3.1.4 Ligands of the EGFR regulate the expression of AKR1C genes in a dose dependent manner

In order to determine if a higher concentration of ligands of the EGFR causes a higher transcription rate of AKR1C genes, a concentration series was implemented. The ligands were chosen whether they showed significant results in the previous experiment, which was fulfilled by EGF and AREG. They were added in EV- and shAHR HaCaT keratinocytes, analyzing the influence of the AHR towards EGFR ligand-induced AKR gene transcription.

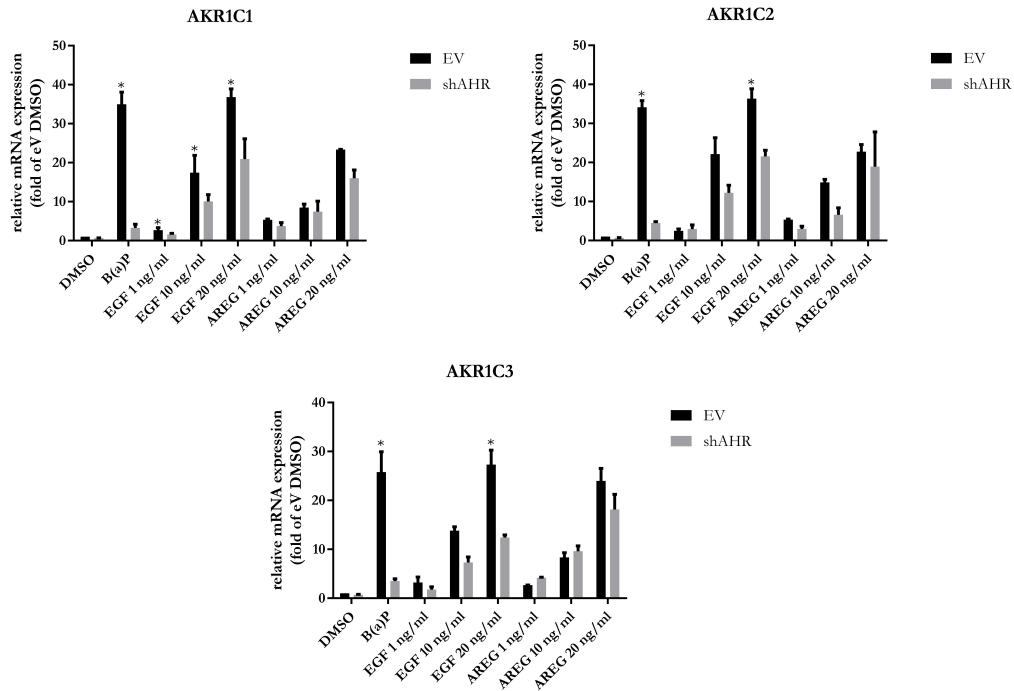


Figure 3.7: AKR1C1, -1C2 and -1C3 gene transcription in EV- and shAHR HaCaT after treatment with medium, DMSO, B(a)P, EGF and AREG. n for EGF = 4, n for AREG = 2, Two-way ANOVA, $p \geq 0.05$, Turkey's multiple comparison test, error bar = SD

Exposure to B(a)P led to an increased transcription of every measured AKR1C subfamily member. In fact, AKR1C1 was increased to 34.99-fold of EV-DMSO, AKR1C2 34.14-fold, and AKR1C3 25.79-fold, which was significant for AKR1C1, -2 and -3 compared to the amount of transcribed DNA in shAHR cells exposed to B(a)P. The exposure to ligands and the amount of transcribed AKR genes correlated positively. Overall, EV-HaCaT keratinocytes showed higher amounts than shAHR cells. Exceptions were the amount of transcribed AKR1C3 DNA in cells exposed to 1 and 10 ng/ml of AREG, and the amount of AKR1C2 transcripts in cells exposed to 1 ng/ml of EGF. For AKR1C1, every concentration of EGF used led to significantly higher amounts of transcribed DNA in EV-HaCaT cells compared to shAHR cells. In AKR1C2, this significant difference was only shown between EV- and shAHR-HaCaT keratinocytes exposed to 20 ng/ml EGF. Regarding AKR1C3, again only the concentration of 20 ng/ml EGF led to a significant difference between the used cells. Unfortunately, the data sheet was devoid of a third n for AREG and the level of significance could not be calculated.

3.1.5 Influence of the inhibition of the EGFR

Since the influence of the AHR and the EGFR towards the expression of AKR1C subfamily members had been investigated, it was necessary to analyze if both recep-

tors would have a functional connection to each other. Therefore, HaCaT wt cells were exposed to either B(a)P or B(a)P in combination with an EGFR-blocking AB. Afterwards, the expression of AKR1C subfamily members was measured.

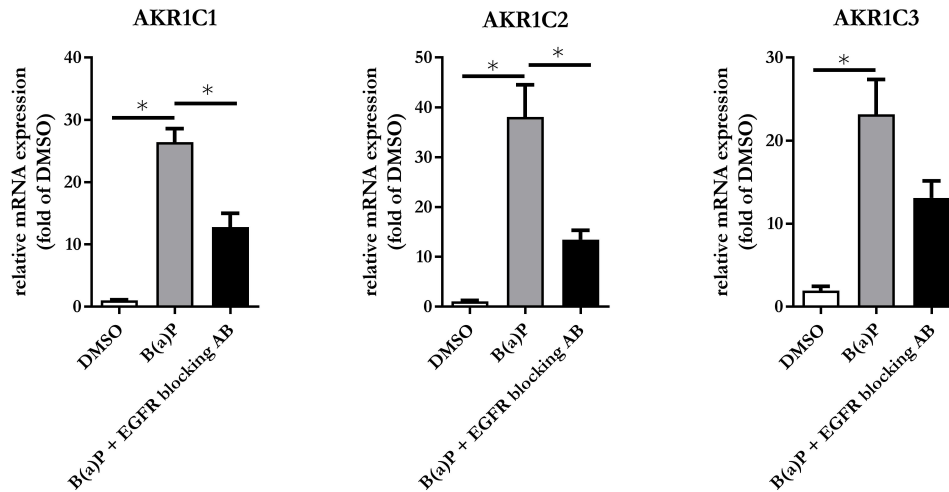


Figure 3.8: AKR1C1, -2 & 3 transcription after exposure anti-EGFR antibody. Executed by Dr. rer. nat. Christian Vogeley, $n = 4$, ordinary one-way ANOVA-test, $p \geq 0.05$, Tukey's multiple comparisons test, error bar = SD

The expression of AKR1C1 and -1C2 was significantly decreased when simultaneously exposed to an EGFR-blocking AB and B(a)P. After B(a)P, the expression of AKR1C1 was increased to 26.42-fold of DMSO. By adding an EGFR-blocking AB, an increase of 12.77-fold of DMSO was measured, which was statistically significant compared to the exposure of B(a)P alone. AKR1C2's expression decreased from a 38.08-fold of DMSO after exposure to B(a)P down to 13.45-fold of DMSO in cells exposed to the EGFR-blocking AB, which, again, was significant. Regarding AKR1C3, it's gene expression was increased to 23.17-fold of DMSO in cells exposed to B(a)P, and increased to 13.1-fold of DMSO in cells exposed to both B(a)P and the AB. However, the calculated result was not significant.

3.1.6 Influence of the inhibition of MMPs and tyrosine kinases

Finally, checkpoints of the postulated pathway were tested. Therefore, WT-HaCaT keratinocytes were exposed to Marimastat, an inhibitor of MMPs like TACE, and Bosutinib, an inhibitor of tyrosine kinases like PKC or c-src. Additionally, the cells were simultaneously exposed to B(a)P and PCB126 to analyze if the combination of those agonists of the AHR would have an influence towards the gene expression of AKR1C subfamily members.

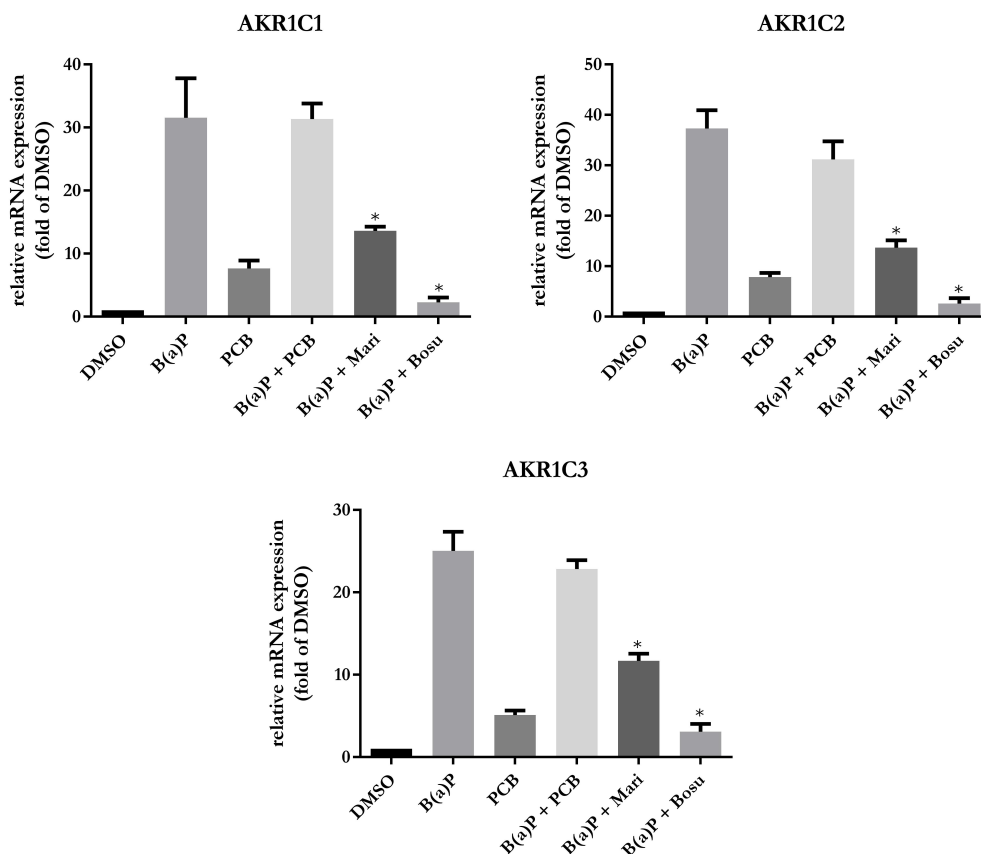


Figure 3.9: AKR1C1, -2 & 3 transcription after exposure to DMSO, B(a)P, PCB126, B(a)P + PCB126, B(a)P + Marimastat and B(a)P + Bosutinib. $n = 4$, RM one way ANOVA, $p \geq 0.05$, Tukey's multiple comparisons test, error bar = SD

Marimastat significantly decreased the gene transcription of AKR1C1. Cells exposed to B(a)P alone showed an increase up to 31.55-fold of DMSO, whereas, combined with Marimastat, an increase of 13.62-fold of DMSO was detected. With only 2.29-fold of DMSO, Bosutinib dampened the effect of B(a)P towards the gene transcription of AKR1C1 significantly. AKR1C2's gene expression showed a similar pattern. Cells exposed to both B(a)P and Marimastat showed a gene transcription of 13.70-fold of DMSO, whereas it's transcription was 37.31-fold of DMSO when exposed to B(a)P alone. The combination of B(a)P and Bosutinib led to a gene expression of 2.59-fold of DMSO. Both measurements were statistically significant. Measurements of AKR1C3's gene transcription were similar. Cells exposed to B(a)P alone showed an expression 25.04-fold of DMSO. Combined with Marimastat, the effect of B(a)P was dampened to 11.69-fold of DMSO and combined with Bosutinib, 3.1-fold of DMSO. Compared to the effect of B(a)P alone, the combination of B(a)P and PCB126 led to no statistically significant difference in the gene expression of AKR1C1, -C2 or C3.

3.2 AKR1C3 protein level

3.2.1 Role of the AHR

Strengthening the results of the mRNA analysis, the next step was to investigate if the transcription process is followed by translation as well. In the experimental setup EV- and shAHR-HaCaT keratinocytes were either exposed to B(a)P or PCB126. After 24 hours, the amount of AKR1C3 protein was determined using WB.

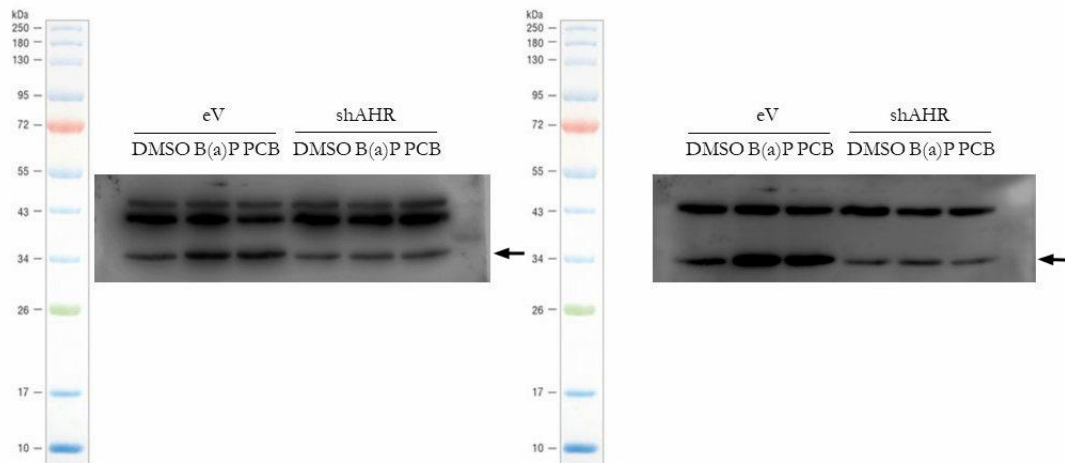


Figure 3.10: Western blot of AKR1C3 in EV- and shAHR-HaCat after treatment with DMSO, B(a)P and PCB126. $n = 4$. The arrow points at the protein band of AKR1C3.

The first experiment can be seen above. The loading control used was β -actin with a mass of 42 kDa. With a mass of 36 kDa, AKR1C3 was successfully detected. At approximately 45 kDa, an unspecific band was detected as well.

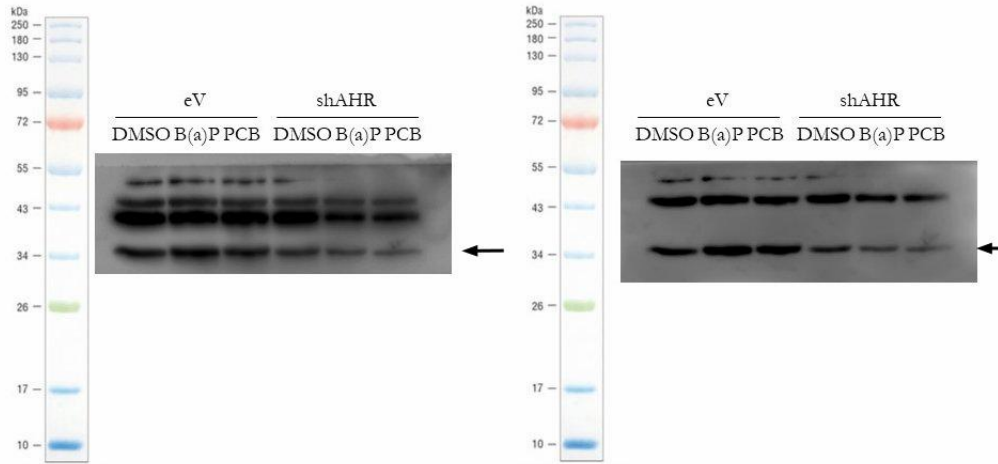


Figure 3.11: Western blot of AKR1C3 in EV- and shAHR-HaCat after treatment with DMSO, B(a)P and PCB126. $n = 4$. The arrow points at the protein band of AKR1C3.

The second experiment showed a similar pattern as the first. Again, β -actin and AKR1C3 were detected, an unspecific band at 45 kDa additionally.

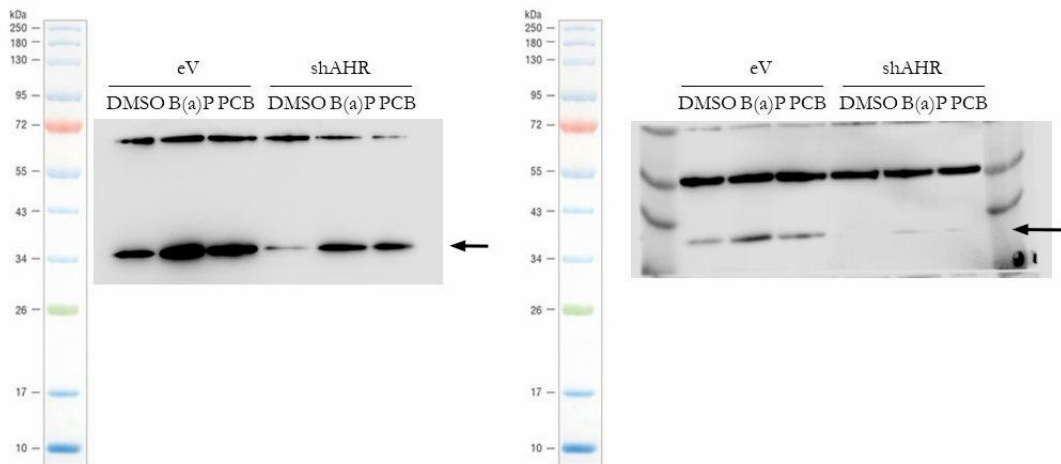


Figure 3.12: Western blot of AKR1C3 in EV- and shAHR-HaCat after treatment with DMSO, B(a)P and PCB126. $n = 4$. The arrow points at the protein band of AKR1C3.

In the third and fourth experiment, the loading control changed from β -actin to β -tubulin, another housekeeping protein with a mass of 55 kDa. Again, both proteins of interest were detected, as well as another unspecific band at approximately 70 kDa.

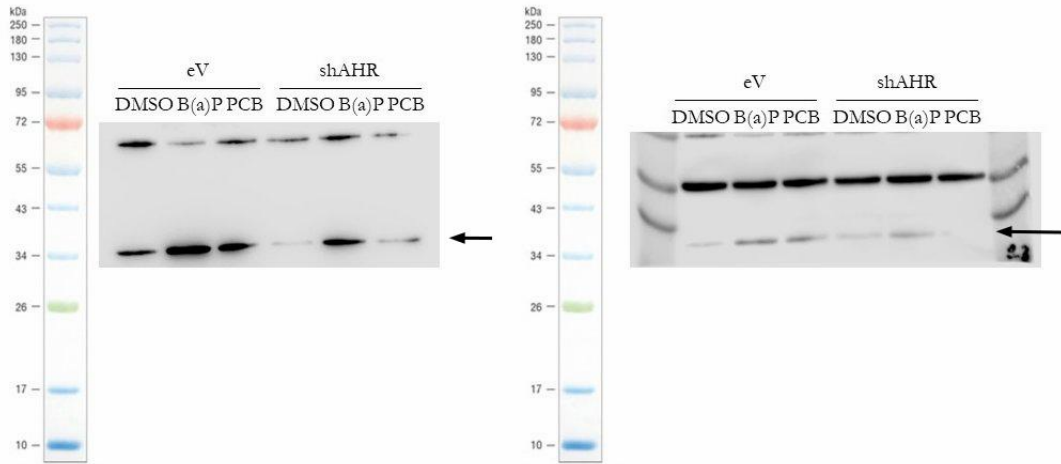


Figure 3.13: Western blot of AKR1C3 in EV- and shAHR-HaCat after treatment with DMSO, B(a)P and PCB126. $n = 4$. The arrow points at the protein band of AKR1C3.

The fourth experiment showed a similar pattern as the third. Then, the intensity of protein bands was calculated into a graph to make them easily comparable.

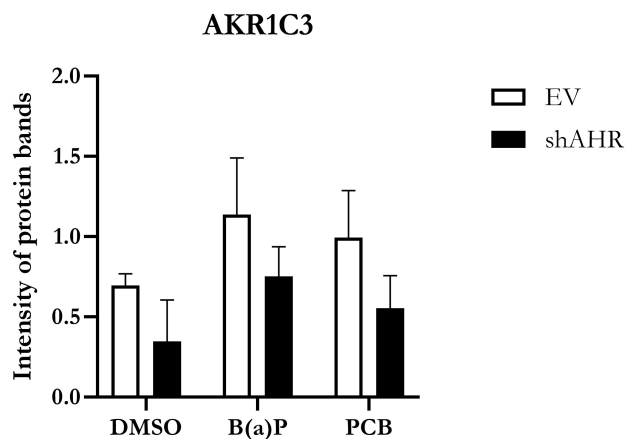


Figure 3.14: Densitometric of western blot of AKR1C3 in EV- and shAHR-HaCat after treatment with DMSO, B(a)P and PCB126. $n = 4$, Two-way ANOVA, $p \geq 0.05$, Tukey's multiple comparisons test, error bar = SD

In EV-HaCaT cells, the intensity of the protein bands were higher compared to those of shAHR cells. With a mean protein ratio of 1.14, the intensity was highest in EV-HaCaT cells exposed to B(a)P. In order to calculate significance, a two-way ANOVA with a Tukey's multiple comparisons test as a follow-up test were performed. Between B(a)P-exposed EV- and shAHR-HaCaT keratinocytes, no statistically significant difference was determined.

4 Discussion

Defense mechanisms against exogenous influences protect life despite a possibly harmful environment. In contrast, dysregulation of such mechanisms eventually leads to acute or chronic diseases. In the skin, the AHR is an important mediator of the xenobiotic response [38]. In SCC of the skin, AKR1C3 is upregulated and its PGF-synthase activity is proposed as a major contributor to carcinogenesis [5]. In 2019, the research team of Yamashita et al. proved that the expression of AKR1C3 is under control of the AHR in TNBC [8]. We proposed that the enzyme could be mediated by the AHR in the skin as well, especially because both are considered as negative regulators of apoptosis [38, 255]. Furthermore, AHR activating tobacco smoke was found to activate TACE through PKC and src, predicting a possible link towards the EGFR [11, 213]. In conclusion, these findings raised the question of a possible crosstalk between the AHR, the EGFR and AKR1C3. Analysis of such a pathway was performed by measuring the amount of transcribed AKR genes in EV- and shAHR HaCaT keratinocytes via qRT-PCR. Measurements of the mature AKR1C3 protein were done using western blot. Our findings reveal a significant difference in the expression of AKR1C subfamily enzymes between EV- and shAHR cells, substantiating the possibility of interactions between the AHR and this enzyme family in the skin. In contrast, linking the EGFR into the pathway could not be shown on protein level, although the measurements of AKR's gene transcription after exposure to ligands of the EGFR were promising.

4.1 Active AHR signaling influences AKR1C subfamily gene expression

After the exposure to B(a)P, the DNA transcription of AKR1C1, -1C2 and 1C3 increased significantly in EV-HaCaT keratinocytes. In contrast, we could not observe this effect in shAHR cells, clearly demonstrating a link between activation of the AHR and gene expression of the AKR1C subfamily. The significance of this result is emphasized by a p-value of $p < 0.001$ for AKR1C1, -2 and -3. The interaction could not be shown in the other investigated enzymes, which were AKR1A1, -1B1, -7A2, and -7A3. Therefore, they were disregarded in the following experiments. In sum-

mary, the transcription of AKR1C subfamily members is connected to the presence of agonists of the AHR. The results were obtained using B(a)P in a concentration of $2.5\ \mu\text{M}$ *in vitro*. Determining the concentration of B(a)P in the environment remains difficult due to the "broad range of potential sources and ubiquitous nature of contamination" [270]. For instance, the concentration of B(a)P found in Australian soil was estimated to range from 0.5-1,000 mg/kg, with higher amounts found in areas known to have been used as industrial workplaces [270]. Comparing the concentrations, it is very likely that humans are exposed to a concentration of B(a)P that could have an effect of AKR1C transcription *in vivo*. Furthermore, the AHR also increases the availability of NADPH, the cofactor of AKR1C subfamily enzymes [38].

Our finding that the transcription of AKR1C subfamily genes is increased in cells exposed to agonists of the AHR runs in contrary to other published research. Surprisingly, the research team of Burczynski et al. reported, that there was no enhanced AKR1C subfamily gene transcription after they exposed HepG2 hepatoma and HT29 colon carcinoma cells to the high-affinity AHR ligand TCDD [271]. Additionally, they stated that only AKR1C1 would be inducible by PAH's [271]. Furthermore, they suggested that the AKR1C subfamily genes would be regulated by AREs and not by XREs [271]. With XREs as the target gene structures of the AHR [84], their theory suggests that AKR1C subfamily members could not be regulated by the AHR. In 2007, Penning et al. even proposed, that the interaction was reverse: The AKR1C subfamily metabolize PAH's to provide the availability of ligands for the AHR just as they do for steroid receptors [268]. Maybe, the regulation of AKR1C subfamily members by the AHR is as Janus-faced as the receptor's role in healthy versus inflamed skin [114] and different regulatory pathways exist between cancer- and cell lines that are immortalized.

In contrast to the work of Burczynski et al. and Penning et al. the work of Yamashita et al. supports our findings. Similar to the designed experimental setup shown in 3.2, they also created MDA-MB 231 cells in which the AHR was knocked out [8]. Just as the results presented here, the expression of AKR1C3 was significantly lower in AHR knocked out cells compared to WT cells, reported in both RT-qPCR and WB [8]. Besides, it has to be noted that certain splice variants of AKR1C3, therefore, dependent on the primer used for the annealing, "PCR may give false estimate of the expression of mature transcripts that would be translated in full-length, active protein" [219]. Here, the solution could be the usage of RNAseq, an analysis more reliable for expressional studies of AKR1C3 [219].

4.2 The EGFR affects the AKR1C subfamily on the RNA level

Active EGFR signaling enhanced the transcription of AKR1C subfamily members. Further, significance was only measured regarding EGF and AREG, and only for AKR1C1 in particular. When those ligands were investigated, their concentration correlated positively with the expression of AKR1C subfamily members. Additionally, the blockage of the EGFR with an AB did show a significant decrease in AKR1C1 and -C2 transcription. The decrease was also detected in AKR1C3, although it was not statistically significant. Finally, the blockage of MMPs by Marimastat and tyrosine kinases by Bosutinib led to a significant decrease in AKR1C1-3's gene expression. Although the analysis by WB did not produce usable results for the EGFR (data not shown), the data obtained from the experiments where cells were exposed to ligands of the EGFR, an AB against the EGFR and Marimastat strongly implicate a connection between EGFR signaling and AKR expression.

Our hypothesis relied on the observation that in lungs exposed to tobacco smoke, TACE was activated through src [11]. We suggested that in this setup, src originated from the AHR, because it is one of its chaperoning members in its inactive state and tobacco smoke is a known activator of the AHR [14, 15]. As previously mentioned, the EGFR can be phosphorylated by c-src at Tyr-845 even in absence of a ligand [158]. Therefore, in one experimental setup in this research, the AB against the EGFR phosphorylated at the residue Tyr-1068 ensured to detect only ligand-bound EGFR. Unfortunately, the data obtained from those WBs could not be used for further calculations.

As mentioned before, the gene expression mediated by the EGFR follows a strict time course [10]. The experimental setup designed for this research scheduled the measurement of phosphorylated EGFR, phosphorylated Erk and phosphorylated TACE after an incubation time of 1, 3 or 6 hours (data not shown). Probably, this time period was too long to measure the actual amount of translated protein due to the different time courses. Additionally, it is unknown whether AKR1C3 could belong to the immediate early, the delayed early, or the delayed up- or down-regulated genes controlled by the EGFR. If further analysis reveals a significant connection between the EGFR and AKR1C3, designing a setup in which the time course mirrors the dynamics of EGFR controlled gene expression should possibly be considered. Potentially, transcript time course analysis (TTCA) could clarify this question, the method being known to detect "transient dynamics and slow expression changes" where other methods often fail [10]. Additionally, Singh et al. reported, that phosphorylated EGFR was detectable after "10 minutes post-UV

radiation, remained high for up to 2 hr, [and] returning to lower levels after 6 hr.” in HaCaT keratinocytes [213]. Although this time dependency was detected after UV radiation, this report emphasizes that another scheduling could have been in use for the detection of phosphorylated EGFR in this research as well. In the same experimental setup, the team noted that EGFR signaling is highly affected by cell culture conditions [213]. When they analyzed the amount of phosphorylated EGFR, PBS covered cells had decreased levels after exposure to UV compared to DMEM covered cells [213]. Therefore, analyses of how culture conditions affect the signaling pathway could have been implemented here as well.

Regarding the ligands of the EGFR, it has to be noted that AREG and EREG are low affinity ligands [173]. Therefore, when used in the same concentration as EGF, misleading results could result. This was prevented by the setup of a concentration series, revealing a positive correlation between a higher concentration of both EGF and AREG and the expression of AKR1C subfamily members. Importantly, AREG is the main ligand in keratinocytes, strengthening the measurements in which it enhances AKR1C subfamily transcription significantly [202, 272]. Interestingly, HB-EGF and EGN are other ligands that are expressed in keratinocytes and EGN is considered as an epithelial mitogen [167, 202, 203]. When future experiments are designed to further investigate the link between the EGFR and AKR gene expression, it should be considered whether analyses of those two ligands including neuregulins would be useful.

Regarding EGFR signaling, it is known that ADAM10 is the main sheddase of EGF. However, this does not mean that ADAM17/TACE is not involved in this process at all [12]. As already noted, AKR1C3 is controlled by the AHR in TNBC. Interestingly, ADAM10 is responsible for the constitutive kinase activity of Her2/neu in breast cancer by shedding its ectodomain [273]. Just recently, src was identified as a promotor of ADAM10 activity [274]. Further experiments could therefore focus on the question of whether ADAM17/TACE or ADAM10 is the link between AHR and EGFR activity. Additionally, ADAM17/TACE is known to be activated by p38/MAPK [275, 276]. In recent studies, BDE-47 (short for: 2,2',4,4'-Tetrabromodiphenyl ether) was able to activate a variety of compounds, including p38/MAPK [277]. Interestingly, BDE-47 is an agonist of the AHR. This finding strengthens the research hypothesis that the EGFR could be activated by active AHR signaling, but p38/MAPK and not src is their possible link.

In summary, more experiments would have been needed to clarify if a pathway exists where the EGFR is activated by the AHR and, in turn, activates AKR1C3. Notably, it is already known that AKRs are controlled by the Keap1/Nrf-2 pathway [229]. Interestingly, this pathway, in turn, is controlled by the AHR [278]. Recently, it was found that skin damage induced by UV was enhanced through KGF-2 (short for:

keratinocyte growth factor 2), activating the AHR that then triggers Nrf-2 signaling [279]. Maybe, analysis of the link between AHR, Nrf-2 and AKR1C3 could be investigated in further experiments.

4.3 The postulated pathway could not be shown on the protein level

The postulated pathway rooted from the reports of Lemjabbar-Alaoui et al. in 2011 and Mantel et al. in 2014. The first paper noted that TACE was activated in smoke exposed lungs [11]. Therefore, our working group concluded that this mechanism could happen due to active AHR transcriptional activity. Due to the fact that it were the ROS that induced the phosphorylation of TACE, experiments where AHR, TACE, EGFR and AKR1C3 activity is measured in HaCaT cells exposed and not exposed to different inducers of ROS might be a potential setup that could emphasize the findings reported here.

Regarding the cells, it has to be noted that the behavior of primary keratinocytes was not investigated. This might lower the relevance of the results presented here *in vitro*. However, primary keratinocytes show poor transfection efficiency, therefore the implementation of shAHR keratinocytes could have been of unnecessary difficulty [26]. Instead, establishing a stable knockdown is much more effective when using HaCaT cells [26]. In order to emphasize the possible overexpression or enhanced activity of the AHR, EGFR and AKR1C3, a research setup analyzing SCC cell lines such as Ca127, HN6, or HN12 could have been additionally used [280]. Furthermore, it could have been useful to test the expression of AKR1C3 and the amount of $9\alpha11\beta$ -PGJ₂ in EGFR-dependent cell lines like HN31 or UMSCC25 [280].

4.4 Conclusion

In summary, this work strongly indicates a link between the transcriptional activity of the AHR and the expression of AKR1C subfamily members, especially AKR1C3. Additionally, experiments focusing on active EGFR signaling led to statistically significant results. However, proving a link between src and TACE was not possible, nor was it possible to investigate if the Ras/Raf pathway, activated through the EGFR, led to enhanced AKR1C3 activity. The results presented here strongly implicate a connection between the AHR and AKR1C3 in keratinocytes *in vitro*. Additional experiments that include further analyses of the role of the EGFR and

the behavior of AHR metabolism towards AKR1C3 in keratinocytes *in vivo* need to be carried out. During the research, it became clear that AKR1C3 and the EGFR are expressed in different locations in the epidermal architecture [205, 241]. The enzyme enhances the differentiation process in the upper layers while the EGFR is responsible for replicative processes in the basal layers [205, 241]. However, hints that the AHR, the EGFR and AKR1C3 are connected somehow were given during this research and reported elsewhere. In order to answer the aim of this work, more experiments are needed, maybe considering the suggestions of using other cell lines or testing other possible links. This research concludes with the answer that the transcription of AKR1C3 is upregulated in HaCaT keratinocytes exposed to agonists of the AHR and that this could be a mechanism how carcinogenesis of the skin is initiated and enhanced as can be seen in TNBC [8].

5 Bibliography

1. Vogeley C, Sondermann NC, Woeste S, et al. Unraveling the differential impact of PAHs and dioxin-like compounds on AKR1C3 reveals the EGFR extracellular domain as a critical determinant of the AHR response. *Environment International* 2022;158.
2. Sung H, Ferlay J, Siegel RL, et al. Global Cancer Statistics 2020: GLOBOCAN Estimates of Incidence and Mortality Worldwide for 36 Cancers in 185 Countries. *CA: A Cancer Journal for Clinicians* 2021;71:209–49.
3. Zambrano-Román M, Padilla-Gutiérrez JR, Valle Y, Muñoz-Valle JF, and Valdés-Alvarado E. Non-Melanoma Skin Cancer: A Genetic Update and Future Perspectives. *Cancers* 2022;14.
4. George EA, Baranwal N, Kang JH, Qureshi AA, Drucker AM, and Cho E. Photosensitizing medications and skin cancer: A comprehensive review. *Cancers* 2021;13:1–18.
5. Mantel A, Carpenter-Mendini A, Vanbuskirk J, and Pentland AP. Aldo-keto reductase 1C3 is overexpressed in skin squamous cell carcinoma (SCC) and affects SCC growth via prostaglandin metabolism. *Experimental Dermatology* 2014;23:573–8.
6. Penning TM, Burczynski ME, Jez JM, et al. Human 3α -hydroxysteroid dehydrogenase isoforms (AKR1C1-AKR1C4) of the aldo-keto reductase superfamily: Functional plasticity and tissue distribution reveals roles in the inactivation and formation of male and female sex hormones. *Biochemical Journal* 2000;351:67–77.
7. Suzuki-Yamamoto T, Nishizawa M, Fukui M, et al. cDNA cloning, expression and characterization of human prostaglandin F synthase. *FEBS Letters* 1999;462:335–40.
8. Yamashita N, Kanno Y, Saito N, et al. Aryl hydrocarbon receptor counteracts pharmacological efficacy of doxorubicin via enhanced AKR1C3 expression in triple negative breast cancer cells. *Biochemical and Biophysical Research Communications* 2019;516:693–8.

9. Twardy DJ. Elevated Levels of Transforming Growth Factor α and Epidermal Growth Factor Receptor Messenger RNA Are Early Markers of Carcinogenesis in Head and Neck Cancer. *Cancer Research* 1993;53:3579–84.
10. Uribe ML, Marrocco I, and Yarden Y. EGFR in Cancer: Signaling Mechanisms, Drugs, and Acquired Resistance. *Cancers* 2021;13.
11. Lemjabbar-Alaoui H, Sidhu SS, Mengistab A, Gallup M, and Basbaum C. TACE/ADAM-17 phosphorylation by PKC- ϵ mediates premalignant changes in tobacco smoke-exposed lung cells. *PloS one* 2011;6:e17489.
12. Sahin U, Weskamp G, Kelly K, et al. Distinct roles for ADAM10 and ADAM17 in ectodomain shedding of six EGFR ligands. *Journal of Cell Biology* 2004;164:769–79.
13. Sahin U and Blobel CP. Ectodomain shedding of the EGF-receptor ligand epigen is mediated by ADAM17. *FEBS Letters* 2007;581:41–4.
14. Enan E and Matsumura F. Identification of c-Src as the integral component of the cytosolic Ah receptor complex, transducing the signal of 2,3,7,8-tetrachlorodibenzo-p-dioxin (TCDD) through the protein phosphorylation pathway. *Biochemical Pharmacology* 1996;52:1599–612.
15. Esser C, Bargon I, Weighardt H, Haarmann-Stemmann T, and Krutmann J. Functions of the aryl hydrocarbon receptor in the skin. *Seminars in immunopathology* 2013;35:677–91.
16. Kamstrup MR, Gniadecki R, and Skovgaard GL. Putative cancer stem cells in cutaneous malignancies. 2007. DOI: 10.1111/j.1600-0625.2007.00547.x.
17. Welsch U and Deller T. Sobotta, Lehrbuch Histologie. 2010:465–83.
18. Nanney LB. Epidermal and dermal effects of epidermal growth factor during wound repair. 1990. DOI: 10.1111/1523-1747.ep12876204.
19. Alberts B, Johnson A, Lewis J, et al. *Molecular Biology of the Cell*. 5th editio. Garland Science, 2008:1205–13, 1224–40.
20. Vogeley C, Esser C, Tüting T, Krutmann J, and Haarmann-Stemmann T. Role of the aryl hydrocarbon receptor in environmentally induced skin aging and skin carcinogenesis. *International Journal of Molecular Sciences* 2019;20.
21. Baudouin C, Charveron M, Tarroux R, and Gall Y. Environmental pollutants and skin cancer. *Cell Biology and Toxicology* 2002;18:341–8.
22. Zhang L, Jin Y, Huang M, and Penning TM. The role of human aldo-keto reductases in the metabolic activation and detoxication of polycyclic aromatic hydrocarbons: Interconversion of PAH catechols and PAH o-quinones. *Frontiers in Pharmacology* 2012;3 NOV:1–12.

23. Katiyar SK, Matsui MS, and Mukhtar H. Ultraviolet-B exposure of human skin induces cytochromes P450 1A1 and 1B1. *Journal of Investigative Dermatology* 2000;114:328–33.
24. Park JY, Shigenaga MK, and Ames BN. Induction of cytochrome P4501A1 by 2,3,7,8-tetrachlorodibenzo-p-dioxin or indolo(3,2-b)carbazole is associated with oxidative DNA damage. *Proceedings of the National Academy of Sciences of the United States of America* 1996;93:2322–7.
25. Hajeyah AA, Griffiths WJ, Wang Y, Finch AJ, and O'Donnell VB. The Biosynthesis of Enzymatically Oxidized Lipids. *Frontiers in Endocrinology* 2020;11:1–32.
26. Marín YE, Seiberg M, and Lin CB. Aldo-keto reductase 1C subfamily genes in skin are UV-inducible: Possible role in keratinocytes survival. *Experimental Dermatology* 2009;18:611–8.
27. Burczynski ME, Harvey RG, and Penning TM. Expression and characterization of four recombinant human dihydrodiol dehydrogenase isoforms: Oxidation of trans-7,8-dihydroxy-7,8- dihydrobenzo[a]pyrene to the activated o-quinone metabolite benzo[a]pyrene- 7,8-dione. *Biochemistry* 1998;37:6781–90.
28. Bray F, Ferlay J, Soerjomataram I, Siegel RL, Torre LA, and Jemal A. Global cancer statistics 2018: GLOBOCAN estimates of incidence and mortality worldwide for 36 cancers in 185 countries. *CA: A Cancer Journal for Clinicians* 2018.
29. Mühlstädt M. *Kurzlehrbuch Dermatologie*. 1. Auflage. Urban & Fischer, 2014:254 ff.
30. Ratushny V, Gober MD, Hick R, Ridky TW, and Seykora JT. From keratinocyte to cancer: The pathogenesis and modeling of cutaneous squamous cell carcinoma. 2012. DOI: 10.1172/JCI57415.
31. Nghiem DX, Kazimi N, Clydesdale G, Ananthaswamy HN, Kripke ML, and Ullrich SE. Ultraviolet a radiation suppresses an established immune response: Implications for sunscreen design. *Journal of Investigative Dermatology* 2001.
32. Gailani MR, Leffell DJ, Ziegler AM, Gross EG, Brash DE, and Bale AE. Relationship between sunlight exposure and a key genetic alteration in basal cell carcinoma. *Journal of the National Cancer Institute* 1996.
33. Benjamin CL, Ullrich SE, Kripke ML, and Ananthaswamy HN. p53 tumor suppressor gene: A critical molecular target for UV induction and prevention of skin cancer. In: *Photochemistry and Photobiology*. 2008. DOI: 10.1111/j.1751-1097.2007.00213.x.

34. Toll A, Salgado R, Yébenes M, et al. MYC gene numerical aberrations in actinic keratosis and cutaneous squamous cell carcinoma. *British Journal of Dermatology* 2009.
35. Toll A, Salgado R, Yébenes M, et al. Epidermal growth factor receptor gene numerical aberrations are frequent events in actinic keratoses and invasive cutaneous squamous cell carcinomas. 2010. DOI: 10.1111/j.1600-0625.2009.01028.x.
36. Zhao L, Li W, Marshall C, et al. Srcasm inhibits fyn-induced cutaneous carcinogenesis with modulation of Notch1 and p53. *Cancer Research* 2009.
37. Mescher M and Haarmann-Stemmann T. Modulation of CYP1A1 metabolism: From adverse health effects to chemoprevention and therapeutic options. *Pharmacology & therapeutics* 2018;187:71–87.
38. Nebert DW. Aryl hydrocarbon receptor (AHR): “pioneer member” of the basic-helix/loop/helix per-Arnt-sim (bHLH/PAS) family of “sensors” of foreign and endogenous signals. 2017. DOI: 10.1016/j.plipres.2017.06.001.
39. Poland AP, Glover E, Robinson JR, and Nebert DW. Genetic expression of aryl hydrocarbon hydroxylase activity. Induction of monooxygenase activities and cytochrome P1-450 formation by 2,3,7,8 tetrachlorodibenzo p dioxin in mice genetically 'nonresponsive' to other aromatic hydrocarbons. *Journal of Biological Chemistry* 1974;249:5599–606.
40. Poland A, Glover E, and Kende AS. Stereospecific, high affinity binding of 2,3,7,8 tetrachlorodibenzo p dioxin by hepatic cytosol. Evidence that the binding species is receptor for induction of aryl hydrocarbon hydroxylase. *Journal of Biological Chemistry* 1976;251:4936–46.
41. Conney AH, Miller EC, and Miller JA. Substrate-Induced Synthesis And Other Properties Of Benzpyrene Hydroxylase In Rat Liver. *Journal of Biological Chemistry* 1957;228:753–66.
42. Elferink CJ and Whitlock JPJ. 2,3,7,8-Tetrachlorodibenzo-p-dioxin-inducible, Ah receptor-mediated bending of enhancer DNA. *The Journal of biological chemistry* 1990;265:5718–21.
43. Burbach KM, Poland A, and Bradfield CA. Cloning of the Ah-receptor cDNA reveals a distinctive ligand-activated transcription factor. *Proceedings of the National Academy of Sciences of the United States of America* 1992;89:8185–9.
44. Dolwick KM, Schmidt JV, Carver LA, Swanson HI, and Bradfield CA. Cloning and expression of a human Ah receptor cDNA. *Molecular pharmacology* 1993;44:911–7.

45. Ema M, Matsushita N, Sogawa K, et al. Human Arylhydrocarbon Receptor: Functional Expression and Chromosomal Assignment to 7p211. *The Journal of Biochemistry* 1994;116:845–51.
46. Gu YZ, Hogenesch JB, and Bradfield CA. The PAS Superfamily: Sensors of Environmental and Developmental Signals. *Annual Review of Pharmacology and Toxicology* 2000;40:519–61.
47. Murre C, Bain G, Dijk MA van, et al. Structure and function of helix-loop-helix proteins. 1994. DOI: 10.1016/0167-4781(94)90001-9.
48. Ikuta T, Eguchi H, Tachibana T, Yoneda Y, and Kawajiri K. Nuclear localization and export signals of the human aryl hydrocarbon receptor. *Journal of Biological Chemistry* 1998;273:2895–904.
49. Reddy P, Jacquier AC, Abovich N, Petersen G, and Rosbash M. The period clock locus of *D. melanogaster* codes for a proteoglycan. *Cell* 1986;46:53–61.
50. Citri Y, Colot HV, Jacquier AC, et al. A family of unusually spliced biologically active transcripts encoded by a *Drosophila* clock gene. *Nature* 1987;326:42–7.
51. Nambu JR, Lewis JO, Wharton KA, and Crews ST. The *Drosophila* single-minded gene encodes a helix-loop-helix protein that acts as a master regulator of CNS midline development. *Cell* 1991;67:1157–67.
52. Hoffman EC, Reyes H, Chu FF, et al. Cloning of a factor required for activity of the Ah (dioxin) receptor. *Science* 1991;252:954–8.
53. Jackson FR, Bargiello TA, Yun SH, and Young MW. Product of per locus of *drosophila* shares homology with proteoglycans. *Nature* 1986;320:185–8.
54. Coumailleau P, Poellinger L, Gustafsson JA, and Whitelaw ML. Definition of a minimal domain of the dioxin receptor that is associated with Hsp90 and maintains wild type ligand binding affinity and specificity. *Journal of Biological Chemistry* 1995;270:25291–300.
55. Abel J and Haarmann-Stemmann T. An introduction to the molecular basics of aryl hydrocarbon receptor biology. *Biological Chemistry* 2010;391:1235–48.
56. Rowlands JC, Mcewan IJ, and Gustafsson JA. Trans-activation by the human aryl hydrocarbon receptor and aryl hydrocarbon receptor nuclear translocator proteins: Direct interactions with basal transcription factors. *Molecular Pharmacology* 1996;50:538–48.
57. Rothhammer V and Quintana FJ. The aryl hydrocarbon receptor: an environmental sensor integrating immune responses in health and disease. *Nature Reviews Immunology* 2019;19:184–97.

58. Perdew GH. Association of the Ah receptor with the 90-kDa heat shock protein. *Journal of Biological Chemistry* 1988;263:13802–5.
59. Whitelaw ML, Gottlicher M, Gustafsson JA, and Poellinger L. Definition of a novel ligand binding domain of a nuclear bHLH receptor: Co-localization of ligand and hsp90 binding activities within the regulable inactivation domain of the dioxin receptor. *EMBO Journal* 1993;12:4169–79.
60. Fukunaga BN, Probst MR, Reisz-Porszasz S, and Hankinson O. Identification of functional domains of the aryl hydrocarbon receptor. *Journal of Biological Chemistry* 1995;270:29270–8.
61. Ma Q and Whitlock JP. A novel cytoplasmic protein that interacts with the Ah receptor, contains tetratricopeptide repeat motifs, and augments the transcriptional response to 2,3,7,8-tetrachlorodibenzo-p-dioxin. *Journal of Biological Chemistry* 1997;272:8878–84.
62. Meyer BK, Pray-Grant MG, Vanden Heuvel JP, and Perdew GH. Hepatitis B Virus X-Associated Protein 2 Is a Subunit of the Unliganded Aryl Hydrocarbon Receptor Core Complex and Exhibits Transcriptional Enhancer Activity. *Molecular and Cellular Biology* 1998;18:978–88.
63. Meyer BK and Perdew GH. Characterization of the AhR-hsp90-XAP2 core complex and the role of the immunophilin-related protein XAP2 in AhR stabilization. *Biochemistry* 1999;38:8907–17.
64. Petrusis JR, Kusnadi A, Ramadoss P, Hollingshead B, and Perdew GH. The hsp90 co-chaperone XAP2 alters importin β recognition of the bipartite nuclear localization signal of the Ah receptor and represses transcriptional activity. *Journal of Biological Chemistry* 2003;278:2677–85.
65. Kazlauskas A, Poellinger L, and Pongratz I. The immunophilin-like protein XAP2 regulates ubiquitination and subcellular localization of the dioxin receptor. *Journal of Biological Chemistry* 2000;275:41317–24.
66. Kazlauskas A, Poellinger L, and Pongratz I. Evidence that the co-chaperone p23 regulates ligand responsiveness of the dioxin (aryl hydrocarbon) receptor. *Journal of Biological Chemistry* 1999;274:13519–24.
67. Pappas B, Yang Y, Wang Y, et al. p23 protects the human aryl hydrocarbon receptor from degradation via a heat shock protein 90-independent mechanism. *Biochemical pharmacology* 2018;152:34–44.
68. Vogel C, Boerboom AMJ, Baechle C, et al. Regulation of prostaglandin endoperoxide H synthase-2 induction by dioxin in rat hepatocytes: Possible c-Src-mediated pathway. *Carcinogenesis* 2000;21:2267–74.

69. Köhle C, Gschaidmeier H, Lauth D, Topell S, Zitzer H, and Bock KW. 2,3,7,8-Tetrachlorodibenzo-p-dioxin (TCDD)-mediated membrane translocation of c-Src protein kinase in liver WB-F344 cells. *Archives of Toxicology* 1999;73:152–8.
70. Liu X and Jefcoate C. 2,3,7,8-Tetrachlorodibenzo-p-dioxin and epidermal growth factor cooperatively suppress peroxisome proliferator-activated receptor- γ 1 stimulation and restore focal adhesion complexes during adipogenesis: Selective contributions of Src, Rho, and Erk disting. *Molecular Pharmacology* 2006;70:1902–15.
71. Waller CL and McKinney JD. Three-Dimensional Quantitative Structure-Activity Relationships of Dioxins and Dioxin-like Compounds: Model Validation and Ah Receptor Characterization. *Chemical Research in Toxicology* 1995;8:847–58.
72. Denison MS and Nagy SR. Activation of the aryl hydrocarbon receptor by structurally diverse exogenous and endogenous chemicals. *Annual review of pharmacology and toxicology* 2003;43:309–34.
73. Paine AJ. Comparison of the photochemical and enzymic generation of excited states of oxygen on the induction of benzo(alpha)pyrene mono-oxygenase in liver cell cultures. *Chemico-biological interactions* 1977;16:309–14.
74. Rannug A, Rannug U, Rosenkranz HS, et al. Certain photooxidized derivatives of tryptophan bind with very high affinity to the Ah receptor and are likely to be endogenous signal substances. *Journal of Biological Chemistry* 1987;262:15422–7.
75. Rannug U, Rannug A, Sjöberg U, Li H, Westerholm R, and Bergman J. Structure elucidation of two tryptophan-derived, high affinity Ah receptor ligands. *Chemistry and Biology* 1995;2:841–5.
76. Ciolino HP, Daschner PJ, Wang TT, and Yeh GC. Effect of curcumin on the aryl hydrocarbon receptor and cytochrome P450 1A1 in MCF-7 human breast carcinoma cells. *Biochemical Pharmacology* 1998;56:197–206.
77. Ciolino HP, Wang TT, and Yeh GC. Diosmin and diosmetin are agonists of the aryl hydrocarbon receptor that differentially affect cytochrome P450 1A1 activity. *Cancer Research* 1998;58:2754–60.
78. Loub WD, Wattenberg LW, and Davis DW. Aryl hydrocarbon hydroxylase induction in rat tissues by naturally occurring indoles of cruciferous plants. *Journal of the National Cancer Institute* 1975;54:985–8.

79. Quattrochi LC and Tukey RH. Nuclear uptake of the Ah (dioxin) receptor in response to omeprazole: Transcriptional activation of the human CYP1A1 gene. *Molecular Pharmacology* 1993;43:504–8.
80. Bass SE, Sienkiewicz P, MacDonald CJ, et al. Novel dithiolethione-modified nonsteroidal anti-inflammatory drugs in human hepatoma HepG2 and colon LS180 cells. *Clinical Cancer Research* 2009;15:1964–72.
81. Delescluse C, Ledirac N, Li R, et al. Induction of cytochrome P450 1A1 gene expression, oxidative stress, and genotoxicity by carbaryl and thiabendazole in transfected human HepG2 and lymphoblastoid cells. *Biochemical Pharmacology* 2001;61:399–407.
82. Avilla MN, Malecki KM, Hahn ME, Wilson RH, and Bradfield CA. The Ah Receptor: Adaptive Metabolism, Ligand Diversity, and the Xenokine Model. *Chemical Research in Toxicology* 2020;33:860–79.
83. Ikuta T, Tachibana T, Watanabe J, Yoshida M, Yoneda Y, and Kawajiri K. Nucleocytoplasmic Shuttling of the Aryl Hydrocarbon Receptor1. *The Journal of Biochemistry* 2000;127:503–9.
84. Probst MR, Reisz-Porszasz S, Agbunag RV, Ong MS, and Hankinson O. Role of the aryl hydrocarbon receptor nuclear translocator protein in aryl hydrocarbon (dioxin) receptor action. *Molecular Pharmacology* 1993;44:511–8.
85. Yao EF and Denison MS. DNA Sequence Determinants for Binding of Transformed Ah Receptor to a Dioxin-Responsive Enhancer. *Biochemistry* 1992;31:5060–7.
86. Hankinson O. Role of coactivators in transcriptional activation by the aryl hydrocarbon receptor. *Archives of Biochemistry and Biophysics* 2005;433:379–86.
87. Huang G and Elferink CJ. A novel nonconsensus xenobiotic response element capable of mediating aryl hydrocarbon receptor-dependent gene expression. *Molecular Pharmacology* 2012;81:338–47.
88. Wormke M, Stoner M, Saville B, et al. The Aryl Hydrocarbon Receptor Mediates Degradation of Estrogen Receptor α through Activation of Proteasomes. *Molecular and Cellular Biology* 2003;23:1843–55.
89. Ohtake F, Takeyama K ichi, Matsumoto T, et al. Modulation of oestrogen receptor signalling by association with the activated dioxin receptor. *Nature* 2003;423:545–50.

90. Wilson SR, Joshi AD, and Elferink CJ. The tumor suppressor kruppel-like factor 6 is a novel aryl hydrocarbon receptor DNA binding partner. *Journal of Pharmacology and Experimental Therapeutics* 2013;345:419–29.
91. Tian Y, Ke S, Denison MS, Rabson AB, and Gallo MA. Ah receptor and NF- κ B interactions, a potential mechanism for dioxin toxicity. *Journal of Biological Chemistry* 1999;274:510–5.
92. Gradin K, McGuire J, Wenger RH, et al. Functional interference between hypoxia and dioxin signal transduction pathways: competition for recruitment of the Arnt transcription factor. *Molecular and Cellular Biology* 1996;16:5221–31.
93. Davarinis NA and Pollenz RS. Aryl hydrocarbon receptor imported into the nucleus following ligand binding is rapidly degraded via the cytoplasmic proteasome following nuclear export. *Journal of Biological Chemistry* 1999;274:28708–15.
94. Ikuta T, Kobayashi Y, and Kawajiri K. Phosphorylation of nuclear localization signal inhibits the ligand-dependent nuclear import of aryl hydrocarbon receptor. *Biochemical and Biophysical Research Communications* 2004;317:545–50.
95. Ma Q and Baldwin KT. 2,3,7,8-tetrachlorodibenzo-p-dioxin-induced degradation of aryl hydrocarbon receptor (AhR) by the ubiquitin-proteasome pathway. Role of the transcription activation and DNA binding of AhR. *Journal of Biological Chemistry* 2000;275:8432–8.
96. Ma Q and Baldwin KT. A cycloheximide-sensitive factor regulates TCDD-induced degradation of the aryl hydrocarbon receptor. *Chemosphere* 2002;46:1491–500.
97. Mimura J, Ema M, Sogawa K, and Fujii-Kuriyama Y. Identification of a novel mechanism of regulation of Ah (dioxin) receptor function. *Genes and Development* 1999;13:20–5.
98. Ahmad N and Mukhtar H. Cytochrome P450: A target for drug development for skin diseases. *Journal of Investigative Dermatology* 2004;123:417–25.
99. Rowe JM, Welsh C, Pena RN, Wolf CR, Brown K, and Whitelaw CBA. Illuminating role of CYP1A1 in skin function. *Journal of Investigative Dermatology* 2008;128:1866–8.
100. Fritsche E, Schäfer C, Calles C, et al. Lightening up the UV response by identification of the arylhydrocarbon receptor as a cytoplasmatic target for ultraviolet B radiation. *Proceedings of the National Academy of Sciences of the United States of America* 2007;104:8851–6.

101. Yu J, Luo Y, Zhu Z, et al. A tryptophan metabolite of the skin microbiota attenuates inflammation in patients with atopic dermatitis through the aryl hydrocarbon receptor. *Journal of Allergy and Clinical Immunology* 2019;143:2108–2119.e12.
102. Rademacher F, Simanski M, Hesse B, et al. Staphylococcus epidermidis Activates Aryl Hydrocarbon Receptor Signaling in Human Keratinocytes: Implications for Cutaneous Defense. *Journal of Innate Immunity* 2019;11:125–35.
103. Krämer HJ, Podobinska M, Bartsch A, et al. Malassezin, a novel agonist of the aryl hydrocarbon receptor from the yeast *Malassezia furfur*, induces apoptosis in primary human melanocytes. *ChemBioChem* 2005;6:860–5.
104. Loertscher JA, Sattler CA, and Allen-Hoffmann BL. 2,3,7,8-Tetrachlorodibenzo-p-dioxin alters the differentiation pattern of human keratinocytes in organotypic culture. *Toxicology and Applied Pharmacology* 2001;175:121–9.
105. Sutter CH, Bodreddigari S, Champion C, Wible RS, and Sutter TR. 2,3,7,8-Tetrachlorodibenzo-p-dioxin increases the expression of genes in the human epidermal differentiation complex and accelerates epidermal barrier formation. *Toxicological sciences : an official journal of the Society of Toxicology* 2011;124:128–37.
106. Van Den Bogaard EH, Podolsky MA, Smits JP, et al. Genetic and pharmacological analysis identifies a physiological role for the AHR in epidermal differentiation. *Journal of Investigative Dermatology* 2015;135:1320–8.
107. Muku GE, Blazanin N, Dong F, et al. Selective Ah Receptor Ligands Mediate Enhanced SREBP1 Proteolysis to Restrict Lipogenesis in Sebocytes. *Toxicological Sciences* 2019;171:146–58.
108. Hu T, Wang D, Yu Q, et al. Aryl hydrocarbon receptor negatively regulates lipid synthesis and involves in cell differentiation of SZ95 sebocytes in vitro. *Chemico-Biological Interactions* 2016;258:52–8.
109. Luecke S, Backlund M, Jux B, Esser C, Krutmann J, and Rannug A. The aryl hydrocarbon receptor (AHR), a novel regulator of human melanogenesis. *Pigment Cell and Melanoma Research* 2010;23:828–33.
110. Haas K, Weighardt H, Deenen R, et al. Aryl Hydrocarbon Receptor in Keratinocytes Is Essential for Murine Skin Barrier Integrity. *Journal of Investigative Dermatology* 2016;136:2260–9.

111. Bogaard EH van den, Esser C, and Perdew G. The aryl hydrocarbon receptor at the forefront of host-microbe interactions in the skin: a perspective on current knowledge gaps and directions for future research and therapeutic applications. *Experimental Dermatology* 2021;0–3.
112. Kimmig J and Schulz KH. Chlorierte aromatische zyklische Äther als Ursache der sogenannten Chlorakne. *Naturwissenschaften* 1957;44:337–8.
113. Fernandez-Salguero PM, Hilbert DM, Rudikoff S, Ward JM, and Gonzalez FJ. Aryl-hydrocarbon receptor-deficient mice are resistant to 2,3,7,8-tetrachlorodibenzo-p-dioxin-induced toxicity. *Toxicology and applied pharmacology* 1996;140:173–9.
114. Haarmann-Stemmann T, Esser C, and Krutmann J. The Janus-Faced Role of Aryl Hydrocarbon Receptor Signaling in the Skin: Consequences for Prevention and Treatment of Skin Disorders. *Journal of Investigative Dermatology* 2015;135:2572–6.
115. Merk HF, Abel J, Baron JM, and Krutmann J. Molecular pathways in dermatotoxicology. *Toxicology and Applied Pharmacology* 2004;195:267–77.
116. Elmetts CA, Ledet JJ, and Athar M. Cyclooxygenases: mediators of UV-induced skin cancer and potential targets for prevention. *The Journal of investigative dermatology* 2014;134:2497–502.
117. Pittayapruek P, Meephansan J, Prapapan O, Komine M, and Ohtsuki M. Role of Matrix Metalloproteinases in Photoaging and Photocarcinogenesis. *International journal of molecular sciences* 2016;17.
118. Pentland AP, Schoggins JW, Scott GA, Khan KNM, and Han R. Reduction of UV-induced skin tumors in hairless mice by selective COX-2 inhibition. *Carcinogenesis* 1999;20:1939–44.
119. Shimizu Y, Nakatsuru Y, Ichinose M, et al. Benzo[a]pyrene carcinogenicity is lost in mice lacking the aryl hydrocarbon receptor. *Proceedings of the National Academy of Sciences of the United States of America* 2000;97:779–82.
120. Frauenstein K, Sydlik U, Tigges J, et al. Evidence for a novel anti-apoptotic pathway in human keratinocytes involving the aryl hydrocarbon receptor, E2F1, and checkpoint kinase 1. *Cell death and differentiation* 2013;20:1425–34.
121. Pollet M, Shaik S, Mescher M, et al. The AHR represses nucleotide excision repair and apoptosis and contributes to UV-induced skin carcinogenesis. *Cell death and differentiation* 2018;25:1823–36.

122. Dusingize JC, Olsen CM, Pandeya NP, et al. Cigarette Smoking and the Risks of Basal Cell Carcinoma and Squamous Cell Carcinoma. *Journal of Investigative Dermatology* 2017;137:1700–8.
123. Hecht SS. Tobacco carcinogens, their biomarkers and tobacco-induced cancer. *Nature reviews. Cancer* 2003;3:733–44.
124. Mitsui H, Suárez-Fariñas M, Gulati N, et al. Gene expression profiling of the leading edge of cutaneous squamous cell carcinoma: IL-24-driven MMP-7. *The Journal of investigative dermatology* 2014;134:1418–27.
125. Chahal HS, Lin Y, Ransohoff KJ, et al. Genome-wide association study identifies novel susceptibility loci for cutaneous squamous cell carcinoma. *Nature communications* 2016;7:12048.
126. Hansen LA, Woodson RL, Holbus S, Strain K, Lo YC, and Yuspa SH. The epidermal growth factor receptor is required to maintain the proliferative population in the basal compartment of epidermal tumors. *Cancer Research* 2000;60:3328–32.
127. Yarden Y and Sliwkowski MX. Untangling the ErbB network. *Nature reviews Molecular Cell Biology* 2001;2:127–37.
128. Savage CRJ and Cohen S. Epidermal growth factor and a new derivative. Rapid isolation procedures and biological and chemical characterization. *The Journal of biological chemistry* 1972;247:7609–11.
129. Cohen S and Carpenter G. Human epidermal growth factor: isolation and chemical and biological properties. *Proceedings of the National Academy of Sciences of the United States of America* 1975;72:1317–21.
130. Carpenter G and Cohen S. Epidermal Growth Factor. *Annual Review of Biochemistry* 1979;48:193–216.
131. Carpenter G, King L, and Cohen S. Epidermal growth factor stimulates phosphorylation in membrane preparations in vitro. *Nature* 1978;276:409–10.
132. Cohen S, Ushiro H, Stoscheck C, and Chinkers M. A native 170,000 epidermal growth factor receptor-kinase complex from shed plasma membrane vesicles. *Journal of Biological Chemistry* 1982;257:1523–31.
133. Schlessinger J. Cell signaling by receptor tyrosine kinases. *Cell* 2000;103:211–25.
134. Yarden Y and Schlessinger J. Epidermal Growth Factor Induces Rapid, Reversible Aggregation of the Purified Epidermal Growth Factor Receptor. *Biochemistry* 1987;26:1443–51.

135. Lemmon MA and Schlessinger J. Regulation of signal transduction and signal diversity by receptor oligomerization. *Trends in Biochemical Sciences* 1994;19:459–63.
136. Downward J, Yarden Y, Mayes E, et al. Close similarity of epidermal growth factor receptor and v-erb-B oncogene protein sequences. *Nature* 1984;307:521–7.
137. Schechter AL, Stern DF, Vaidyanathan L, et al. The neu oncogene: An erb-B-related gene encoding a 185,000-Mr tumour antigen. *Nature* 1984;312:513–6.
138. Coussens L, Yang-Feng TL, Liao YC, et al. Tyrosine kinase receptor with extensive homology to EGF receptor shares chromosomal location with neu oncogene. *Science* 1985;230:1132–9.
139. Kraus MH, Issing W, Miki T, Popescu NP, and Aaronson SA. Isolation and characterization of ERBB3, a third member of the ERBB/epidermal growth factor receptor family: Evidence for overexpression in a subset of human mammary tumors. *Proceedings of the National Academy of Sciences of the United States of America* 1989;86:9193–7.
140. Plowman GD, Culouscou JM, Whitney GS, et al. Ligand-specific activation of HER4/p180erbB4, a fourth member of the epidermal growth factor receptor family. *Proceedings of the National Academy of Sciences of the United States of America* 1993;90:1746–50.
141. Wang Y, Minoshima S, and Shimizu N. Precise mapping of the EGF receptor gene on the human chromosome 7p12 using an improved fish technique. *The Japanese Journal of Human Genetics* 1993;38:399–406.
142. Popescu NC, King CR, and Kraus MH. Localization of the human erbB-2 gene on normal and rearranged chromosomes 17 to bands q12-21.32. *Genomics* 1989;4:362–6.
143. Zimonjic DB, Alimandi M, Miki T, Popescu NC, and Kraus MH. Localization of the human HER4/erbB-4 gene to chromosome 2. *Oncogene* 1995;10:1235–7.
144. Burgess AW, Cho HS, Eigenbrot C, et al. An open-and-shut case? Recent insights into the activation of EGF/ErbB receptors. *Molecular Cell* 2003;12:541–52.
145. Bajaj M, Waterfield MD, Schlessinger J, Taylor WR, and Blundell T. On the tertiary structure of the extracellular domains of the epidermal growth factor and insulin receptors. *Biochimica et Biophysica Acta (BBA)/Protein Structure and Molecular* 1987;916:220–6.

146. Lax I, Johnson A, Howk R, et al. Chicken epidermal growth factor (EGF) receptor: cDNA cloning, expression in mouse cells, and differential binding of EGF and transforming growth factor alpha. *Molecular and Cellular Biology* 1988;8:1970–8.
147. Garrett TP, McKern NM, Lou M, et al. Crystal structure of a truncated epidermal growth factor receptor extracellular domain bound to transforming growth factor α . *Cell* 2002;110:763–73.
148. Kovacs E, Zorn JA, Huang Y, et al. A Structural Perspective on the Regulation of the EGF Receptor. 84. 2015:739–64. DOI: 10.1146/annurev-biochem-060614-034402.A.
149. Ward CW, Hoyne PA, and Flegg RH. Insulin and epidermal growth factor receptors contain the cysteine repeat motif found in the tumor necrosis factor receptor. *Proteins: Structure, Function, and Bioinformatics* 1995;22:141–53.
150. Abe Y, Odaka M, Inagaki F, Lax I, Schlessinger J, and Kohda D. Disulfide bond structure of human epidermal growth factor receptor. *Journal of Biological Chemistry* 1998;273:11150–7.
151. Ogiso H, Ishitani R, Nureki O, et al. Crystal structure of the complex of human epidermal growth factor and receptor extracellular domains. *Cell* 2002;110:775–87.
152. Lemmon MA, Schlessinger J, and Ferguson KM. The EGFR family: Not so prototypical receptor tyrosine kinases. *Cold Spring Harbor Perspectives in Biology* 2014;6:1–18.
153. Lemmon MA, Treutlein HR, Adams PD, Brünger AT, and Engelman DM. A dimerization motif for transmembrane alpha-helices. *Nature structural biology* 1994;1:157–63.
154. Russ WP and Engelman DM. The GxxxG motif: A framework for transmembrane helix-helix association. *Journal of Molecular Biology* 2000;296:911–9.
155. Lu C, Mi LZ, Grey MJ, et al. Structural Evidence for Loose Linkage between Ligand Binding and Kinase Activation in the Epidermal Growth Factor Receptor. *Molecular and Cellular Biology* 2010;30:5432–43.
156. Gajiwala KS. EGFR: Tale of the C-terminal tail. *Protein Science* 2013;22:995–9.
157. Wagner MJ, Stacey MM, Liu BA, and Pawson T. Molecular mechanisms of SH2- and PTB-Domain-containing proteins in receptor tyrosine kinase signaling. *Cold Spring Harbor Perspectives in Biology* 2013;5:1–19.

158. Sato KI, Sato A, Aoto M, and Fukami Y. c-SRC phosphorylates epidermal growth factor receptor on tyrosine 845. 1995. DOI: 10.1006/bbrc.1995.2574.
159. Klapper LN, Glathe S, Vaisman N, et al. The erbB-2/HER2 oncoprotein of human carcinomas may function solely as a shared coreceptor for multiple stroma-derived growth factors. *Proceedings of the National Academy of Sciences of the United States of America* 1999;96:4995–5000.
160. Tzahar E, Waterman H, Chen X, et al. A hierarchical network of interreceptor interactions determines signal transduction by Neu differentiation factor/neuregulin and epidermal growth factor. *Molecular and Cellular Biology* 1996;16:5276–87.
161. Guy PM, Platko JV, Cantley LC, Cerione RA, and Carraway KL. Insect cell-expressed p180(erbB3) possesses an impaired tyrosine kinase activity. *Proceedings of the National Academy of Sciences of the United States of America* 1994;91:8132–6.
162. Shi F, Telesco SE, Liu Y, Radhakrishnan R, and Lemmon MA. ErbB3/HER3 intracellular domain is competent to bind ATP and catalyze autophosphorylation. *Proceedings of the National Academy of Sciences of the United States of America* 2010;107:7692–7.
163. Elenius K, Choi CJ, Paul S, Santiestevan E, Nishi E, and Klagsbrun M. Characterization of a naturally occurring ErbB4 isoform that does not bind or activate phosphatidylinositol 3-kinase. *Oncogene* 1999;18:2607–15.
164. Schneider MR and Wolf E. The epidermal growth factor receptor ligands at a glance. *Journal of Cellular Physiology* 2009;218:460–6.
165. Bork P, Holm L, and Sander C. The Immunoglobulin Fold. 1994. DOI: 10.1006/jmbi.1994.1582.
166. Stein RA and Staros JV. Evolutionary analysis of the ErbB receptor and ligand families. *Journal of Molecular Evolution* 2000;50:397–412.
167. Stein RA and Staros JV. Insights into the evolution of the ErbB receptor family and their ligands from sequence analysis. *BMC Evolutionary Biology* 2006;6:1–17.
168. Fernández-Larrea J, Merlos-Suárez A, Ureña JM, Baselga J, and Arribas J. A role for a PDZ protein in the early secretory pathway for the targeting of proTGF- α to the cell surface. *Molecular Cell* 1999;3:423–33.

169. Brown CL, Coffey RJ, and Dempsey PJ. The Proamphiregulin Cytoplasmic Domain Is Required for Basolateral Sorting, but Is Not Essential for Constitutive or Stimulus-induced Processing in Polarized Madin-Darby Canine Kidney Cells. *Journal of Biological Chemistry* 2001;276:29538–49.
170. Hieda M, Isokane M, Koizumi M, et al. Membrane-anchored growth factor, HB-EGF, on the cell surface targeted to the inner nuclear membrane. *Journal of Cell Biology* 2008;180:763–9.
171. Buonanno A and Fischbach GD. Neuregulin and ErbB receptor signaling pathways in the nervous system. *Current Opinion in Neurobiology* 2001;11:287–96.
172. Olayioye MA, Neve RM, Lane HA, and Hynes NE. The ErbB signaling network: receptor heterodimerization in development and cancer. *The EMBO journal* 2000;19:3159–67.
173. Kochupurakkal BS, Harari D, Di-Segni A, et al. Epigen, the last ligand of ErbB receptors, reveals intricate relationships between affinity and mitogenicity. *Journal of Biological Chemistry* 2005;280:8503–12.
174. Carraway KL, Sliwkowski MX, Akita R, et al. The erbB3 gene product is a receptor for heregulin. *Journal of Biological Chemistry* 1994;269:14303–6.
175. Tzahar E, Levkowitz G, Karunagaran D, et al. ErbB-3 and ErbB-4 function as the respective low and high affinity receptors of all Neu differentiation factor/heregulin isoforms. *Journal of Biological Chemistry* 1994;269:25226–33.
176. Carraway KL3, Weber JL, Unger MJ, et al. Neuregulin-2, a new ligand of ErbB3/ErbB4-receptor tyrosine kinases. *Nature* 1997;387:512–6.
177. Zhang D, Sliwkowski MX, Mark M, et al. Neuregulin-3 (NRG3): A novel neural tissue-enriched protein that binds and activates ErbB4. *Proceedings of the National Academy of Sciences of the United States of America* 1997;94:9562–7.
178. Harari D, Tzahar E, Romano J, et al. Neuregulin-4: A novel growth factor that acts through the ErbB-4 receptor tyrosine kinase. *Oncogene* 1999;18:2681–9.
179. Riese DJ and Stern DF. Specificity within the EGF family/ErbB receptor family signaling network. *BioEssays* 1998;20:41–8.
180. Ferguson KM, Berger MB, Mendrola JM, Cho HS, Leahy DJ, and Lemmon MA. EGF activates its receptor by removing interactions that autoinhibit ectodomain dimerization. *Molecular Cell* 2003;11:507–17.

181. Ferguson KM, Darling PJ, Mohan MJ, Macatee TL, and Lemmon MA. Extracellular domains drive homo- but not heterodimerization of erbB receptors. *EMBO Journal* 2000;19:4632–43.
182. Berger MB, Mendrola JM, and Lemmon MA. ErbB3/HER3 does not homodimerize upon neuregulin binding at the cell surface. *FEBS Letters* 2004;569:332–6.
183. Lemmon MA, Bu Z, Ladbury JE, et al. Two EGF molecules contribute additively to stabilization of the EGFR dimer. *The EMBO journal* 1997;16:281–94.
184. Massagué J and Pandiella A. Membrane-anchored growth factors. *Annual review of biochemistry* 1993;62:515–41.
185. Seals DF and Courtneidge SA. The ADAMs family of metalloproteases: Multidomain proteins with multiple functions. *Genes and Development* 2003;17:7–30.
186. Maretzky T, Zhou W, Huang XY, and Blobel CP. A transforming Src mutant increases the bioavailability of EGFR ligands via stimulation of the cell-surface metalloproteinase ADAM17. *Oncogene* 2011;30:611–8.
187. Honegger AM, Kris RM, Ullrich A, and Schlessinger J. Evidence that autophosphorylation of solubilized receptors for epidermal growth factor is mediated by intermolecular cross-phosphorylation. *Proceedings of the National Academy of Sciences of the United States of America* 1989;86:925–9.
188. Zhang X, Gureasko J, Shen K, Cole PA, and Kuriyan J. An Allosteric Mechanism for Activation of the Kinase Domain of Epidermal Growth Factor Receptor. *Cell* 2006;125:1137–49.
189. Carpenter G. Employment of the epidermal growth factor receptor in growth factor-independent signaling pathways. *The Journal of cell biology* 1999;146:697–702.
190. Luttrell LM, Delia Rocca GJ, Van Biesen T, Luttrell DK, and Lefkowitz RJ. $G\beta\gamma$ subunits mediate Src-dependent phosphorylation of the epidermal growth factor receptor. A scaffold for G protein-coupled receptor-mediated Ras activation. *Journal of Biological Chemistry* 1997;272:4637–44.
191. Köstler WJ, Zeisel A, Körner C, et al. Epidermal growth-factor - Induced transcript isoform variation drives mammary cell migration. *PLoS ONE* 2013;8.
192. Guo YJ, Pan WW, Liu SB, Shen ZF, Xu Y, and Hu LL. ERK/MAPK signalling pathway and tumorigenesis (Review). *Experimental and Therapeutic Medicine* 2020:1997–2007.

193. Zhong Z, Wen Z, and Darnell JE. Stat3: A STAT family member activated by tyrosine phosphorylation in response to epidermal growth factor and interleukin-6. *Science* 1994;264:95–8.
194. Engelman JA, Luo J, and Cantley LC. The evolution of phosphatidylinositol 3-kinases as regulators of growth and metabolism. *Nature Reviews Genetics* 2006;7:606–19.
195. Shostak K and Chariot A. EGFR and NF- κ B: Partners in cancer. *Trends in Molecular Medicine* 2015;21:385–93.
196. Avraham R and Yarden Y. Feedback regulation of EGFR signalling: Decision making by early and delayed loops. *Nature Reviews Molecular Cell Biology* 2011;12:104–17.
197. Waterman H, Sabanai I, Geiger B, and Yarden Y. Alternative intracellular routing of ErbB receptors may determine signaling potency. *Journal of Biological Chemistry* 1998;273:13819–27.
198. Lenferink AE, Pinkas-Kramarski R, Van De Poll ML, et al. Differential endocytic routing of homo- and hetero-dimeric ErbB tyrosine kinases confers signaling superiority to receptor heterodimers. *EMBO Journal* 1998;17:3385–97.
199. Pentassuglia L and Sawyer DB. The role of Neuregulin-1beta/ErbB signaling in the heart. *Experimental cell research* 2009;315:627–37.
200. Stoll SW, Kansra S, Peshick S, et al. Differential utilization and localization of ErbB receptor tyrosine kinases in skin compared to normal and malignant keratinocytes. *Neoplasia* 2001;3:339–50.
201. Burgess AW. EGFR family: Structure physiology signalling and therapeutic target. *Growth Factors* 2008;26:263–74.
202. Piepkorn M, Pittelkow MR, and Cook PW. Autocrine regulation of keratinocytes: The emerging role of heparin-binding, epidermal growth factor-related growth factors. *Journal of Investigative Dermatology* 1998;111:715–21.
203. Schneider MR, Werner S, Paus R, and Wolf E. Beyond wavy hairs: The epidermal growth factor receptor and its ligands in skin biology and pathology. *American Journal of Pathology* 2008;173:14–24.
204. Maretzky T, Evers A, Zhou W, et al. Migration of growth factor-stimulated epithelial and endothelial cells depends on EGFR transactivation by ADAM17. *Nature Communications* 2011;2:1–25.

205. Pastore S, Lulli D, and Girolomoni G. Epidermal growth factor receptor signalling in keratinocyte biology: Implications for skin toxicity of tyrosine kinase inhibitors. *Archives of Toxicology* 2014;88:1189–203.
206. Pastore S, Mascia F, Mariani V, and Girolomoni G. The epidermal growth factor receptor system in skin repair and inflammation. *Journal of Investigative Dermatology* 2008;128:1365–74.
207. Büchau AS. EGFR (trans)activation mediates IL-8 and distinct human antimicrobial peptide and protein production following skin injury. *Journal of Investigative Dermatology* 2010;130:929–32.
208. Xue M, Chow SO, Dervish S, Chan YKA, Julovi SM, and Jackson CJ. Activated protein C enhances human keratinocyte barrier integrity via sequential activation of epidermal growth factor receptor and tie2. *Journal of Biological Chemistry* 2011;286:6742–50.
209. Elder JT, Fisher GJ, Lindquist PB, et al. Overexpression of transforming growth factor alpha in psoriatic epidermis. *Science (New York, N.Y.)* 1989;243:811–4.
210. Wang S, Zhang Z, Peng H, and Zeng K. Recent advances on the roles of epidermal growth factor receptor in psoriasis. *American journal of translational research* 2019;11:520–8.
211. Ishitoya J, Toriyama M, Oguchi N, et al. Gene amplification and overexpression of EGF receptor in squamous cell carcinomas of the head and neck. *British journal of cancer* 1989;59:559–62.
212. Maxwell SA, Sacks PG, Gutterman JU, and Gallick GE. Epidermal Growth Factor Receptor Protein-Tyrosine Kinase Activity in Human Cell Lines Established from Squamous Carcinomas of the Head and Neck. *Cancer Research* 1989;49:1130–7.
213. Singh B, Schneider M, Knyazev P, and Ullrich A. UV-induced EGFR signal transactivation is dependent on proligand shedding by activated metalloproteases in skin cancer cell lines. *International Journal of Cancer* 2009;124:531–9.
214. Zhang Z, Oliver P, Lancaster JR, et al. Reactive oxygen species mediate tumor necrosis factor alpha-converting, enzyme-dependent ectodomain shedding induced by phorbol myristate acetate. *The FASEB Journal* 2001;15:303–5.
215. Penning TM. Hydroxysteroid dehydrogenases and pre-receptor regulation of steroid hormone action. *Human Reproduction Update* 2003;9:193–205.

216. Penning TM. AKR1C3 (type 5 17β -hydroxysteroid dehydrogenase/prostaglandin F synthase): Roles in malignancy and endocrine disorders. *Molecular and Cellular Endocrinology* 2019;489:82–91.
217. Jez JM, Flynn TG, and Penning TM. A nomenclature system for the aldo-keto reductase superfamily. *Advances in Experimental Medicine and Biology* 1997;414:579–89.
218. Jez JM, Bennett MJ, Schlegel BP, Lewis M, and Penning TM. Comparative anatomy of the aldo-keto reductase superfamily. *Biochemical Journal* 1997;326:625–36.
219. Penning TM, Wangtrakuldee P, and Auchus RJ. Structural and functional biology of aldo-keto reductase steroid-transforming enzymes. *Endocrine Reviews* 2019;40:447–75.
220. Gulbis JM, Mann S, and MacKinnon R. Structure of a Voltage-Dependent K^+ Channel β Subunit. *Cell* 1999;97:943–52.
221. Kelly VP, Sherratt PJ, Crouch DH, and Hayes JD. Novel homodimeric and heterodimeric rat γ -hydroxybutyrate synthases that associate with the Golgi apparatus define a distinct subclass of aldo-keto reductase 7 family proteins. *Biochemical Journal* 2002;366:847–61.
222. Hoog SS, Pawlowski JE, Alzari PM, Penning TM, and Lewis M. Three-dimensional structure of rat liver 3α -hydroxysteroid/dihydrodiol dehydrogenase: A member of the aldo-keto reductase superfamily. *Proceedings of the National Academy of Sciences of the United States of America* 1994;91:2517–21.
223. Liu SQ, Jin H, Zacarias A, Srivastava S, and Bhatnagar A. Binding of pyridine coenzymes to the β -subunit of the voltage sensitive potassium channels. *Chemico-Biological Interactions* 2001;130-132:955–62.
224. Borhani DW, Harter TM, and Petrash JM. The crystal structure of the aldose reductase·NADPH binary complex. *Journal of Biological Chemistry* 1992;267:24841–7.
225. Hara A, Matsuura K, Tamada Y, et al. Relationship of human liver dihydrodiol dehydrogenases to hepatic bile-acid-binding protein and an oxidoreductase of human colon cells. *Biochemical Journal* 1996;313:373–6.
226. Matsuura K, Deyashiki Y, Sato K, Ishida N, Miwa G, and Hara A. Identification of amino acid residues responsible for differences in substrate specificity and inhibitor sensitivity between two human liver dihydrodiol dehydrogenase isoenzymes by site-directed mutagenesis. *The Biochemical journal* 1997;323 (Pt 1:61–4.

227. Qiu W, Zhou M, Labrie F, and Lin SX. Crystal structures of the multispecific 17 β -hydroxysteroid dehydrogenase type 5: Critical androgen regulation in human peripheral tissues. *Molecular Endocrinology* 2004;18:1798–807.
228. Nishizawa M, Nakajima T, Yasuda K, et al. Close kinship of human 20 α -hydroxysteroid dehydrogenase gene with three aldo-keto reductase genes. *Genes to Cells* 2000;5:111–25.
229. Tebay LE, Robertson H, Durant ST, et al. Mechanisms of activation of the transcription factor Nrf2 by redox stressors, nutrient cues, and energy status and the pathways through which it attenuates degenerative disease. *Free radical biology & medicine* 2015;88:108–46.
230. Platt A, Xia Z, Liu Y, Chen G, and Lazarus P. Impact of nonsynonymous single nucleotide polymorphisms on in-vitro metabolism of exemestane by hepatic cytosolic reductases. *Pharmacogenetics and Genomics* 2016;26:370–80.
231. Luo DX, Huang MC, Ma J, Gao Z, Liao DF, and Cao D. Aldo-keto reductase family 1, member B10 is secreted through a lysosome-mediated non-classical pathway. *Biochemical Journal* 2011;438:71–80.
232. Matsunaga T, Haga M, Watanabe G, et al. 9,10-Phenanthrenequinone promotes secretion of pulmonary aldo-keto reductases with surfactant. *Cell and Tissue Research* 2012;347:407–17.
233. Weber S, Salabei JK, Möller G, et al. Aldo-keto Reductase 1B15 (AKR1B15): A mitochondrial human aldo-keto reductase with activity toward steroids and 3-keto-acyl-CoA conjugates. *Journal of Biological Chemistry* 2015;290:6531–45.
234. Grimshaw CE, Bohren KM, Lai CJ, and Gabbay KH. Human Aldose Reductase: Rate Constants for a Mechanism Including Interconversion of Ternary Complexes by Recombinant Wild-Type Enzyme. *Biochemistry* 1995;34:14356–65.
235. Cooper WC, Jin Y, and Penning TM. Elucidation of a complete kinetic mechanism for a mammalian hydroxysteroid dehydrogenase (HSD) and identification of all enzyme forms on the reaction coordinate: The example of rat liver 3 α -HSD (AKR1C9). *Journal of Biological Chemistry* 2007;282:33484–93.
236. Jin Y and Penning TM. Multiple steps determine the overall rate of the reduction of 5 α -dihydrotestosterone catalyzed by human type 3 3 α -hydroxysteroid dehydrogenase: Implications for the elimination of androgens. *Biochemistry* 2006;45:13054–63.

237. Bennett MJ, Schlegel BP, Jez JM, Penning TM, and Lewis M. Structure of 3 α -hydroxysteroid/dihydrodiol dehydrogenase complexed with NADP⁺. *Biochemistry* 1996;35:10702–11.
238. Ratnam K, Ma H, and Penning TM. The arginine 276 anchor for NADP(H) dictates fluorescence kinetic transients in 3 α -hydroxysteroid dehydrogenase, a representative aldo-keto reductase. *Biochemistry* 1999;38:7856–64.
239. Schlegel BP, Jez JM, and Penning TM. Mutagenesis of 3 α -hydroxysteroid dehydrogenase reveals a 'push -pull' mechanism for proton transfer in aldo-keto reductases. *Biochemistry* 1998;37:3538–48.
240. Zeng CM, Chang LL, Ying MD, et al. Aldo-keto reductase AKR1C1-AKR1C4: Functions, regulation, and intervention for anti-cancer therapy. *Frontiers in Pharmacology* 2017;8:1–9.
241. Mantel A, Carpenter-Mendini AB, Vanbuskirk JB, De Benedetto A, Beck LA, and Pentland AP. Aldo-keto reductase 1C3 is expressed in differentiated human epidermis, affects keratinocyte differentiation, and is upregulated in atopic dermatitis. *The Journal of investigative dermatology* 2012;132:1103–10.
242. Rižner TL, Šmuc T, Rupreht R, Šinkovec J, and Penning TM. AKR1C1 and AKR1C3 may determine progesterone and estrogen ratios in endometrial cancer. *Molecular and Cellular Endocrinology* 2006;248:126–35.
243. Flück CE, Meyer-Böni M, Pandey AV, et al. Why boys will be boys: Two pathways of fetal testicular androgen biosynthesis are needed for male sexual differentiation. *American Journal of Human Genetics* 2011;89:201–18.
244. Deyashiki Y, Ogasawara A, Nakayama T, et al. Molecular cloning of two human liver 3 alpha-hydroxysteroid/dihydrodiol dehydrogenase isoenzymes that are identical with chlordecone reductase and bile-acid binder. *The Biochemical journal* 1994;299 (Pt 2):545–52.
245. Yepuru M, Wu Z, Kulkarni A, et al. Steroidogenic enzyme AKR1C3 is a novel androgen receptor-selective coactivator that promotes prostate cancer growth. *Clinical Cancer Research* 2013;19:5613–25.
246. Kabututu Z, Manin M, Pointud JC, et al. Prostaglandin F₂ α synthase activities of aldo-keto reductase 1B1, 1B3 and 1B7. *Journal of Biochemistry* 2009;145:161–8.
247. Komoto J, Yamada T, Watanabe K, and Takusagawa F. Crystal Structure of Human Prostaglandin F Synthase (AKR1C3). *Biochemistry* 2004;43:2188–98.

248. Matsuura K, Shiraishi H, Hara A, et al. Identification of a principal mRNA species for human 3 α -hydroxysteroid dehydrogenase isoform (AKR1C3) that exhibits high prostaglandin D2 11-ketoreductase activity. *Journal of biochemistry* 1998;124:940–6.
249. Desmond JC, Mountford JC, Drayson MT, et al. The aldo-keto reductase AKR1C3 is a novel suppressor of cell differentiation that provides a plausible target for the non-cyclooxygenase-dependent antineoplastic actions of nonsteroidal anti-inflammatory drugs. *Cancer Research* 2003;63:505–12.
250. Zouboulis CC, Chen WC, Thornton MJ, Qin K, and Rosenfield R. Sexual hormones in human skin. *Hormone and Metabolic Research* 2007;39:85–95.
251. Sator PG, Schmidt JB, Sator MO, Huber JC, and Hönigsmann H. The influence of hormone replacement therapy on skin ageing: A pilot study. *Maturitas* 2001;39:43–55.
252. Holzer G, Riegler E, Hönigsmann H, Farokhnia S, and Schmidt B. Effects and side-effects of 2% progesterone cream on the skin of peri- and postmenopausal women: Results from a double-blind, vehicle-controlled, randomized study. *British Journal of Dermatology* 2005;153:626–34.
253. Zhang Y, Dufort I, Rheault P, and Luu-The V. Characterization of a human 20 α -hydroxysteroid dehydrogenase. *Journal of molecular endocrinology* 2000;25:221–8.
254. Dufort I, Labrie F, and Luu-The V. Human Types 1 and 3 3 α -Hydroxysteroid Dehydrogenases: Differential Lability and Tissue Distribution1. *The Journal of Clinical Endocrinology & Metabolism* 2001;86:841–6.
255. Kanda N and Watanabe S. 17 β -Estradiol Inhibits Oxidative Stress-Induced Apoptosis in Keratinocytes by Promoting Bcl-2 Expression. *Journal of Investigative Dermatology* 2003;121:1500–9.
256. Chow KC, Lu MP, and Wu MT. Expression of dihydrodiol dehydrogenase plays important roles in apoptosis- and drug-resistance of A431 squamous cell carcinoma. *Journal of Dermatological Science* 2006;41:205–12.
257. Smith PK, Krohn RI, Hermanson GT, et al. Measurement of protein using bicinchoninic acid. *Analytical Biochemistry* 1985.
258. Laemmli UK. Cleavage of structural proteins during the assembly of the head of bacteriophage T4. *Nature* 1970.
259. Towbin H, Staehelin T, and Gordon J. Electrophoretic transfer of proteins from polyacrylamide gels to nitrocellulose sheets: procedure and some applications. *Proceedings of the National Academy of Sciences* 1979.

260. Renart J, Reiser J, and Stark GR. Transfer of proteins from gels to diazobenzyloxymethyl-paper and detection with antisera: a method for studying antibody specificity and antigen structure. *Proceedings of the National Academy of Sciences* 1979.
261. Burnette WN. "Western Blotting": Electrophoretic transfer of proteins from sodium dodecyl sulfate-polyacrylamide gels to unmodified nitrocellulose and radiographic detection with antibody and radioiodinated protein A. *Analytical Biochemistry* 1981.
262. Thorpe GHG, Kricka LJ, Moseley SB, and Whitehead TP. Phenols as enhancers of the chemiluminescent horseradish peroxidase-luminol-hydrogen peroxide reaction: Application in luminescence-monitored enzyme immunoassays. *Clinical Chemistry* 1985.
263. Leong MM and Fox GR. Enhancement of luminol-based immunodot and Western blotting assays by iodophenol. *Analytical Biochemistry* 1988.
264. Summers WC. A simple method for extraction of RNA from *E. coli* utilizing diethyl pyrocarbonate. *Analytical Biochemistry* 1970;33:460–3.
265. Haugland RP and Haugland RP. *Handbook of fluorescent probes and research products*. 9th ed. Eugene, OR: Molecular Probes, 2002.
266. Livak KJ and Schmittgen TD. Analysis of relative gene expression data using real-time quantitative PCR and the $2^{-\Delta\Delta CT}$ method. *Methods* 2001;25:402–8.
267. Macleod AK, McMahon M, Plummer SM, et al. Characterization of the cancer chemopreventive NRF2-dependent gene battery in human keratinocytes: Demonstration that the KEAP1-NRF2 pathway, and not the BACH1-NRF2 pathway, controls cytoprotection against electrophiles as well as redox-cycling compounds. *Carcinogenesis* 2009;30:1571–80.
268. Penning TM and Drury JE. Human aldo-keto reductases: Function, gene regulation, and single nucleotide polymorphisms. *Archives of Biochemistry and Biophysics* 2007;464:241–50.
269. Karin M. Inflammation-activated protein kinases as targets for drug development. *Proceedings of the American Thoracic Society* 2005;2:386–90.
270. CRC CARE 2017. Risk-based management and remediation guidance for benzo(a)pyrene. Tech. rep. CRC CARE Technical Report no. 39, CRC for Contamination Assessment and Remediation of the Environment, Newcastle, Australia.

271. Burczynski ME, Lin HK, and Penning TM. Isoform-specific induction of a human aldo-keto reductase by polycyclic aromatic hydrocarbons (PAHs), electrophiles, and oxidative stress: Implications for the alternative pathway of PAH activation catalyzed by human dihydrodiol dehydrogenase. *Cancer Research* 1999;59:607–14.
272. Piepkorn M. Overexpression of Amphiregulin, a Major Autocrine Growth Factor for Cultured Human Keratinocytes, in Hyperproliferative Skin Diseases. *The American Journal of Dermatopathology* 1996;18.
273. Liu PC, Liu X, Li Y, et al. Identification of ADAM10 as a major source of HER2 ectodomain sheddase activity in HER2 overexpressing breast cancer cells. *Cancer Biology and Therapy* 2006;5:657–64.
274. Huang J, Pan Y, Hu G, et al. SRC fine-tunes ADAM10 shedding activity to promote pituitary adenoma cell progression. *The FEBS Journal* 2020;287:190–204.
275. Winograd-Katz SE and Levitzki A. Cisplatin induces PKB/Akt activation and p38MAPK phosphorylation of the EGF receptor. *Oncogene* 2006;25:7381–90.
276. Xu P and Derynck R. Direct Activation of TACE-Mediated Ectodomain Shedding by p38 MAP Kinase Regulates EGF Receptor-Dependent Cell Proliferation. *Molecular Cell* 2010;37:551–66.
277. Tang J, Hu B, Zheng H, et al. 2,2',4,4'-Tetrabromodiphenyl ether (BDE-47) activates Aryl hydrocarbon receptor (AhR) mediated ROS and NLRP3 inflammasome/p38 MAPK pathway inducing necrosis in cochlear hair cells. *Ecotoxicology and Environmental Safety* 2021;221.
278. Miao W, Hu L, Scrivens PJ, and Batist G. Transcriptional regulation of NF-E2 p45-related factor (NRF2) expression by the aryl hydrocarbon receptor-xenobiotic response element signaling pathway: Direct cross-talk between phase I and II drug-metabolizing enzymes. *Journal of Biological Chemistry* 2005;280:20340–8.
279. Gao S, Guo K, Chen Y, et al. Keratinocyte Growth Factor 2 Ameliorates UVB-Induced Skin Damage via Activating the AhR/Nrf2 Signaling Pathway. *Frontiers in Pharmacology* 2021;12:1–13.
280. Korpela SP, Hinz TK, Oweida A, et al. Role of epidermal growth factor receptor inhibitor-induced interferon pathway signaling in the head and neck squamous cell carcinoma therapeutic response. *Journal of Translational Medicine* 2021;19:1–15.

6 Appendix

6.1 List of Figures

| | | |
|-----|---|----|
| 2.1 | Stimulation of cells with AHR ligands | 32 |
| 3.1 | Stable knockdown of the AHR in shAHR HaCaT keratinocytes shown after exposure to the ligands B(a)P and PCB126. Two-way ANOVA, $n = 5$, $p \geq 0.05$, Tukey's multiple comparisons test, error bar = SD | 44 |
| 3.2 | AKR1C1, -C2 and C3 transcription in EV and shAHR HaCaT after treatment with DMSO, B(a)P and PCB126. $n = 6$, Two-way ANOVA-test, $p \geq 0.05$, Tukey's multiple comparisons test, error bar = SD | 45 |
| 3.3 | AKR1A1, -B1 and -B10 transcription in EV and shAhR HaCaT after treatment with DMSO, B(a)P and PCB126. $n = 6$, Two-way ANOVA-test, $p \geq 0.05$, Tukey's multiple comparisons test, error bar = SD | 46 |
| 3.4 | AKR7A2 & -3 transcription in EV and shAhR HaCaT after treatment with DMSO, B(a)P and PCB126. $n = 6$, Two-way ANOVA-test, $p \geq 0.05$, Tukey's multiple comparisons test, error bar = SD | 46 |
| 3.5 | AKR1C1, -C2 and -C3 transcription in WT HaCaT after treatment with DMSO, B(a)P, EGF, $TGF\alpha$, $TNF\alpha$, AREG and EREG. $n = 6$, Kruskal-Wallis-test, $p \geq 0.05$, Dunn's multiple comparisons test, error bar = SD | 47 |
| 3.6 | AKR1A1, -1B1 and -1B10 transcription in WT HaCaT after treatment with DMSO, B(a)P, EGF, $TGF\alpha$, $TNF\alpha$, AREG and EREG. $n = 1$ for AKR1A1 and -B1, $n = 6$ for AKR1B10, Kruskal-Wallis-test, $p \geq 0.05$, Dunn's multiple comparisons test, error bar = SD | 48 |
| 3.7 | AKR1C1, -1C2 and -1C3 gene transcription in EV- and shAHR HaCaT after treatment with medium, DMSO, B(a)P, EGF and AREG. n for EGF = 4, n for AREG = 2, Two-way ANOVA, $p \geq 0.05$, Turkey's multiple comparison test, error bar = SD | 49 |

| | | |
|------|--|----|
| 3.8 | AKRC1, -2 & 3 transcription after exposure anti-EGFR antibody. Executed by Dr. rer. nat. Christian Vogele, n = 4, ordinary one-way ANOVA-test, p >= 0.05, Tukey's multiple comparisons test, error bar = SD | 50 |
| 3.9 | AKRC1, -2 & 3 transcription after exposure to DMSO, B(a)P, PCB126, B(a)P + PCB126, B(a)P + Marimastat and B(a)P + Bosutinib. n = 4, RM one way ANOVA, p >= 0.05, Tukey's multiple comparisons test, error bar = SD | 51 |
| 3.10 | Western blot of AKR1C3 in EV- and shAHR-HaCat after treatment with DMSO, B(a)P and PCB126. n = 4. The arrow points at the protein band of AKR1C3. | 52 |
| 3.11 | Western blot of AKR1C3 in EV- and shAHR-HaCat after treatment with DMSO, B(a)P and PCB126. n = 4. The arrow points at the protein band of AKR1C3. | 53 |
| 3.12 | Western blot of AKR1C3 in EV- and shAHR-HaCat after treatment with DMSO, B(a)P and PCB126. n = 4. The arrow points at the protein band of AKR1C3. | 53 |
| 3.13 | Western blot of AKR1C3 in EV- and shAHR-HaCat after treatment with DMSO, B(a)P and PCB126. n = 4. The arrow points at the protein band of AKR1C3. | 54 |
| 3.14 | Densitometric of western blot of AKR1C3 in EV- and shAHR-HaCat after treatment with DMSO, B(a)P and PCB126. n = 4, Two-way ANOVA, p >= 0.05, Tukey's multiple comparisons test, error bar = SD | 54 |

6.2 List of Tables

| | | |
|------|--|----|
| 1 | List of abbreviations | VI |
| 2.1 | List of chemicals | 27 |
| 2.2 | List of stimulants | 28 |
| 2.3 | List of Kits | 28 |
| 2.4 | List of Devices | 28 |
| 2.5 | Software | 28 |
| 2.6 | List of primary antibodies | 29 |
| 2.7 | List of secondary antibodies | 29 |
| 2.8 | Human Cell Lines | 30 |
| 2.9 | AHR ligands | 32 |
| 2.10 | EGFR ligands | 32 |

| | | |
|------|---|----|
| 2.11 | Concentration series of EGF and AREG | 33 |
| 2.12 | Anti-EGFR antibody | 33 |
| 2.13 | Pathway promoters and inhibitors | 33 |
| 2.14 | AHR ligands for WB | 34 |
| 2.15 | 2x RIPA buffer | 34 |
| 2.16 | 1 ml completed lysis buffer | 35 |
| 2.17 | 4x Laemmli sample buffer | 35 |
| 2.18 | SDS-polyacrylamide gel 10% | 36 |
| 2.19 | SDS-Page, 5x Running buffer | 37 |
| 2.20 | Western blot, 5x transfer buffer | 38 |
| 2.21 | Western blot, 2l finished transfer buffer | 38 |
| 2.22 | Western blot, 10x washing buffer | 39 |
| 2.23 | Synthesis Step 1: Primer annealing | 41 |
| 2.24 | Synthesis Step 2: cDNA-Synthesis | 41 |
| 2.25 | PCR reaction mixture | 41 |
| 2.26 | qRT-PCR Sequences | 42 |
| 6.1 | Amino acid code | 89 |

6.3 Amino Acid Code

| Amino Acid | 3-Letter Code | 1-Letter Code |
|-------------------------|---------------|---------------|
| Alanine | Ala | A |
| Cysteine | Cys | C |
| Aspartic acid/Aspartate | Asp | D |
| Glutamic Acid/Glutamate | Glu | E |
| Phenylalanine | Phe | F |
| Glycine | Gly | G |
| Histidine | His | H |
| Isoleucine | Ile | I |
| Lysine | Lys | K |
| Leucine | Leu | L |
| Methionine | Met | M |
| Asparagine | Asn | N |
| Proline | Pro | P |
| Glutamine | Gln | Q |
| Arginine | Arg | R |
| Serine | Ser | S |

| Amino Acid | 3-Letter Code | 1-Letter Code |
|-------------------|----------------------|----------------------|
| Threonine | Thr | T |
| Valine | Val | V |
| Tryptophan | Trp | W |
| Tyrosine | Tyr | Y |

Table 6.1: Amino acid code

Acknowledgements

In the end, I want to thank the persons that took part in this research.

First of all, I would like to express my gratitude to PD Dr. med. Stephan Meller for making this dissertation possible by taking the role of my doctoral supervisor.

I am also grateful to Univ.-Prof. Dr. med. Ellen Fritsche for being my co-supervisor.

This work would not have been possible without the research team of Dr. rer. nat. Thomas Haarmann-Stemmann. My sincere thanks go to PD Dr. Thomas Haarmann-Stemmann himself and Dr. Christian Vogeley for being my advisors during the research and answering each of my questions with patience. Additionally, I would like to thank Dr. Melina Mescher and Dr. Marius Pollet for introducing me into the world of cell culture-based research. Additionally, huge thanks go to Katharina Rolfes, Selina Woeste and Ragnhild Wirth for being my office mates, helpful advisors and sympathetic colleagues.

My life would not have been what it was without my parents, Stephan Maaß and Brigitte Kohl. Additionally, I feel sincere gratitude towards my sister, Alexandra Neuwirth, for always being there for me, representing a role model, and, therefore, affecting my personality, always for the better.

I am and will always be indebted to my friends for their companionship and continuous support: Rebekka Oppermann, Matthias and Jennifer Buchholz, Jan Wiske-
mann, Jasmin Laufenberg, Karola Schmitz, Frederike Klee, Gesche Stratmann, and Olivia Wilson-Piper. Special thanks go to the friends I made at Heinrich-Heine uni-
versity, Mia Lohmann, Isabelle Reuter, Katharina Greger and Nguyen Khoa Tran. I also want to thank Tanja Bergmann, my partner in crime. Special gratitude goes to Dr. Livia Arianna Belfiore, for both being the person and being the friend she is.

The first persons who made me think that I can follow a scientific career path were my teachers. Without their support, I would never have tried to strive for being a doctor one day. Therefore, I feel a deep gratitude towards them and the *Siebengebirgsgymnasium*.

I am also in deep gratitude to Ruth Bläser and Mrs. Robin Lohmann for proofreading. I deeply thank both of you for your correction and that you let me participate

in your knowledge about the English language.

Lastly, I want to express my gratitude towards Dr. med. Philippe Bissen. When you submitted your thesis, I was mentioned as your girlfriend in the acknowledgements. Now, I am able to mention you as my husband. Thank you, in return, for being part of my life. I hope that we will continue this journey together.